CUKUROVA UNIVERSITY
INSTITUTE OF NATURAL AND APPLIED SCIENCES

PhD THESIS

Toufique AHMED

ANALYSIS OF THE EFFECT OF DIFFERENT ANTIMICROBIAL FINISHES WITH MULTIPLE METHODS ON VARIOUS COTTON FABRICS

DEPARTMENT OF TEXTILE ENGINEERING

ADANA, 2022

ABSTRACT

PhD THESIS

ANALYSIS OF THE EFFECT OF DIFFERENT ANTIMICROBIAL FINISHES WITH MULTIPLE METHODS ON VARIOUS COTTON FABRICS

Toufique AHMED

CUKUROVA UNIVERSITY
INSTITUTE OF NATURAL AND APPLIED SCIENCES
DEPARTMENT OF TEXTILE ENGINEERING

Supervisor : Prof. Dr. R. Tuğrul OĞULATA
Year: 2022, Pages 150
Jury : Prof. Dr. R. Tuğrul OĞULATA
: Prof. Dr. Ahmet TEKE
: Assoc. Prof. Dr. Serin MEZARCIÖZ
: Assist. Prof. Dr. Halil İbrahim İÇOĞLU
: Assist. Prof. Dr. Pınar PARLAKYİĞİT

Antibacterial textiles are used to protect from microbial infection by inhibiting the growth of microbes or annihilating them. This study compares different methods, fabric types, and pretreatments for antibacterial performance with green synthesized silver nanoparticles (AgNPs). It also aims to explain the influence of plant extract, silver nitrate ($AgNO_3$) molarity and volume, fabric pH etc., on silver nanoparticles synthesis and antibacterial efficiency. This research demonstrated synthesizing AgNPs from *C.arvensis* weeds and *C.reticulata* fruit peels. For this purpose, after preparing plant extract, the silver nanoparticles (AgNPs) were synthesized from silver nitrate ($AgNO_3$) using plant extract. The synthesized nanoparticles were incorporated into the fabrics by various methods such as padding, immersion, sol-gel, etc. Next, the AgNps-loaded fabrics were characterized by SEM, EDS, and XRD. Latter, antibacterial tests were done for the fabrics. This study derived an equation for plant extract amount, explained nanoparticle morphology, and investigated the best AgNPs loading method and fabric structure for antibacterial activity. It also discovered recoverable antibacterial property loss of AgNPs-loaded fabrics. The reason behind this exceptional behavior of AgNPs-loaded fabrics is also explained. It is envisaged that this study might contribute to producing cheap and effective antibacterial products.

Key Words: Green synthesis, sol-gel, antibacterial textiles, silver nanoparticles, nanoparticle morpholog

ÖZ

DOKTORA TEZİ

FARKLI ANTİMİKROBİYAL BİTİM İŞLEMLERİNİN PAMUKLU KUMAŞLAR ÜZERİNDEKİ ETKİSİNİN ANALİZİ

Toufique AHMED

ÇUKUROVA ÜNİVERSİTESİ
FEN BİLİMLERİ ENSTİTÜSÜ
TEKSTİL MÜHENDİSLİĞİ ANABİLİM DALI

Danışman : Prof. Dr. R. Tuğrul OĞULATA
Yıl: 2022, Sayfa 150
Jüri : Prof. Dr. R. Tuğrul OĞULATA
: Prof. Dr. Ahmet TEKE
: Doç. Dr. Serin MEZARCIÖZ
: Dr. Öğr. Üyesi Halil İbrahim İÇOĞLU
: Dr. Öğr. Üyesi Pınar PARLAKYİĞİT

Antibakteriyel tekstiller, mikropların büyümesini engelleyerek veya onları yok ederek mikrobiyal enfeksiyondan korunmak için kullanılır. Bu çalışmada, yeşil sentezlenmiş gümüş nanopartiküller (AgNP'ler) ile yüksek antibakteriyel performans için farklı yöntemler, kumaş türleri ve ön işlemler karşılaştırılmıştır. Ayrıca bitki özü, gümüş nitrat molaritesi ve hacmi, kumaş pH'ı vb.'nin sentezlenen gümüş nanopartiküller ve antibakteriyel verim üzerindeki etkisinin incelenmesi amaçlanmaktadır. Gümüş nanopartiküller (AgNP'ler) ex-situ ve in-situ yöntemleri uygulanarak sentezlenmiştir. Ex-situ sentez yönteminde sentezlenen nanopartiküller, dolgu, daldırma, sol-jel vb. gibi çeşitli yöntemlerle kumaşlara dahil edilmiştir. Daha sonra, kumaşlara dahil edilen gümüş nanopartiküller, SEM, EDS, ve XRD ile karakterize edilmiştir. Ardından kumaşlar için antibakteriyel testler yapılmıştır. Bu çalışma, bitki özü miktarı için bir denklem formüle edilmiştir, nanopartiküller morfolojisini açıklamış ve antibakteriyel aktivite için en iyi AgNP yükleme yöntemini ve kumaş yapısını açıklamıştır. Ayrıca AgNP'ler yüklü kumaşların geri kazanılabilir antibakteriyel özellik kaybını keşfetti. AgNP'ler yüklü kumaşların bu istisnai davranışının arkasındaki neden de açıklanmıştır. Çalışmanın minimum maliyet ve minimum sağlık veya çevresel tehlike ile antibakteriyel tekstil üretimine katkı sağlayabileceği öngörülmektedir.

Anahtar Kelimeler: Yeşil sentez, sol-jel, antibakteriyel tekstiller, gümüş nanoparçacıklar, nanoparçacık morfoloji

EXTENDED SUMMARY

The antibacterial textile market is expanding day by day. The Covid-19 pandemic accelerated the market demand to a larger extent. Cotton is the most popular among all the fibres so far due to its unparalleled comfortability. But it is a great nutrient source for microbes. Hence, the microbes attack cotton fibre easily, which caused an unpleasant odour, loss of strength, loss of colour, etc. For antibacterial fabrics, there are multiple agents such as QAC, Triclosan, PHMB, metal ions etc. Among all, silver nanoparticles (AgNPs) are a great antibacterial agent regarding performance, comparatively harmless to the environment and human health. AgNPs can be synthesized from $AgNO_3$ in multiple ways, such as physical and chemical methods. Physical methods are costly, imperfect, low production etc. on the contrary, chemical methods need a separate reducing and capping agent. Besides, these chemicals are not eco-friendly. On the other hand, green synthesis is the most eco-friendly, cost-effective, and straightforward. Here only organic extract can simultaneously reduce, agglomerate, and stabilize the AgNPs. This study aims to find out the best method and fabric type for higher antibacterial efficiency by comparing various methods and fabrics- using green synthesized silver nanoparticles. It is also intended to investigate the correlating factors on antibacterial efficiency. For example, the influce of silver nitrate molarity and volume, plant extract quantity, fabric pretreatment, AgNPs incorporation methods etc. on antibacterial property. Almost all types of organic sources can do green synthesis. However, *Calendula arvensis*, a widely found weed from December to April in Turkey, has been selected for this study. To the best of our knowledge, there has been no such type of study before. AgNPs were also synthesized using *citrus reticulata*, the available mandarin orange peel extract. For an effective nanoparticle synthesis plant extract, quantity is most crucial. Hence, an equation was formulated to determine the optimum required plant extract amount for *in-situ* and *ex-situ* methods. As textiles materials, four types of fabrics were used: - plain (1/1, GSM

123), twill (3/1, GSM 230), knit (plain, GSM 154), and non-woven (GSM 20). AgNPs can be incorporated into fabrics by various incorporation methods. This study implemented four basic methods (*padding*, *immersion*, *in-situ*, *sol-gel*) and three derivative methods: *2-times-padding*, *in-situ-pad*, and *immersion (in-situ)*. Although the previous works claimed room temperature is enough for green synthesis. However, this study found below 40 °C AgNPs will not form from *C.arvensis* extract, and 60 °C is optimum for high stability. The influence of temperature was investigated using Surface Plasmon Resonance (SPR) of UV-vis spectroscopy. It showed temperature affects nanoparticle size (in terms of UV-vis SPR). But the effect was not statistically significant. The Kruskal-Wallis test (non-parametric test, equivalent to ANOVA) was used for the statistical test. For more confirmation, Dunn's post hoc test was also conducted. Any significant results were not found in those statistical tests. Among other parameters, $AgNO_3$ molarity and volume were most influential in AgNPs size (in terms of UV-vis SPR) and stability. In this case, the effect of $AgNO_3$-molarity was found statistically significant by the ANOVA test. Tukeys' HSD test was also used to determine which specific group had a significant result. The plant extracts have electron-donating $NADPH_2$ co-enzymes, which donate electrons to the Ag^+ ion, and in this way, it gets reduced to Ag^0. The formation of Ag^0 will cause free surface energy which will initiate nucleation. However, for uniform size distribution, short nucleation is desirable. Therefore, the functional groups (-OH, >C=C<, etc.) will come forward to stop the nucleation process. In this way, AgNPs will be formed.

Sol-gel is an excellent antibacterial agent carrier for textiles. It is simple and does not require high temperatures. Sol-gel comprises hydrolysis and condensation process. The acid hydrolysis is done by adding acid (such as citric acid or hydrochloric acid). It will take a long time. The required time was investigated at three different temperatures. At 60 °C, the acid hydrolysis time is about 4.50 hours; at room temperature (25 °C), it is 6.30 hours; and at 3 °C, it is 8 hours. But condensation will take a minuscule amount of alkaline presence. The condensation

is a comparatively faster reaction; it will take about 30 min. The AgNPs formation was conformed by the UV-vis spectrum. The peaks were between 416 to 430 nm, which is in the range of AgNPs peaks. For more confirmation, SEM and EDS were done. The SEM images illustrate 3 different shapes (spherical, irregular, and cubic) for various conditions. The EDS also identified the presence of Ag in the samples. To investigate the crystal system and lattice parameters of the AgNPs, XRDs were done. The XRD images revealed that the crystallinity of green synthesized AgNPs is 74%, and the average crystal size is about 6.6 nm. The irregularly shaped nanoparticle is mostly closed packed, having hkl values such as (111). On the other hand, the cubic shapes have mostly loose packs having hkl values similar to (110). Primarily orthorhombic and hexagonal crystal systems have been obtained for cubic and irregular shapes. On the other hand, XRD for sol-gel methods showed various hkl values with cubic crystal structure for only Tetraethyl orthosilicate (TEOS). However, adding AgNPs will cause more peaks related to silver with various crystal systems such as monoclinic, cubic, anorthic, etc. The more AgNPs added, the more silver peaks are obtained, according to the ratios of AgNPs in sol-gel. By analysing SEM images, it was understood that the size changes for various parameters. Smaller nanoparticles and cubic shapes are desirable for antibacterial properties. Size and shape were analyzed in detail. The AgNps size depends on multiple parameters. The Pearson correlation and mutual information show that AgNPs size is related to $AgNO_3$ morality, plant extract amount, silver volume, and pH of the fabric. The high amount of plant extract will cause an increased number of AgNPs. However, the low concentration of $AgNO_3$ along with the high amount of plant extract or vice versa will produce larger AgNPs. It is also evident that the plant extract to $AgNO_3$ morality (Plant Extract: $AgNO_3$) is the most influential in AgNPs size. To have an increase number of AgNPs with smaller size the Plant Extract: $AgNO_3$-molarity ratio should be below 20, and pH should be around 8. Besides, high $AgNO_3$ volume almost always produces smaller AgNPs. But the number of AgNPs may depend on other factors such as the pH of fabric, plant extract, etc. In general, pH will have a

proportional relation to the mean size of AgNPs and the number of AgNPs. Incorporation methods also affect AgNPs size. For example, the *padding* method produces smaller AgNPs, and the *in-situ* method makes the bigger AgNPs. But the *in-situ* method is the highest number of AgNPs producers. It is also observed that a simple water wash of the AgNPs incorporated dried sample will decrease the AgNPs size. On the contrary, the AgNPs shape is closely associated with crystallinity. The close-packed structure (111) tends to form irregular shapes, but the loosely packed (011) form square shapes. The loose-packed crystal will have more free energy than that of closed packed. Hence the loosely packed crystals will orient in a more regular way. Moreover, the slight alkalinity will produce some smaller nanoparticles attached to the regular AgNPs. For this reason, the cubic AgNPs are a little bit bigger than the spherical AgNPs. The fabric pH was found the most influential factor on different shapes. A pH less than 7 will cause spherical nanoparticles, but pH between 7.1- 7.8 will cause a cubic shape. The reason behind these shape changes is related to Gibbs free energy and surface free energy. Besides, the incorporation method also has a significant influence on cubic shape synthesis. If the fabric is bulky (high areal density), it will form a cubic shape in the *padding* method, whereas the *padding* method for a low areal density fabric will fail to form a cubic shape, because of the non-thermodynamic equilibrium conditions and squeezing out some NaOH by the pressure roller. The plant extract also influences shape. For example, the orange peel extract will always produce spherical AgNPs due to its acidic nature. The citric acid treatment also makes spherical AgNPs. Antibacterial tests are done according to the AATCC-100 standard with a slight modification in the untreated sample. *Staphylococcus aureus* and *Klebsiella pneumoniae* are used as Gram-positive and Gram-negative bacteria. The mutual information (MI) and Pearson correlation indicate that AgNPs size, $AgNO_3$ molarity, plant extract ratio, and pH of fabric are highly correlated to the antibacterial activity. A large mean size will have low antibacterial activity. Low $AgNO_3$ molarity will have suitable antibacterial properties due to well dispersion. Although plant extract works in combination with

$AgNO_3$ molarity, generally, it is proportional to the antibacterial activity. Fabrics without pretreatment will have the lowest antibacterial activity. Silver nitrate ($AgNO_3$) volume is also proportional to the antibacterial activity. Fabric type is also essential for antibacterial action. The plain fabric (low areal density and high interlacement) have high antibacterial property and low leaching. On the other hand, polypropylene nonwoven fabric will have low antibacterial properties. Besides, the high areal density and low interlaced fabric (such as 3/1 twill with 230 GSM) will have lower antibacterial efficiency than low GSM fabrics. Different incorporation methods were also compared and found that 2-times padding is the best for antibacterial activity. For wash fastness, fabric pretreatment is found to be the most influential. NaOH pretreated fabric and Span-80 pretreated fabric have more than 96% and 98% efficiency, respectively, even after 20 home washes. However, the simultaneous pretreatment with two or more chemicals will not work well since they will interact.

The AgNPs incorporated fabric lose antibacterial properties with time. However, they can again recover their antibacterial property once washed with detergent. Probably, it is caused due to the forming of non-antibacterial zero-valent AgNPs. The antibacterial activity of AgNPs depends on chemisorbed Ag^+, which interacts with the surrounding environment to form zero-valent AgNPs. It is termed as the "*time-effect"* of AgNPs. It was found a high amount of plant extract can minimize the time effect; a high volume of $AgNO_3$ also has a low *time-effect*. The padding and immersion method will have the highest *time-effect*. Because the ex-situ synthesized, AgNPs will have more chemisorbed Ag^+ than that of the *in-situ* method. More chemisorbed Ag^+ cause more zero-valent AgNPs, and hence *time-effect* will be more. Besides, high pH will have more *time-effect* and need more washing to recover antibacterial activity. However, the zero-valent AgNPs will convert back to the chemisorbed Ag^+ again while washing with detergent. This way, the AgNPs will redeem their antibacterial activity.

GENİŞLETİLMİŞ ÖZET

Antibakteriyel tekstil pazarı gün geçtikçe genişlemektedir. Piyasa talebindeki artış Covid-19 pandemisi ile büyük ölçüde hızlanmıştır. Pamuk eşsiz konforu nedeniyle lifler arasında en çok kullanılan hammaddelerden birisidir. Ancak pamuk lifi, mikroplar için ideal bir besin kaynağıdır. Bu nedenle mikroplar pamuk lifine kolayca saldırarak kötü kokuya, mukavemet kaybına, renk kaybına vb. neden olmaktadır. Bu çalışmanın amacı, antibakteriyel tekstiller için ucuz ve etkili bir üretim yolu bulmaktır. Antibakteriyel tekstiller için, QAC, Triklosan, PHMB, metal iyonları vb. gibi birden fazla ajan vardır. $AgNO_3$ (Gümüş nitrat), performans açısından çevreye ve insan sağlığına diğer antibakteriyel maddelere nispeten zararsız, mükemmel bir ajandır. $AgNO_3$'ten AgNP'leri sentezlemek için fiziksel, kimyasal yöntemler gibi birçok farklı metot bulunmaktadır. Fiziksel yöntemlerin yüksek maliyet, az miktarda üretim vb. gibi dezavantajları bulunmaktadır. Bunun yanında kimyasal yöntemlerde ayrı indirgeme ve yakalayıcı maddeleri gibi çevre dostu olmayan kimyasallar gerekebilmektedir. Yeşil sentezleme yöntemi diğer kimyasal metotlar arasında en çevre dostu olan, basit ve maliyeti düşük olan bir metottur. Bu yöntemde elde edilen biyolojik özüt, AgNP'leri aynı anda indirgeyebilmekte (reduction), kümeleştirebilmekte (neucleation) ve stabilize (stabilization) edebilmektedir. Bu çalışma, yeşil sentezlenmiş gümüş nanopartikülleri kullanarak çeşitli yöntemler ve kumaşları karşılaştırarak daha yüksek antibakteriyel etkisi için en iyi yöntemi ve kumaş türünü bulmayı amaçlamaktadır. Ayrıca antibakteriyel etkinlik açısından gümüş nitrat molaritesi ve hacmi, bitki özü miktarı, kumaş ön terbiyesi, AgNP'lerin dahil etme yöntemleri vb. parametrelerin araştırılması amaçlanmıştır. Yeşil sentezleme işlemi yaklaşık olarak her türlü biyolojik kaynakla yapılabilmektedir. Bu çalışmada yeşil sentezleme için Türkiye'de Aralık-Nisan ayları arasında yaygın olarak bulunan bir yabani ot olan ve literatürde bu işlemde kullanılmamış *Calendula arvensis* (Öküzgözü) bitkisi ve mandalina kabuğu özütü olan *Citrus reticulate* (Çukurova Üniversitesinden

toplanmıştır) seçilmiştir. Etkili bir AgNPs sentezi için bitki özütü miktarı çok önemlidir. Bu nedenle, in-situ ve ex-situ yöntemler için gerekli optimum bitki özü miktarını belirlemek için bir denklem formüle edilmiştir. Bu çalışmada dört tip kumaş kullanılmıştır: düz (1/1, gramaj 123), dimi (3/1, gramaj 230), örgü (düz, gramaj 154) ve dokusuz (gramaj 20). AgNP'ler sentezlendikten sonra kumaşlara kaplama, emdirme, püskürtme, daldırma (immersion), insitu vb. gibi farklı metodlarla aktarılmıştır. Önceki çalışmalarda belirtildiği üzere oda sıcaklığı yeşil sentez için yeterlidir. Ancak bu çalışmada, 40 °C'nin altında *C.arvensis* ekstraktından AgNP'lerin oluşmadığı ve 60 °C'nin yüksek stabilite için optimum sıcaklık değeri olduğu bulunmuştur. UV-vis'in Yüzey Plazmon Rezonansı (SPR) kullanılarak sıcaklığın etkisi araştırılmaya çalışılmıştır. Sıcaklığın nanopartikül boyutunu etkilediği görülmüştür (UV-vis SPR açısından). Ancak etkisi istatistiksel olarak önemsiz çıkmıştır. İstatistiksel test için burada Kruskal-Wallis testi (ANOVA eşittir parametrik olmayan test) kullanıldı. Daha fazla doğrulama için Dunn'in post hoc testi de yapıldı. Bu istatistiksel testlere göre anlamlı bir sonuç bulunamadı. $AgNO_3$ molaritesi gibi hacim molaritesinin diğer parametreler arasında AgNP boyutunda (UV-vis SPR'den) ve stabilitede en etkili faktör olduğu tespit edildi. Bu durumda $AgNO_3$ molaritesinin etkisi ANOVA testi ile istatistiksel olarak anlamlı bulundu. Hangi grubun anlamlı sonuç verdiğini belirlemek için Tukeys'in HSD testi yapılmıştır. Yalnızca $AgNO_3$ molaritesinin UV-vis'i önemli ölçüde etkileyebileceği tespit edilmiştir. Bitki özleri Ag^+ iyonuna elektron veren $NADPH_2$ ko-enzimlerine sahiptir ve bu şekilde Ag^+ den Ag^0'a dönüşmektedir. Ag^0 oluşumu çekirdeklenmeyi başlatacak olan serbest yüzey enerjisine **(**Surface Free Energy**)** neden olmaktadır. Ancak üniform boyut dağılımı için kısa bir birleştirme gerekmektedir. Birleştirme sürecini durdurmak için fonksiyonel gruplar (-OH, >C=C< vb.) devreye girmektedir.

Sol-jel, tekstiller için antibakteriyel ajan taşıyabilmesi, uygulamasının kolay oluşu ve düşük sıcaklıklarda çalışılabilmesi açısından avantajlı bir metottur. Sol-jel metodu hidroliz ve kondenzasyon şeklinde iki temel adımda gerçekleşmektedir. Hidroliz, sitrik asit veya hidroklorik asit eklenerek gerçekleştirilir. Deneysel

çalışmalarda üç farklı sıcaklıkta hidroliz süreleri ayrı ayrı tespit edilmiştir. Sonuçlara göre; asidik ortamda hidroliz süresinin 60°C'de 4.50 saat , oda sıcaklığında 6.50 saat olduğu ve 3°C sıcaklıkta 8 saat olduğu sonucuna varılmıştır. Yoğuşma (kondenzasyon) işlemi ise zayıf bazik ortamda gerçekleşmektedir. Kondenzasyon reaksiyonu bu şekilde daha hızlı ve yaklaşık 30 dakika sürmektedir. AgNPs oluşumu UV-vis spektrumu ile belirlenmiştir. AgNP'lerin pik aralığında olan 416 ila 430 nm arasında olduğu tespit edilmiştir. Kumaşlarda etkili antibakteriyel özellik sağlayabilmek için nanopartikül boyutlarının küçük ve kübik şekillerde olması gerekmektedir. Bundan dolayı boyut ve şekil ayrıntılı olarak çalışmada analiz edilmiştir. Ayrıntılı inceleyebilmek için SEM (Taramalı elektron mikroskobu) ve EDS analizleri yapılmıştır. SEM görüntüleriyle, üç farklı şekilde (küresel, düzensiz ve kübik) AgNPler elde edildiği görülmüştür. EDS sonuçlarına göre numunelerdeki Ag varlığı da tanımlanmıştır. AgNP'lerin kristal sistemini ve kafes parametrelerini araştırmak için ise XRD analizleri yapılmıştır. XRD görüntüleri yeşil sentezlenmiş AgNP'lerin kristalliğinin %74 olduğunu ve ortalama kristal boyutunun yaklaşık 6.6 nm olduğunu ortaya çıkarmıştır. Düzensiz şekilli nanopartikül çoğunlukla (111) gibi hkl değerlerine sahip kapalı paketlenir. Öte yandan, kübik şekiller çoğunlukla (110)'a benzer hkl değerlerine sahip gevşek pakete sahip olduğu tespit edilmiştir. Kübik ve düzensiz şekiller için öncelikli olarak ortorombik ve altıgen kristal sistemler elde edilmiştir. Ayrıca, sol-jel yöntemi uygulanan kumaşlara yapılan XRD analizleri, sadece Tetrat Etil Ortosilikat (TEOS) için kübik kristal yapılı ve çeşitli hkl değerleri göstermiştir. Ancak sol-jel yönteminde AgNP'lerin eklenmesinin, monoklinik, kübik, anortik vb. gibi çeşitli kristal sistemlerinin olduğu görülmüştür. Bu metotta AgNP'ler sol içine ne kadar fazla eklenirse, o kadar fazla gümüş piki elde edilmiştir. SEM görüntüleri analiz edilerek çeşitli parametreler için boyutların değiştiği sonucuna varılmıştır. AgNps boyutu birden çok parametreye bağlıdır. Pearson korelasyonu ve ortak bilgiye (Mutual Information) göre, AgNP'lerin boyutuyla, $AgNO_3$'ün molaritesiyle, bitki özü miktarıyla, gümüş hacmiyle ve kumaşın pH'ı ile ilişkili olduğunu göstermektedir. AgNP'lerin boyutu üzerindeki çeşitli faktörler

analiz edildiğinde, bitki özütü miktarı arttıkça, üretilen AgNP'ler miktarının arttığı ve $AgNO_3$ konsantrasyonu azaldıkça ve bitki özütü miktarı arttıkça AgNPs boyutlarının büyüdüğü gözlemlenmiştir. Aynı şekilde, yüksek miktarda bitki özütü ve düşük molarite daha büyük boyutta partikül oluşumuna neden olmuştur. Bitki ekstraktının $AgNO_3$ molaritesinde (bitki özütü: $AgNO_3$-molarite) AgNP'ler boyutunda en etkili parametre olduğu sonucuna varılmıştır. Küçük boyutta AgNP'lerin elde edilmesi için bitki özütü: $AgNO_3$-molaritesinin 20'nin altında ve ortamın pH seviyesinin 8 civarında olması gerektiği belirlenmiştir. $AgNO_3$ molaritesinin, AgNP'lerin boyutuyla ilişkisinin az olduğu, buna karşılık yüksek hacimdeki $AgNO_3$ ile daha küçük boyutta AgNP'lerin üretildiği gözlemlenmiştir. Çalışmada AgNP sentez yöntemleri de karşılaştırılmıştır. Emdirme yönteminde in-situ yöntemine göre daha küçük boyutta AgNP'ler üretilmiştir. Ancak in-situ yönteminde üretilen AgNP miktarı daha fazladır. AgNP'lerin dahil olduğu kuru numunenin basit bir su ile yıkanmasının AgNP'lerin boyutunu azaltacağını da gözlemlenmiştir. AgNP'lerin şekli, kristallik ile yakından ilişkilidir. Gevşek bir şekilde paketlenmiş kristal, kapalı paketlenmiş kristalden daha fazla serbest enerjiye sahip olmaktadır. Bu nedenle, gevşek bir şekilde paketlenmiş kristaller daha düzenli bir şekilde yönlendirilmektedir. Ayrıca, az miktarda alkali, küçük bir nanoparçacık üretmektedir ve ardından ana AgNP'lerle birleşmektedir. Bu nedenle, kübik AgNP'ler küresel AgNP'lerden biraz daha büyüktür. Küresel, düzensiz ve kübik olmak üzere üç çeşit nanopartiküller elde edilmiştir. Farklı şekillerin nedeni de araştırılmış ve kumaş pH'ının en etkili faktör olduğunu bulundu. pH seviyesi asidik ise üretilen gümüş nanoparçacıklar küre şeklinde oluşmaktadır. pH 7,1 - 7,8 seviyeleri arasına geldiğinde parçacıklar kübik şeklinde meydana gelmektedir. Bu şekil değişikliklerinin nedeni Gibbs serbest enerjisi ve yüzey serbest enerjisi ile ilgilidir. Gibbs serbest enerjisi, Ag^0 atomlarını gevşek paketlenmiş (110) ortorombik kristal sistemine yönlendirmektedir. Yine gevşek paket kristali, onları kübik bir şekilde yönlendirerek daha fazla yüzey serbest enerjisine sahip olmaktadır. Aksine yüksek pH seviyesi yüksek miktarda Gibbs içermeyen enerjiye neden olmaktadır.

Bu nedenle kapalı paketlenmiş (111) altıgen (hexagonal) kristaller meydana gelmektedir. Kristaller, onları düzensiz şekle götüren düşük yüzey serbest enerjisine sahip olmaktadır. Bunların yanında kumaşa aktarma yöntemlerinin de kübik şekil sentezi üzerinde önemli bir etkisi bulunmaktadır. Kumaşın gramaj değeri yüksekse, emdirme yönteminde kübik bir şekil oluşturduğu, düşük gramaj kumaş için emdirme yöntemi uygulandığında ise kübik bir şekil meydana gelmediği görülmüştür. Bunun nedeni, silindirlerin basıncı yüksek gramajli kumaştan biraz fazla NaOH çıkarmasıdır. Basınç silindiri ayrıca yüksek gramajli dokusunda basınçla meydana gelen mekanik dengedeki bir değişiklik nedeniyle daha fazla termodinamik dengesizlik yaratmıştır. Deneysel çalışmada bitki özütü yapısının ve miktarının da partikül şeklini etkilediği tespit edilmiştir. Örneğin mandalina kabuğu özü, asidik yapısı nedeniyle her zaman küresel AgNP'ler üretecektir. İşlemlerde sitrik asit kullanımının küresel biçimde AgNP'lerin üretimine neden olduğu görülmüştür. Çalışmada antibakteriyel testler, işlenmemiş numunelere küçük bir değişiklikle AATCC-100 standardına göre yapılmaktadır. Bu testlerde *Staphylococcus aureus* ve *Klebsiella pneumonia* bakterileri kullanılmaktadır. Çalışmada istatiksel analiz olarak uygulanan karşılıklı bilgi ve Pearson korelasyonlarına göre; AgNPs boyutunun, $AgNO_3$ molaritesinin, bitki ekstrakt oranının ve kumaş pH'ının antibakteriyel aktivite ile yüksek oranda ilişkili olduğu ortaya koyulmuştur. Parçacıkların büyük boyuta sahip olması, düşük antibakteriyel aktiviteye sebep olmaktadır. Düşük $AgNO_3$ molaritesinin iyi dağılma nedeniyle uygun antibakteriyel özelliklere sahip olduğu, bitki özütünün ve $AgNO_3$ molaritesi kombinasyonunun genel olarak antibakteriyel aktivite ile orantılı olduğu sonucuna varılmıştır. Nötr civarındaki kumaş pH seviyesi işlem görmemiş kumaşlar nedeniyle en düşük antibakteriyel özelliğe sahip olmuştur. Gümüş nitrat hacmi de antibakteriyel aktivite ile doğru orantılıdır. Kumaş türünün de antibakteriyel özellik kazandırma açısından önemli olduğu görülmüştür. Düz kumaşın (düşük gramaj ve yüksek bağlantı sayısına sahip) yüksek antibakteriyel özelliğinin ve düşük sızıntıya sahiptir. Öte yandan, polipropilen dokunmamış kumaş düşük antibakteriyel özelliklere sahip çıkmıştır.

Ayrıca, yüksek gramajli ve düşük geçmeli kumaşın (230 gramaj ve 3/1 dimi gibi) düşük antibakteriyel etkinliğe sahip olduğu görülmüştür. Kumaşlara gümüş nanoparçacıkları uygulama metodları karşılaştırıldığında - 2-kat-emdirme yönteminin kumaşlara antibakteriyel aktivite kazandırma açısından en iyisi olduğu tespit edilmiştir. Kumaşlara kazandırılan antibakteriyel özelliklerin yıkamaya karşı kalıcılığının sağlanabilmesi için kumaş ön terbiyesinin gerekli olduğu görülmüştür. NaOH (Sodyum Hidroksit) ön işlem görmüş kumaşın ve Span-80 ön işlem görmüş kumaşın 20 defa evsel yıkamadan sonra bile sırasıyla %96 ve %98'den fazla verimliliğe sahip olduğu tespit edilmiştir. Bununla birlikte, kumaşlara iki veya daha fazla kimyasal ile eş zamanlı ön işlem uygulandığında, etkileşime girdikleri için antibakteriyel özellik kazandırılamamıştır.

AgNP'lerin zamanla antibakteriyel özelliklerini kaybettiği tespit edilmiştir. Ancak deterjanla yıkandıklarında antibakteriyel özelliklerini tekrar kazandıkları görülmüştür. Antibakteriyel aktivitenin olmaması sıfır değerli AgNP'lerin oluşumundan kaynaklanmaktadır. AgNP'lerin antibakteriyel aktivitesi, çevreyle etkileşime giren kimyasal olarak emilmiş Ag^{+}'ya bağlıdır. Çalışmada bu durum AgNP'lerin *"zaman-etkisi"* olarak adlandırılmıştır. Yüksek miktarda bitki özünün zaman etkisini en aza indirebileceği tespit edilmiştir; yüksek hacimli $AgNO_3$ ise düşük zaman etkisine (*low time-effect*) sahiptir, yani zamanla düşük sayıda bakteri üremesine yol açmaktadır. Emdirme ve daldırma yöntemi en yüksek zaman etkisine sahip olduğu tespit edilmiş, ancak her ikisinin de yıkamadan sonra %100 geri kazanıma sahip olduğu görülmüştür. Çünkü *ex-situ* yönteme sentezlenen AgNP'ler, *in-situ* yönteme göre kimyasal olarak daha fazla absorbe edilmiş Ag^{+}'ya sahip olmaktadır. Daha fazla kimyasal absorbe edilmiş Ag^{+}, daha fazla sıfır değerli AgNP'ler ve dolayısıyla daha fazla *zaman-etkisi* (time-effect) anlamına gelmektedir. Ayrıca, yüksek pH seviye daha fazla 'zaman-etkisine' sahip olacak ve antibakteriyel aktiviteyi geri kazanmak için daha fazla yıkamaya ihtiyaç duyacaktır. Bununla birlikte, sıfır değerli AgNP'ler (zero-valent AgNPs) kimyasal olarak emilmiş Ag^{+}'ya geri dönecektir. Bu şekilde antibakteriyel aktivitelerini kullanacaklardır.

ACKNOWLEDGEMENT

Throughout the writing of this dissertation I have received a great deal of support and assistance from different persons and organization.

I would first like to thank my supervisor, Prof. Dr. R. Tuğrul OĞULATA, whose expertise was invaluable in formulating the research questions and methodology. His insightful feedback pushed me to sharpen my thinking and brought my work to a higher level.

I would like to acknowledge my gratitude and thanks to Prof. Dr. OSMAN GÜLNAZ, for his unprecedented and patient support for UV-vis spectroscopy and antibacterial tests to further my research.

I would like to thank Dr. Sabiha SEZGİN BOZOK, who helped me a lot through the whole research work-from materials purchasing to thesis writing. Additionally I am grateful to Ms Sevgi Erdoğan for her help related to antibacterial tests. Besides, I am also thankful to Prof. Dr. Ahmet TEKE and Doç. Dr. Serin MEZARCIÖZ for their kind support in my research progress. I am thankful to Muhittin ÖZKAN for his research support and ideas. Aditionally, I am expressing my gratidute to Dr. Halil İbrahim İÇOĞLU and Dr. Pınar PARLAKYİĞİT for their review and feedbacks.

I would like to express my gratitude and thanks to the Turkish government for the scholarship which cover my academic and living expenditure in Turkey. I would like to acknowledge my gratitude to the Scientific Research Project of Çukurova University (BAP), Project No: FDK-2021-13527, for its financial support for my research.

I am garetul to my friend Mr. İbrahim Korkmaz for his kind support in research materials. I am also thankful to my colleagues Md.Sultan Mahmud and Md. Mahabubur Rahman for their support and ideas.

CONTENTS **PAGE**

ABSTRACT I
ÖZ II
EXTENDED SUMMARY III
GENİŞLETİLMİŞ ÖZET IX
ACKNOWLEDGEMENT XV
CONTENTS …… XVI
INDEX OF TABLES…….. XXII
INDEX OF FIGURE…… XXIV
SYMBOLS AND ABBREVIATIONS XXVIII
1. INTRODUCTION 1
1.1. Fabrics types 2
1.2. Fabrics for antibacterial textiles 3
1.3. Bacterial cell 4
1.3.1. Size of bacteria 5
1.3.2. Types of bacteria 6
1.3.2.1. Gram-negative bacteria 6
1.3.2.2. Gram-positive bacteria 6
1.4. Antibacterial Textiles in Health Sector 7
1.5. Various antibacterial agents 8
1.6. Problems of commercial antibacterial agents 8
1.7. Silver: a low toxic antibacterial agent 9
1.7.1. Toxicity of silver on animal 9
1.7.2. Toxicity of silver on ecosystem 10
1.8. Synthesis of AgNPs 10
1.9. The best method for AgNPs synthesis 12

1.9.1. Drawbacks of physical and chemicals methods 13
1.9.2. Advantages of Green synthesis 13
1.9.3. Biological source for Green synthesis 14
1.9.3.1. *Calendula arvensis* 15
1.9.3.2. Mandarin orange (*Citrus reticulata*) 17
1.10. Incorporation Methods 17
2. LITERATURE REVIEW 21
2.1. Fabric structure on antibacterial activity 21
2.2. Antibacterial textiles 21
2.3. Green synthesis for antibacterial textiles 22
2.3.1. Effect of pH on green synthesis of silver 23
2.3.2. Effect of temperature on green synthesis 24
2.3.3. $AgNO_3$ molarity on green synthesis 24
2.4. Sol-gel Method 25
2.5. Nanoparticle size and shape 26
3. MATERIALS AND METHODS 29
3.1. Required Materials 29
3.2. Plant Extraction Preparation 29
3.2.1. *C.arvensis* (Field marigold) plant Extract 29
3.2.2. FTIR of *C.arvensis* plant extract 29
3.2.3. *C.raticulata* Peel Extract 30
3.3. Green Synthesis 30
3.3.1. Temperature for green synthesis 31
3.3.1.1. Different amounts of plant extract 31
3.3.1.2. UV-vis Spectroscopy 33
3.3.2. Fabric pretreatment 34
3.4. Formulating the amount of plant extract 34
3.4.1. For the Immersion method 35
3.4.2. For the in-situ method: 36

3.5. AgNPs incorporation methods 37
3.5.1. Padding 37
3.5.2. Immersion 37
3.5.3. In-situ 37
3.5.4. Immersion (in-situ) 37
3.5.5. Two-times-padding 38
3.5.6. In-situ-pad 38
3.5.7. Sol-gel 38
3.5.7.1. Sol-gel Preparation 38
3.5.7.2. Applied on textiles 38
3.5.7.2.(1). Method -1 (In-situ- sol-gel) 39
3.5.7.2.(2). Method-2 (Dip coating) 39
3.5.7.2.(3). Method-3 (In-situ AgNPs) 40
3.5.7.2.(4). Method-4 (Spray) 40
3.5.7.2.(5). Method-5 (insitu-1:1) 41
3.5.7.2.(6). Method-6 (immersion 2:1) 41
3.5.7.2.(7). Method-7 (immersion 1:1) 41
3.6. Characterization 41
3.6.1. XRD 41
3.6.2. SEM and EDS 42
3.7. Antibacterial Test 42
3.8. Wash fastness 42
3.9. Fabric's pH test 43
3.10. Data Analysis and visualization 43
3.10.1. Data Correlation 43
3.10.2. Mutual information 44
4. RESULT AND DISCUSSION 45
4.1. Influence of Temperature on UV-Vis SPR of AgNPs 45
4.1.1. Data distribution for effect on temperature 46

4.1.1.1. Shapiro-Wilks test of Normality 47
4.1.1.2. Bartlett's Homogeneity test 48
4.1.1.3. Dunn’s post hoc Test 48
4.2. Different concentration of $AgNO_3$ on AgNPs formation 49
4.3. The different volumes of $AgNO_3$ on AgNPs formation 50
4.3.1. Data distribution 52
4.3.1.1. Shapiro-Wilks test of Normality 53
4.3.1.2. Levene’s and Bartlett’s Test for homogeneity 53
4.3.2. ANOVA 54
4.3.3. TUKEY’S HSD test 54
4.4. Amount of Plant Extracts on AgNps formation: 56
4.5. Green Synthesis Mechanism 57
4.6. Sol-gel Mechanism 60
4.6.1. Influence of pH 60
4.6.2. Influence of acid hydrolysis time 62
4.6.3. Influence of temperature on gelation 64
4.7. XRD of Green synthesized AgNPs 65
4.8. XRD of AgNPs incorporated with Sol-gel method 67
4.9. SEM-image of Green Synthesized AgNPs 69
4.10. EDS of AgNPs 74
4.11. AgNPs number, shape and size of different samples 76
4.11.1. Pearson Correlation of AgNPs synthesis 80
4.11.2. Mutual information 81
4.11.3. Plant Extract on AgNPs size 81
4.11.4. Influence of $AgNO_3$ Molarity 83
4.11.5. Influence of $AgNO_3$ Volume 84
4.11.6. Fabric pH on AgNPs size and number 84
4.11.7. Different methods on AgNps size and number 85
4.11.8. Different methods on AgNPs amounts 87

4.12. Comparison of square and spherical AgNPs:.....88
4.13. Mechanism of shape.....88
4.13.1. Growth.....88
4.13.2. Crystallinity.....89
4.14. Various parameters on AgNPs shape.....90
4.14.1. The pH of fabric:.....90
4.14.2. Incorporation methods.....91
4.14.3. Plant Extract on the shape.....91
4.15. Antibacterial Performance.....94
4.15.1. Antibacterial Mechanism.....95
4.15.2. Adhesion to the microbes.....95
4.15.2.1. Electrostatic interaction.....95
4.15.2.2. Acid-basic theory.....96
4.15.3. Pit formation and penetration.....96
4.15.4. Inside the cell.....96
4.15.5. Cytotoxicity.....96
4.15.6. Free radical generation.....97
4.16. Correlating factors of antibacterial performance.....98
4.16.1. AgNPs mean size on antibacterial activity.....100
4.16.2. $AgNO_3$ Molarity on Antibacterial performance:.....101
4.16.3. Plant extract amount on antibacterial performance.....101
4.16.4. Influence of pH.....103
4.16.5. Influence of $AgNO_3$ Volume on antibacterial activity.....104
4.16.6. Different fabrics on antibacterial performance.....105
4.16.7. Different methods of antibacterial performance.....107
4.16.8. Wash fastness.....109
4.16.9. Importance of fabric pre-treatment.....111
4.17. An interesting phenomenon of AgNPs treated cloth and time.....112
4.17.1. Plant extract on time effect.....114

4.17.2. $AgNO_3$ Volume on time effect 115
4.17.3. Various methods on time effect 116
4.17.4. Fabric pH on time effect 118
5. CONCLUSION AND RECOMMENDATIONS 119
5.1. Conclusion 119
5.2. Recommendations 120
REFERENCES 123
CURRICULUM VITAE 149

INDEX OF TABLES **PAGE**

Table 1.1 Various antibacterial agents 8
Table 1.2 Various methods for silver nanoparticle synthesis 12
Table 1.3 Different nanoparticle loading methods 18
Table 3.1. Different amount of plant extract at room temperature 31
Table 3.2. Effect of temperature on AgNPs (0.1M) formation and stability 32
Table 4.1. Effect of temperature on AgNPs UV-SPR and absorption 45
Table 4.2. Shapiro-Wilks Normality test 47
Table 4.3. Bartlett's Homogeneity test 48
Table 4.4. Kruskal-Wallis test 48
Table 4.5. Dunn's post hoc test 49
Table 4.6. Different concentration of silver nitrate on UV-vis spectrum 49
Table 4.7. $AgNO_3$ volume on UV spectrum and stability 51
Table 4.8. Shapiro-Wilks normality test for $AgNO_3$ Molarity 53
Table 4.9. Tests for homogeneity of $AgNO_3$ molarity on UV-vis 54
Table 4.10. ANOVA table for different variable 54
Table 4.11. TUKEY's HSD test 55
Table 4.12. Effect of different plant extract on AgNPs 56
Table 4.13. Influence of time on esterification and sol-gel formation 63
Table 4.14. Temperature has effect on sol-gel formation of hydrolyzed solution .. 64
Table 4.15. XRD parameters for C.arvensis synthesized AgNPs 66
Table 4.16. Various factors on AgNPs size 78
Table 4.17. Effect of Methods with constant molarity, volume 86
Table 4.18. Square or cubic shaped AgNPs formation 93
Table 4.19. Main factors of antibacterial activity 94
Table 4.20. Influence of plant extract on antibacterial performance 103
Table 4.21. $AgNO_3$ volume on antibacterial activity (only the worst 10 rows) ... 105

Table 4.22. The 2-times-padding against other methods for wash fastness..... 109
Table 4.23. Antibacterial activity and wash fastness of different samples 110
Table 4.24. Antibacterial activity of fabric having no pretreatment 111
Table 4.25. Effect of different pretreatment on Antibacterial wash fastness..... 112
Table 4.26. Time effect on various samples 113

INDEX OF FIGURES **PAGE**

Figure 1.1 Different types of fabrics 3
Figure 1.2 Bacterial, animal and plant cell comparison 5
Figure 1.3 Relative sizes of different microscopic objects 6
Figure 1.4 Gram positive and gram negative bacteria 7
Figure 1.5 Top-down and bottom-up 11
Figure 1.6 Different physical and chemical methods of AgNPs synthesis 11
Figure 1.7 C.arvensis flower 15
Figure 1.8 Geographical distribution of Calendula genus 16
Figure 1.9 Taxonomy of C.arvensis plant 17
Figure 3.1. FTIR of C.arvensis plant extract 30
Figure 3.2. The temperature of AgNPs stability and reaction time 32
Figure 3.3. UV-vis spectrum for AgNPs 33
Figure 3.4. Different peak positions 34
Figure 3.5 Process flow of method-2 (dip-coating) 40
Figure 4.1. Temperature on AgNPs formation and UV spectrum 46
Figure 4.2 Q-Q plot of UV- spectrum for different $AgNO_3$ temperature 47
Figure 4.3 UV spectrum of $AgNO_3$ having various molarity 50
Figure 4.4 $AgNO_3$ volume on AgNPs 52
Figure 4.5. Q-Q plot of UV on the influence of $AgNO_3$ Molarity and Volume 53
Figure 4.6. $AgNO_3$ molarity on AgNPs stability 55
Figure 4.7. Plant Extract on UV spectrum 57
Figure 4.8. Green synthesis mechanism 59
Figure 4.9. Green synthesis mechanism (in-situ method) 60
Figure 4.10. Acid hydrolysis of TEOS 61
Figure 4.11. Condensation after acid hydrolysis 62
Figure 4.12. Time required for gel and colloidal gel 64
Figure 4.13. XRD of spherical shaped AgNPs 66

Figure 4.14. XRD of squared shaped AgNPs 66
Figure 4.15. XRD of only sol-gel, sol:AgNPs= 1:2, and sol:AgNPs = 1:1 67
Figure 4.16. XRD of only sol-gel 67
Figure 4.17. XRD of sol:AgNPs = 1:2 67
Figure 4.18. XRD of sol:AgNPs = 1:1 67
Figure 4.19. in-9mM-0.10-p 69
Figure 4.20. imn-2mM-.04-p 69
Figure 4.21. imn-2mM-.03-p 69
Figure 4.22. in-2mM-.04-k 69
Figure 4.23. in-2mM-.04-p 69
Figure 4.24. im-2mM-.04-p 69
Figure 4.25. in-2mM-.04-t 70
Figure 4.26. imn-2mM-.04-wk 70
Figure 4.27. pad-2mM-.04-x4 70
Figure 4.28. pad-2mM-.04-x8 70
Figure 4.29. in-2mM-2.6-F3 70
Figure 4.30. in-1mM-.52-or-t 70
Figure 4.31. in-2mM-2.6-nw-sc 71
Figure 4.32. ip-1mM-2.6-nw-r 71
Figure 4.33. in-2mM-2.6-F1 71
Figure 4.34. p2x-1mM-.03-F2 71
Figure 4.35. p2x-1mM-.03-F3 71
Figure 4.36. im-1mM-.04-F4 71
Figure 4.37. p2x-1mM-.03-F5 72
Figure 4.38. p2x-2mM-.04-wk 72
Figure 4.39. p2x-1mM-.03-F7 72
Figure 4.40. in-1mM-1.04-t 72
Figure 4.41. in-.05M-2.6-tm 72
Figure 4.42. ip-1mM-2.6-k-r 72

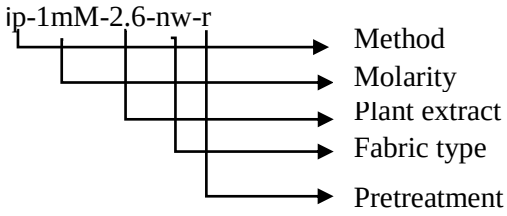
Figure 4.43. ip-1mM-2.6-sk 73
Figure 4.44. in-2mM-.03-or-t 73
Figure 4.45. pad-2mM-.04-wash 73
Figure 4.46. im-2mM-.03-or-rt 73
Figure 4.47. p2x-2mM-2.6-F6 73
Figure 4.48. in-2mM-2.6-F1-d 73
Figure 4.49. in-0.1M-0.1-t 74
Figure 4.50. EDS of green synthesized AgNPs 75
Figure 4.51. Sol-gel (Sol: AgNPs = 1:2) 75
Figure 4.52. Sol-gel (Sol: AgNPs = 1:1) 76
Figure 4.53. Overall information about synthesized AgNPs 77
Figure 4.54. Pearson correlation of different factors related to AgNPs number 80
Figure 4.55. Mutual informations 81
Figure 4.56. Plant Extract on AgNPs size and AgNPs number 82
Figure 4.57. $AgNO_3$ molarity, AgNPs number and AgNPs mean size relation 83
Figure 4.58. $AgNO_3$ volume on AgNPs size 84
Figure 4.59. pH of fabric on AgNPs mean size and number 85
Figure 4.60. Effect of methods 87
Figure 4.61. Distribution of AgNPs spherical and square shapes 88
Figure 4.62. Antimicrobial action of AgNPs 97
Figure 4.63. AgNPs size and antibacterial performance 99
Figure 4.64. Mutual Information for antibacterial activity 99
Figure 4.65. AgNPs mean size (nm) vs. number of survival bacteria 100
Figure 4.66. Influence of $AgNO_3$ molarity on antibacterial property 101
Figure 4.67. Influence of Plant extract on antibacterial activity 102
Figure 4.68. Influence of pH on antibacterial 104
Figure 4.69. Influence of $AgNO_3$ volume on antibacterial activity 105
Figure 4.70. Influence of fabric types on antibacterial performance 106
Figure 4.71. Comparison of different AgNPs incorporation methods 108

Figure 4.72. Antibacterial and wash fastness 109
Figure 4.73. Influence of plant extract on time effect 114
Figure 4.74. $AgNO_3$ volume on time effect 115
Figure 4.75. Different AgNPs incorporation methods on time effect 117
Figure 4.76. pH on time effect on AgNPs loaded fabrics 118

SYMBOLS AND ABBREVIATIONS

µl	: microliter
1 drop	: 1/26 milliliter = 38.46 microliter
$AgNO_3$	: silver nitrate
$AgNO_3$_M	: Silver Nitrate Molarity
$AgNO_3$_M	: Molarity of $AgNO_3$
$AgNO_3$_Vol	: Volume of $AgNO_3$
AgNPs	: silver nanoparticles
ANOVA	: Analysis of Variance
CA	: Citric acid
df	: degree of freedom
F	: F-statistics
M	: Molarity
min	: minute
NaOH	: Sodium Hydroxide
NI	: Non-ionic Surfactant
PE	: Plant Extract
S-80	: Span -80
sec	: second
SS	: sum of Square
TEOS	: Tetra Ethyl Ortho-Silicate
TUKEY's HSD	: TUKEY's Honestly Significant Difference Test
UV-vis	: Ultraviolet–visible spectroscopy
V	: Volume
WPU	: wet pick up
SPR	: Surface Plasmon Resonance
QAC	: Quaternary Ammonium Compound

Sample numbering



imm : immersion

imn : inmersiont (in-situ)

in : insitu

ip : insitu-pad

k : knit

NI : Non-ionic surfactant (Span-80)

nw : non-woven

or : orange extract

p : plain

p2x : 2-times-pad

r : no-pretreatment

sc : scoured

t : twill

1. INTRODUCTION

Antimicrobial textiles have an expanding market share in today's world. But there is a conspicuous lack of research in this field, especially correlating textile parameters to antimicrobial performance. Therefore, this study aimed to- synthesize silver nanoparticles using plant extracts, their incorporation in textiles in different methods, various correlated parameters of AgNPs (such as mean size, shape, amount, etc.), and fabrics (such as structure, GSM, etc.) to antibacterial efficiency as well as wash fastness.

The purpose of antimicrobial textiles is to prevent the spreading of various diseases by inhibiting the growth of bacteria, viruses, and other noxious microbes. Due to the advent of a different pandemic, it is getting more popular day by day. Especially different types of epidemics and pandemics, especially the Covid-19 pandemic, accelerated the market demand. Previously antimicrobial textiles were only related to the medical sector. But now it is used by people from all walks of life. Besides microbial protection, it also prevents unpleasant odor, fabric discoloration, strength loss, etc., created by human sweat. Various natural and chemical agents are used for antimicrobial textiles, such as metal nanoparticles, phenol, polybiguanides, chitosan, plant-based chemicals, and others. But the chemical agents are harmful to human health and the environment. Some are toxic and forbidden by different health organizations (such as triclosan). So, considering all side effects and high antimicrobial activity AgNPs were chosen. Because AgNPs is the least harmful but highly active ingredients. However, making AgNPs from $AgNO_3$ needs some additional chemicals. Which again may cause some environmental effects. But, the green synthesis can synthesize AgNPs from $AgNO_3$ using simple organic extract (such as plants, bacterial, or fungal extract). This process is super simple, eco-friendly, and cost-effective. Later, the antimicrobial agents can be incorporated into textiles by various methods such as pad-dry-cure, immersion, in-situ, laser ablation, chemical vapor disposition, physical vapor disposition, etc. However, in the scope

of the present work, pad-dry-cure, in-situ, immersion, and sol-gel methods were investigated.

Antibacterial treatment may be applied to regular clothes to protect them from unwanted odor, color staining, or strength loss. Especially the sports wears are ideal candidate here. As well as medical clothing, hygienic products such as masks, gloves, etc., a high wash fastness antimicrobial agents incorporation can open the horizon of reusable medical and hygienic clothing instead of disposable ones, which will save the world from huge wastage of textiles and also money.

The covid-19 pandemic placed the antibacterial textile market in a strong position in world market share. The antibacterial market had more than 10.48 billion USD in 2019, having a CAGR (Compound annual growth rate) of 9.8% from 2020 to 2026. Hence it is predicted to have a 20.50 billion USD. The application areas of antibacterial textiles extend to multiple fields, including the health sector, weather applications including personal protective equipment (PPE), home textiles, sportswear, intimate clothing, and so on (Monica Periolatto, 2017).

1.1. Fabrics types

Basically the fabrics are classified into three groups of fabrics are there according to manufacturing process. They are weaving, knitting and non-woven.
Weaving: in weaving two sets of yarns are used: warp and weft yarn. The interlacement of warp and weft yarn will produce woven fabrics. Based on this interlacement the woven fabrics are further classified into three groups: plain, twill, satin.

Knitting: knitting is transforming a continuous strand of yarn into series of loops and interlocking them. The knit fabrics basically two kinds: warp knit and weft knit. The weft knitted items are widely used as clothing. The weft knitting items are divided into four groups based on structure: plain, rib, interlock and purl.

Non-woven: The non-woven fabrics are made from fibers directly through a fibrous film. Non-woven items are widely used healthcare sectors and disposable clothing. Figure 1.1 depicts the major three types of fabrics.

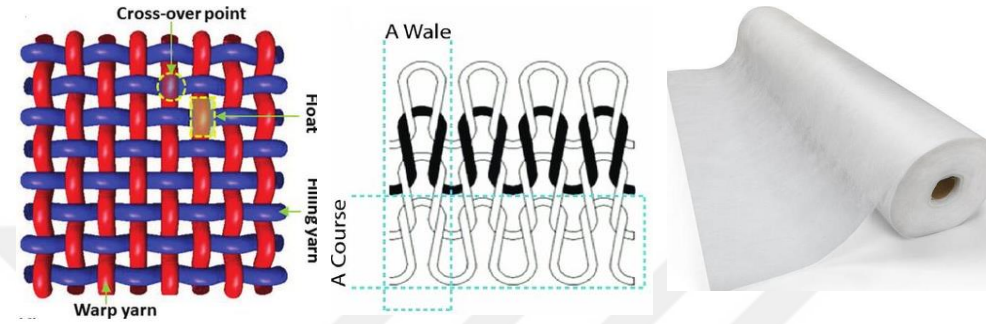


Figure 1.1 Different types of fabrics (Agcayazi et al. 2018)

1.2. Fabrics for antibacterial textiles

For antibacterial textiles, synthetic fibers are typically used, as the synthetic fibers are cheap and resistant to microbial growth. On the contrary, natural fibers are a great nutrient source for microbes due to their hydrophilic nature (S.-H. Lim and Hudson 2004)(Cappitelli and Sorlini 2008). But regarding comfort, natural fibers are unparalleled to any others.

Cotton is the most versatile textile fiber still now. The average cotton consumption is about 20 million tons out of 45 million textile fibers (Moses and Venkataraman 2016). Three types of fabrics are available, woven, knit, and nonwoven. Most antimicrobial textiles are non-woven, primarily used in the medical sector. But nowadays, antimicrobial fabrics can be used in sportswear, personal clothing, protective clothing, etc.; antimicrobial garments are useful for the base layer (close to the skin) that prevents skin infections. It also prevents the transfer of microbes from one person to another, which is essential, especially for sharing communal items like protective athletic equipment.

Nevertheless, the cotton gowns fail to meet the required standards (EN 13795 standards for surgical clothing and drapes) due to the absence of antimicrobial protection. However, surprisingly it is still primarily favored in hospitals due to its unparalleled comfort (Türler et al., 2000). Therefore, AgNPs incorporated in cotton fabric might be an excellent approach to simultaneously achieving both comfort and antimicrobial protection.

1.3. Bacterial cell

The bacteria, singular bacterium, is a microscopic organism abandouly found in everywhere of the planet. It lacks some essential cell components such as membrane-bound nucleus and hence are placed in prokaryotes. Bacterial cells are distinct from animal and plant cells in a number of ways. The absence of internal organelles such as mitochondria, chloroplasts, and a nucleus, which are present in both animal and plant cells, is one of the most significant differences (Kara and Robert J 2022). Figure 1.2 shows the differnces of animal, plant and bacterial cells

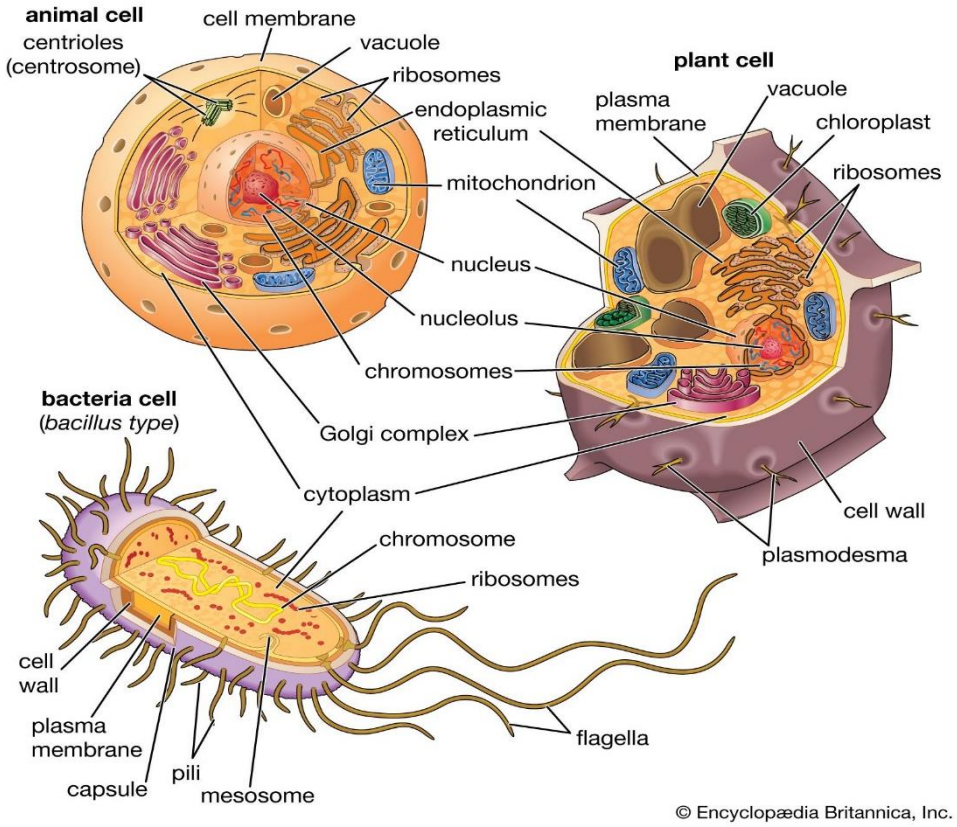


Figure 1.2 Bacterial, animal and plant cell comparison (Encyclopaedia Britanica)

1.3.1. Size of bacteria

Bacteria are single cell microbes. This implies that each bacteria consists of only one cell. This is in contrast to humans, who have billions of cells in their bodies.Bacterial cells are a fraction of the size of human cells. Bacterial cells can range in length from 1 to 10 meters. The majority of them are only 1 to 2 meters in diameter. A micrometre, or one millionth of a millimetre, is 1000 times smaller than a millimetre. That is really small! It's a fraction of the size of a human red blood cell, which is roughly 7 m in diameter on average (Introduction to Bacteria 2022) . Figure 1.3 shows the relative size of some microbial objects.

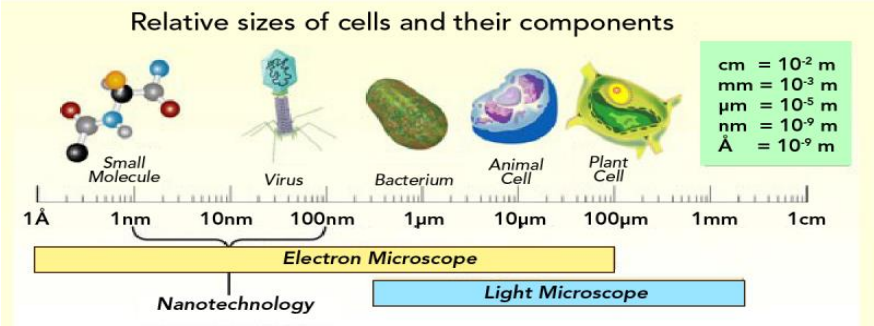


Figure 1.3 Relative sizes of different microscopic objects

1.3.2. Types of bacteria

There are 2 types of bacteria: 1) Gram-positive and 2) Gram-negative. The comparison has been illustrated in figure 1.4.

1.3.2.1. Gram-negative bacteria

Gram-negative bacterial extracellular vesicles harbor LPS, proteins, lipids, genetic materials, and other virulence factors. In the following subsections, we will present the current under- standing

a) **Proteins**: so far 3500 vesicular proteins of gram-negative bacteria have been identified.
b) **Lipids**: it is an important component of Gram- negative bacteria extra cellular vesicles.
c) **DNA & RNAs:** gram negative bacteria contain both luminal and surface-associated DNAs. The presence of RNAs in extracellular vesicles was also reported.

1.3.2.2. Gram-positive bacteria

The gram-positive bacteria has the following components:

a) Cytoplasmic lipid membrane

b) Thick layer of peptidoglycan

c) It contains Teichoic acids and lipoids those serve as chelating agents.

d) Smaller volume of periplasm (lied between 2 cytoplasm) in comparison of gram-negative bacteria (Miller and Salama 2018).

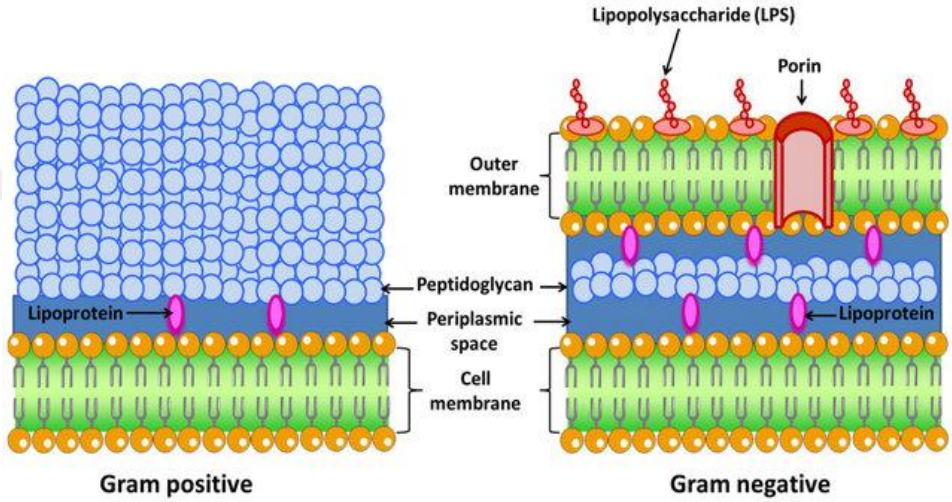


Figure 1.4 Gram positive and gram negative bacteria (Jiménez-Jiménez, Moreno, and Vallet-Regí 2022)

1.4. Antibacterial Textiles in Health Sector

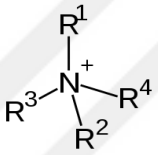
People working in health care are in danger because of healthcare-associated infections (HAI) (Kiran Pulidindi 2020). Healthcare workers are at high risk of contamination as they directly contact infected people. Moreover, inside the hospitals, used HVAC (heating, ventilation, and air conditioning) systems prone to high microorganism retention capacity pose various health hazards like asthma, allergies, etc. (Möritz et al. 2001). During the Covid-19 pandemic, it was experienced that the confined air or environment in different meeting places, even the public transport, has converted into a hot spot for viral extents. For these reasons, disinfection is a dire need in different sections like personal equipment, mass gathering places, and particularly hospitals. Various chemicals such as liquid

chlorine, UV light, chlorine dioxide, sodium hypochlorite, ozone, etc., are used in hospitals to disinfect. But most of these are perilous in terms of health hazards, storage, transport, pollution, high operation costs, and hazardous by-products (Wang et al. 2020). During the post-Covid-19 pandemic, people from all walks of life realize the need for antibacterial textiles- which can also work against viruses.

1.5. Various antibacterial agents

There are quite a large number of antibacterial agents on the market. Some are depicted in table 1.1.

Table 1.1 Various antibacterial agents

Sl	Material	Chemical formula	Commercial name	Manufacturer/ remarks
1	Quaternary Ammonium Compound (QAC);		BIOGUARD® Sanitized Saniguard-7500	AEGIS, New Zealand SNITIZED, Switzerland L N chemical industries
2.	Metal ions	$AgNO_3$, $CuSO_4$ etc	-	-
3	Triclosan	$(C_6H_5)_2O$	Microban Biofresh Irgaguard	Microban, UK BiofresH™ , USA Irgaguard® B 265, Germany (BASF)
4	Polyhexamethylene biguanide (PHMB)	$(C_8H_{17}N_5)n$		Reputex Purista Biozac ZS
5	Chitosan / chitin	$C_6H_{11}NO_4X_2$		

1.6. Problems of commercial antibacterial agents

Antibacterial agents such as Si-QAC or Triclosan may cause dermatological problems and environmental hazards. The QAC is non-biodegradable in anaerobic conditions however can degrade in aerobically. For this reason, a large amount of QAC has been detected in the sediment and sludge. Moreover, it is toxic for sea

creatures, including algae, rotifers, and other useful and innocent microbes (C. Zhang et al. 2015).

On the other hand, Triclosan is a widely used bisphenol having extraordinary antimicrobial action, whereas other bisphenols (such as hexachlorophene) are highly toxic (Orhan, Kut, and Gunesoglu 2007). If used widely, it may be a potential health risk (Yazdankhah et al. 2006). As a result, people had a declining interest in using commercial antimicrobial textiles, considering health and environmental issues (Durán et al. 2007).

1.7. Silver: a low toxic antibacterial agent

In comparison with other antibacterial agents, Silver is non-toxic and harmless for human health but highly toxic to bacteria (Zhuang et al. 2010) (Windler, Height, and Nowack 2013). Silver can inhibit more than 16 bacterial species and 7 fungi species (Zhao and Stevens 1998). It is also used in food packaging to preserve food from bacteria due to its low toxicity (Mei et al. 2017). For the same reason, silver-based compounds have a potentially wide range of application domains such as wound dressing, medical equipment, food containers, paints, etc.

1.7.1. Toxicity of silver on animal

Silver is not totally free from toxicity. It has some toxicity on the environment, although it is still a controversial issue whether silver is harmful or not. The silver nanoparticle and silver ions show toxicity (Lubick 2008), but small nanoparticles are more toxic due to their high surface area (Choi and Hu 2008). The Lethal Dose 50 (LD50) of colloidal AgNPs is about 5000 mg/kg. (It means, 5000mg AgNPs per kilogram body weight of animals will cause 50% animal die). Moreover, it is relatively harmless to animals' skin, eyes, and oral (Maneewattanapinyo et al. 2011). However, high silver exposure to the skin may cause argyria (Fabrega et al. 2011). Christensen claimed AgNPs cause no toxicity in inhalation, mucins in respiratory mucosa and cause no skin irritation or sensitisation. Nevertheless, a high

dose (for risk assessment purposes) can elevate liver enzyme, which gets back to normal condition after treatment removal (Christensen et al. 2010). Additionally, after a detailed discussion on Silver's toxicity, Lansdown concluded systematic absorption of silver ions has a low health risk (Lansdown 2010). Ji et al. ended AgNPs show no significant health effects in the rat (J. H. Ji et al. 2007).

1.7.2. Toxicity of silver on ecosystem

On the other hand, AgNPs can have a negative impact on the ecosystem in the short and long term; but this has yet to be fully explained (Quadros and Marr 2010). Some researchers claim that the Ag^{+} is harmful to prokaryotes and marine creatures (Bianchini et al. 2002). However, there are scopes of arguments as water contains sulfide, Cl^{-}, organic matter (having logK>9.0) - which can mitigate the silver toxicity by producing silver compounds. Besides, alkalinity and hardness may decrease the toxicity (Erickson et al. 1998). More research is needed to investigate silver toxicity on animal health and ecology. In parallel with this, new silver compounds can be made to reduce toxicity. For example, Plotnikov et al. developed low toxic but high antiviral silver-based compounds (Plotnikov et al. 2016). Silver release depends predominantly on the nanoparticle incorporation method into the fabric. Up to 145 µg Ag/L can leach from AgNPs during the initial washing (Reidy et al. 2013). Hence it needs an efficient nanoparticle incorporation method to limit silver nanoparticle release.

1.8. Synthesis of AgNPs

Nanoparticles are synthesized in two ways: 1) Top-down (Physical method) 2) Bottom-up (chemical method) (Behzad et al. 2021). Figure 1.5 and figure 1.6 illustrate the various silver nanoparticles AgNPs synthesis method.

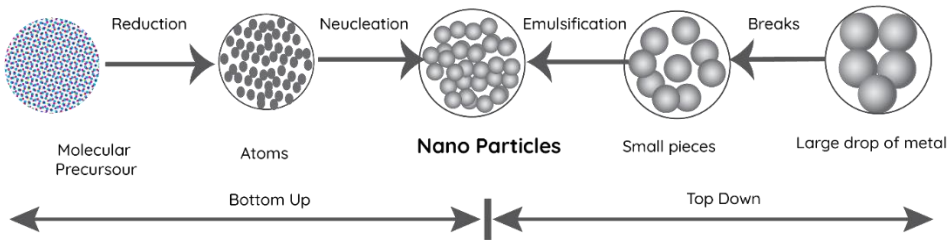


Figure 1.5 Top-down and bottom-up

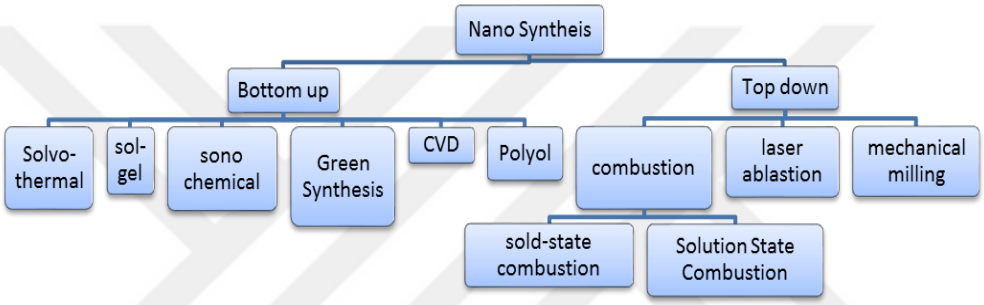


Figure 1.6 Different physical and chemical methods of AgNPs synthesis

Among them, chemical methods are more popular. Table 1.2 briefly illustrates some popular chemical methods.

Table 1.2 Various methods for silver nanoparticle synthesis

Method	Main Reducer	Condition	Feature	Ref
Lee Meisel	Mainly Citrate (or $NaBH_4$)	Boiling	Size: 60- 200 nm Shape: spherical	(Lee and Meisel 1982) (Wan et al. 2013)
Turkevich	Tri sodium citrate	High pH, 70 ^{0}C, 80 ^{0}C, or 100 ^{0}C (standard)	Nontoxic, most popular method, Shape: spherical, Size :1.6 nm	(Turkevich, Stevenson, and Hillier 1951) (Gorup et al. 2011)
Creighton	$NaBH_4$	Ice cold temperature	Shape: spherical and Size: 10-20 nm	(Trefry et al. 2010)
Thermolytic	Primary-alkylamines; DMF*(reducing), APS or PVP (stabilizing) for nano prism; or only PPh3 ligand	120 ^{0}C or 180 ^{0}C	Size: dispersed small AgNPs; can produce nano prism; no reducing or stabilizing agent if PPh3 is used	(Kashiwagi, Yamamoto, and Nakamoto 2006) (Pastoriza-Santos and Liz-Marzán 2000) (Yamamoto and Nakamoto 2003)
Tollen	sodium hydroxide, ammonia, and formaldehyde	Room temperature	Size: 2- 10 nm (if Chemical etching is applied)	(D. C. Lim, Lopez-Salido, and Kim 2006) (Yin et al. 2002)
Green synthesis	Biological extract	Room temperature	Super simple, The biological extract acts as capping and reducing agents	(Kanchi and Ahmed 2018)

*dimethylformamide (DMF), aminopropyltriethoxysilane (APS) polvinylpyrrolidone (PVP)

1.9. The best method for AgNPs synthesis

Among dozens of nanoparticle synthesis methods, which should be used regarding all aspects? First, the drawback of different methods should be discussed.

1.9.1. Drawbacks of physical and chemicals methods

Physical methods include sunlight-induced silver nanoparticle synthesis without reducing or capping agents (Annadhasan et al. 2012). But The leading drawbacks of the top-down (physical) approach are the imperfection of nano surface, high cost, low production, and high energy consumption (Thakkar, Mhatre, and Parikh 2010)

Ordinarily, Chemical methods are cost-effective due to their high production rate. But it requires numerous chemicals as reducing agents such as hydrazine, sodium borohydride, etc. Again, controlling the morphology and preventing the agglomeration of nanoparticles requires stabilizing agents such as thiophenol, mercapto-acetate, thiourea, etc. However, the chemicals are not eco-friendly, toxic, and can produce hazardous by-products (López-Téllez et al. 2013) (Gomathi et al. 2017).

Some early days eco-friendly synthesis methods rely on organic solvents such as Hydrazine, Sodium Borohydride ($NaBH_4$), or Dimethyl Formamide (DMF) because of their hydrophobic capping action (Raveendran, Fu, and Wallen 2003). Using supercritical CO_2 (M. Ji et al. 1999) or fluorinated ligands as stabilizers or capping agents were also considered environmentally benign (Shah et al. 2000). But the intricacies of these eco-friendly methods are- 1) It is challenging to isolate the nanoparticles using CO_2-philic surfactant 2) Micro emulsion ingredients are toxic 3) The reducing agents have high hazards of environmental or biological risk. Hence, it is palpable that most of the available techniques are high-priced and inefficient; therefore, demand for to develop a clean, harmless, eco-friendly benign synthesis procedure (Mandal et al. 2006).

1.9.2. Advantages of Green synthesis

So, physical and chemical means are expensive and linked with noxious chemicals. On the contrary, bio-inspired green synthesis is an ideal solution. It is a low-cost, non-toxic, highly-productive, and eco-friendly means of nanoparticle

synthesis. Importantly, plant extract can simultaneously accomplish the required tasks (reducing and stabilizing). Therefore, unlike other chemical syntheses, there is no need to use separate reducing and stabilizing agents.

Additionally, the antioxidant property of phytochemicals such as phenols, flavonoids, and others can scavenge free radicals. Hence the green-synthesized silver nanoparticles will also have scavenging properties (González-Ballesteros, Rodríguez-González, and Rodríguez-Argüelles 2018) (Mittal, Kaler, and Banerjee 2012) In this way, it can prevent free radicals-related diseases (Fafal et al. 2017).

1.9.3. Biological source for Green synthesis

There are plenty of bilogolical sources for green synthesis have been experimented, such as: sprout (Gardea-Torresdey et al. 2003), fungi (Molnár et al. 2018), yeast (Roy, Sarkar, and Ghosh 2015), algae (Ramakrishna et al. 2016), root and leaves (Behravan et al. 2019) so on and so forth. The botanical extracts provide some fascinating privileges, including extraordinary assembly (S. Ahmed et al. 2016). The plant-extract acts as stabilizing and capping agents for synthesized particles (Parthiban et al. 2019). Eminently, plant extracts are much faster than other biological substances. The effectiveness of bacteria or fungi demands 24 hours to 120 hours whereas, plant extract (neem leaves) requires only a couple of hours (Shankar et al. 2004).

As part of searching for suitable reducing agents, various biological substances were experimented with, ranging from fungi to fruit peels. Among different types of green materials, some are- mango peel (Yang and Li 2013), clove (*Syzygium aromaticum*) (Vijayaraghavan et al. 2012), aloe vera (Zhou et al. 2017b), lemongrass extract (Hiremath, Narendra Kumar, and Sukanya 2018a), flame lily (*Gloriosa superba*) (Naika et al. 2015b) neem/salep (Rohani Shirvan, Kordjazi, and Bashari 2019b). Among different bacteria, *Bacillus subtilis*, Shewanella algae, Rhodococcus, used for gold, Pseudomonas Stutzeri, Lactobacillus used for silver, Desulfobacteriaceae are used for silver Zinc Sulphide (Mandal et al. 2006).

Firdhouse et al. analyzed 16 plants in which *Alternanthera sessilis* provided the best extracts and encountered a range of 5-25 nm particle size and 21-29 mm inhibition zone for many plants (Firdhouse and Lalitha 2016).

1.9.3.1. *Calendula arvensis*

For this study, *Calendula arvensis* was used as the plant source, but it is a seasonal weed; hence *Citrus reticulate* was also used.

Calendula arvensis L. is from the *Calendula* genus. Commonly it is know as 'Field marigold. This genus is widely available from Europe to W.Himalaya, Sahara, and Arabian Peninsula to Macaronesia. Figure 1.7 illustrates the image of *C.arvensis* flower.



Figure 1.7 *C.arvensis* flower

In this genus, three species are there; *C.arvensis* is one. The rest two are *C.officinalis* and *C.suffruticosa* (Servi et al. 2020). *C.arvensis* is a yearly and weeds type herbs. Generally it grows in empty field, roadside, rocky hillside, cultivated field and others. Geographically is available around meditation coastal region

including Turkey, southern Europe, Caucasia, Iran, Afghanistan (TÜBİVES Calendula Arvensis 2021). Figure 1.8 depicts the geographical location of *Calendula* genus whereas figure 1.9 illustrates the taxonomy of the *C.arvensis* plant. It has various antibacterial, anti-mutagenic, anti-inflammatory, antioxidant, hemolytic etc. (Abutaha et al. 2019). Normally, it is used in food coloring, tea or spice, ointment, tincture, and cosmetic cream (Abudunia et al. 2017) (Paolini et al. 2010).

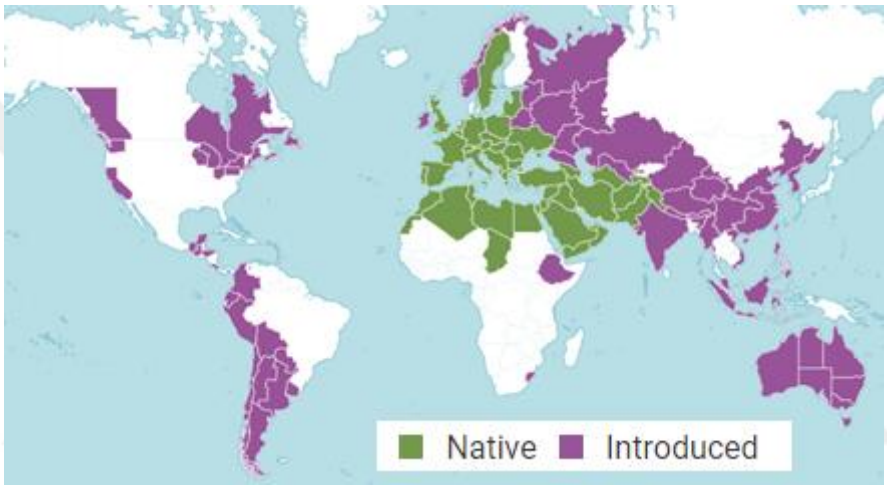


Figure 1.8 Geographical distribution of Calendula genus (Kew 2021)

Paolini et al. identified 85 essential oil components, including monoterpene, Sesquiterpene, alcohol, aldehyde, ketones, and esters from *C.arvensis*. Abutaha et al. (2019) demonstrated it could destroy breast cancer cells. *C.arvensis* is traditionally used as spicy, food color, tea, ointment, tincture, and cosmetic cream (Ruiz De Clavijo 2005). Phytochemical studies showed that *C.arvensis* contains phenolic acids, and flavonoids like different types of chemical compounds (Kırmızıbekmez et al. 2006).

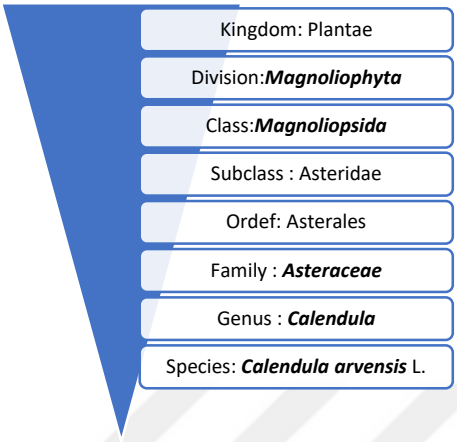


Figure 1.9 Taxonomy of *C.arvensis* plant

1.9.3.2. Mandarin orange (*Citrus reticulata*)

The *Citrus* genus is native to Southeast Asia. Within this genus, there is mandarin orange (*Citrus reticulata* Blanco), lemon (*C. medica*), and pummelo (*C. maxima*) (Froelicher et al. 2008). For this study, *Citrus reticulata* peel was used to compare with *C.arvensis* synthesized AgNPs.

The nanoparticles can be applied in *ex-situ* or *in-situ*. The *ex-situ* methods (such as coating, padding, spray, and others) are also widely used in antimicrobial treatment using various metal nanoparticles. Table 1.3 illustrates some techniques for loading nanoparticles on fabrics.

1.10. Incorporation Methods

Almost all the application methods need binding or cross-linking agents for better fixation and washing fastness (D. Zhang et al. 2013). Because physical entrap cannot protect the nanoparticle from washout during laundering (Nadiger and Shukla 2016). In this case, *in-situ* may be an exception as it performs better without binding or cross-linking agents (Zhou et al. 2017c).

Table 1.3 Different nanoparticle loading methods

Sl	Method	Process	Parameters	Feature	Ref
1)	Immersion	Fabric is immersed in NP suspension. Ultra-sonication for better performance Air-dried at high temp like 120 C	-Constant stirring -Room temp (10 min – 5hours)	Simple and better fixing	(F. Zhang et al. 2009) (Chauhan, Kumar, and Bhushan 2019)
2)	Pad-dry-Cure	Immersed in solution for a specific time (e.g 10 min) Cure: 180 ^{0}C for several minutes	-certain pressure like 1.5 kg/cm2	Most widely used	(Xu et al. 2018) (Abou-Okeil et al. 2012)
3)	Spraying	Spray with spray gun from 8 Cm to 16 cm distance; on both sides	Pressure: 3-4 bar	Simple method	(Rana et al. 2016) (Sasaki et al. 2016)
4)	In-situ	Step-1: Fabric is immersed in $AgNO_3$. Step-2: in reducing agent bath or vice-versa.	Reduction happens inside the fiber and changes the color of the fabric.	Better fixing without any binder or cross linkers.	(Xing et al. 2020) (Zhou et al. 2017c).
5)	Pulsed laser ablation	Nanoparticles were in situ synthesis on textile by laser pulse ablation method. The laser beam does the laser ablation	Laser beam wavelength 1064 nm with 10 Hz repetition	Inexpensive and no by-product	(Shahidi, Rashidian, and Dorranian 2018)

Table 1.4 continuous

6)	Layer by layer assembly	Cotton fabric is immersed sequentially in- a) anionic colloidal solution b) deionized water c) cationic colloid solution d) deionized water repeated until 10-16 multilayers (2 layers formed /cycle)	Dried at 60^0C and cured at 130 ^{0}C for 3 min	UV preventive fabric, good wash fastness	(Uğur et al. 2010)
7)	Sonochemical	Fabric immersed in nanoparticle solution, then irradiated for 1 hour with the ultrasonic horn	20 kHz, 600 W and 70% efficiency, 30 ^{0}C	Better fixing, Nanosynthesis also possible in-situ	(Perelshtein et al. 2008) (Abramov et al. 2009)

This study aims to investigate

1. Finding equations to quantify the exact or least amount of plant extract for *in-situ* and *ex-situ* methods.
2. Determining the minimum acid-hydrolysis time at different temperature.
3. Correlation between different factors on AgNPs size and shape.
4. Probable mechanisms for cubic, spherical and irregular shapes.
5. Correlation between different factors on antibacterial performance.

6. Factors of wash fastness regarding antibacterial performance and a find-out a way to increase wash fastness
7. Time effect on AgNPs incorporated textiles.

2. LITERATURE REVIEW

2.1. Fabric structure on antibacterial activity

C.arvensis is a widely found weed in Turkey. But there is no available study on using *C.arvensis* in green synthesis. Besides, there are very few works on the relation of fabric parameters and antimicrobial finished. Among previous studies, one is characteristic of weaving parameters in micro-capsulated fabric. The author tested woven fabrics (plain, 2/1 twill, honeycomb) for carrying microcapsule. They found that the honeycomb structure is the best for micro-capsulated moxa oil with gelatin-Arabic gum. (L. Li et al. 2013). In another paper, Hashem et al. investigated different antimicrobial actions on finished and dyed woven and knit fabric using Actigard® and later tested physical and mechanical properties and antimicrobial tests. They tested 100% cotton twill (1/3) with carded yarn, plain woven (poplin, GSM= 189 g/m2), simple 1/1 weave (GSM= 73 g/m2), and knitted cotton fabric (58 gm/m^2). They found dyed fabric has high performance than grey fabrics. In this paper, the authors conducted details research on different types of woven and knit fabric and antimicrobial finish under different conditions. Still, they were not eager to correlate weave or fabric structure and antimicrobial finishes (Hashem et al. 2009). There is no study on antimicrobial performance versus antibacterial agent incorporation methods, the mechanism of nanoparticle shapes in textile products, comparing sol-gel with green synthesis methods, and the factors of high wash fastness of antibacterial textiles.

2.2. Antibacterial textiles

Moses et al. investigated anti-odor and UV protection of chemically protected cotton fibers. They treated cotton (woven & knit) fabrics with NaOH, Cellulase, and Morpholine and dyed by 6 dyes Natural dyes & 2 synthetic dyes. They showed that NaOH treated fabric creates higher zones of prohibition when treated

with morpholine, cellulase enzyme. (Moses and Venkataraman 2016). Hashem et al. intended to assess the technical feasibility of combing antimicrobial finishing over other finishing. They found cotton fabrics dyed with reactive, direct, or vat dye and treated with Actigard showed higher antimicrobial than other dyes. (Hashem et al. 2009). Asanović et al. investigated the antimicrobial activity of knitted fabric for medical purposes. They treated the chitosan gel in either gentamicin sulfate or autochthonous essential oil of Picea abies to examine the influence of antimicrobial treatment on compression work, volume resistivity, water sorption, and water retention. A wide range of antimicrobial actions of knit fabric and gentamicin sulfate were found (Asanović et al. 2010).

2.3. Green synthesis for antibacterial textiles

Green synthesis is another critical and contemporary idea for antimicrobial actions. L. Hiremath et al. worked on the green synthesis, and they demonstrated the use of lemon grass to synthesize magnetite particles. They used the dipping and sonication method to synthesize and found that cotton cloth absorbed more nano particles than other cotton samples (like gauze roll). They also concluded that sonication is the best method in this aspect (Hiremath, Narendra Kumar, and Sukanya 2018b). In another article, A. Hebeish et al. Applied green synthesis by using Butanetetracarboxylic Acid (BTCA) to apply chitosan with various molecular weights using chitosanolysis and pectinase enzyme, and they found high crease recovery and presence of antimicrobial agent up to 10 washes (Hebeish et al. 2011).

M.A Sabri et al. reviewed details on green synthesis using grape extract, neem, Triphala, Tulsi, Coriandam leaf extract, Pomegranate peel, etc. (Sabri et al. 2016). Q. Zhou applied in-situ synthesis of AgNps on cotton for UV protection and antibacterial activity using Alovera as a reducing agent. They pretreated the cotton fabric in water and then immersed it in $AgNO_{3;}$ subsequently, Alovera was applied to have excellent antimicrobial and UV protection (Zhou et al. 2017a). A.R Shirvan

(Rohani Shirvan, Kordjazi, and Bashari 2019a) investigated neem/salep synthesized $AgNO_3$ and applied it on cotton by impregnation method. R. Naika et al. synthesize CuO nano particles using *Gloriosa Superba L.* extract (Naika et al. 2015a).

2.3.1. Effect of pH on green synthesis of silver

Because silver salt is resistant to reduction, the pH of the solution is critical. The pH of the solution is proportional to the degree of reduction and colloid formation (Tripathy et al. 2010). The pH varied from 9.8 to 11.0 in the majority of cases. The nanoparticles will be lost until the pH changes. Higher pH speeds up nano production, according to studies. Large-sized nanoparticles are caused by a lower or acidic pH. Higher or alkaline pH, on the other hand, produces tiny nanoparticles. The silver nanoparticles agglomerate in the acidic environment. The alkaline pH, on the other hand, produces a significant number of tiny silver nanoparticles by generating a large number of hydroxyl ions (OH-) (Sathishkumar, Sneha, and Yun 2010) (Andreescu et al. 2007).

At pH 7, microbially produced gold nanoparticles with a diameter of 10-20 nm, whereas pH 1 produces AuNPs with a diameter of 50-500 nm (Thakkar, Mhatre, and Parikh 2010). M.K El Bisi et al. investigated the influence of pH on honey produced silver nanoparticles throughout a pH range of 8 to 11 and discovered that pH less than 9 prevents nanoparticle formation. pH 10-11, on the other hand, is ideal (El-Bisi, et al. 2013). The shape of nanoparticles is also affected by pH. Higher pH results in more spherical and decahedral geometries, whereas ellipsoidal shapes are less common. An isoelectric point is formed when the pH falls below one, but the zeta potential increases proportionately as the pH rises (Sathishkumar, Sneha, and Yun 2010). Sadowski et al. demonstrated isoelectric points at pH 2 in another investigation.Besides, Sadowski et al. described isoelectric points achieved at pH 2, and pH exceeding 8 produce a large amount of zeta potential which is need for stability (Sadowski et al.).

2.3.2. Effect of temperature on green synthesis

The metal reduction usually begins at ambient temperature. The synthesis process will be accelerated as the temperature rises. Heydari et al. investigated a temperature range of 4 ºC to 60 ºC and discovered that 45 ºC is the best temperature for synthesizing AgNPs from oak fruit husk (Heydari and Rashidipour 2015). Another study on the creation of silver nanoparticles using gelatine and glucose found that while temperature is unrelated to particle size, it can speed up the reaction process (Vasireddy, Paul, and Mitra 2012) (Engelbrekt et al. 2009). For some reducing agents, such as honey, which decomposes at 80 ºC, temperature has no effect on metal reduction. The temperature range of 50°C to 70°C is ideal for a greater reduction rate (El-Bisi, et al. 2013).

2.3.3. $AgNO_3$ molarity on green synthesis

The amount and form of nanoparticles are influenced by their $AgNO_3$ molarity. Nonetheless, it is dependent on a number of parameters, including molarity, biological extract capping ability, and the presence of highly active functional groups, etc. Because high molarity agglomerate nanoparticles, on the contrary, a lower concentration of organic extracts creates smaller nanoparticles (10 nm). Sangeetha et al. observed a similar phenomenon, in which an increase in aloe vera content leads to the formation of bigger nanoparticles (Sangeetha, Rajeshwari, and Venckatesh 2011).

It should, however, have a bottom limit beyond which the solution may get insufficient reducing and capping agents. Khalil et al. found that 1 ml olive leaf extract produces bigger nanoparticles (30 nm), whereas 5 ml olive leaf extract produces nanoparticles as tiny as 8 nm. To prevent aggregation, the extract concentration must provide enough capping agents (Khalil et al. 2014).

Larger nanoparticles result from a lack of reducing agent in highly concentric metal precursors (Zain, Stapley, and Shama 2014). Increasing the

concentration of either the precursor or the reducing agent will increase the nanoparticle size for the same reason. As a result, a combination of different concentrations can produce a wide range of nanoparticle sizes (Leung, Wong, and Xie 2010).

2.4. Sol-gel Method

Sol-gel is used to make aerogel- the world's lightest materials, toughest ceramics, protective coatings, biomedical, nano-powder, optomechanical products, medicines, antimicrobial and water repellent substances so on. In textiles, it also has a very promising scope.

Sol-gel is a simple, effective, and one of the most promising technology in functional textiles. It is believed to be an excellent host for different antibacterial agents. The most important benefit is that it needs only room temperature (G. Sun 2016). Mahltig et al. claimed that Sol-gel is good at fixing silver and its compounds within a modified silica matrix (Boris Mahltig, Haufe, and Böttcher 2005). Different researchers used different methods to incorporate antimicrobials agents in sol-gel.
B. Mahltig et al. (2004) incorporated desired materials (such as hydrophobic, antimicrobial, or other properties) into the sol liquid and mixed it for a few minutes before applying. Dai prepared AgNPs with a 1-5 nm size by applying dodecanethiol by sol (Dai, Sharma, and Wu 2005). Tarimala et al. 2006 also used dodecaethiol for capping AgNPs incorporation (Tarimala et al. 2006). In another investigation, (Lin et al. 2019) immersed oxygen plasma activated cotton into anhydrous ethanol, APP, TEOS and HPDMS mixture, and ammonia to control pH (Lin et al. 2019). Sol-gel consists of successive hydrolysis and condensation process (Hernández-Barrios et al. 2017). Hydrolysis takes time. Venkateswara Rao and Bhagat (2004) claimed this time should be 2-3 days. B. Mahltig and Böttcher (2003) mentioned it is 24 hours.

2.5. Nanoparticle size and shape

Qin et al. (2010) demonstrated a pH change from 6 to 11.5 will change the size of AgNPs from 73 nm to 31 nm. Dong et al. demonstrated Ag atoms would be produced at a faster rate at high pH (Dong et al. 2009). They correlated spherical and rod-like shapes (pH 11.1 to pH 8.3), triangular, and polygon shapes (pH 6.1 to pH 5.7) with pH. They got 30 nm, 59 nm, 69 nm, and 96 nm nanoparticles from pH 11.1, pH 8.3, pH 6.1, and pH 5.7. Hence they found high pH will cause small nanoparticles. Luo et al. mentioned Gibbs free energy for synthesized AgNPs by calculating bulk free energy and surface free energy for both solid and liquid phases (Luo, Hu, and Xiao 2008).

If the nanoparticle size is small, then the surface: volume ratio will be increased, and Gibbs free energy will also be raised; consequently, the melting temperature will be decreased. Besides, increasing driving force from crystallization leads to the formation of polyhedrons such as octahedrons, truncated octahedrons, and cubes pyramids (Tang et al. 2009).

The stabilizers, reducer, reaction rate, and preparation method determine the shape of nanoparticles (Haruta 2004). Y. Sun and Xia (2002) demonstrated that $AgNO_3$, ethylene glycol, and PBP produce cubic shape, but when the temperature increases to 190 °C then, the AgNPs will be irregular. Again, if the molar ratio of reducer (PVP): $AgNO_3$ is increased to 3 from 1.5, multiply twinned particles (MTPs) will be produced. Im et al. (2005) produced nanotubes by reducing $AgNO_3$ with ethylene glycol, PVP, and HCl at 140 °C. Molar ratio can also determines the nanoparticle morphology (Tao, Sinsermsuksakul, and Yang 2006). It was suggested that high molar ratio produces nanocubes, whereas a low molar ratio produces nanowires. Wiley et al. (2006) synthesized AgNPs by ethylene glycol (EG) with 3 different shapes. They mentioned the ionic etching by (Hcl, Cl^- etc.).

Noël et al. (2020) claimed nanoparticle formation produces an oxidant that can participate in the etching of nanoparticle surface. This oxidative etching is

relevant to single crystal particle synthesis. Hence, the presence of both reducer and oxidant can control nanoparticles' shape and growth dynamics. When a weak reducer replaces a strong reducer, cubic shape nanoparticles will be formed. However, for the etching process, it need an oxidant, such as O_2, Cl^-, H_2O_2, halogen gas etc.

3. MATERIALS AND METHODS

3.1. Required Materials

Tetra Ethyl Orthosilicate (TEOS), Silver Nitrate ($AgNO_3$), Ethanol, Muller Hinton agar, Nutrient broth, Citric acid were purchased from Sigma-Aldrich. All of these materials were analytical grade. The fabrics were collected from local textile mills. Here four types of fabrics were used: plain (1/1), knit (plain), twill (3/1), and non-woven (melt-blown). All the fabrics were made from cotton except the non-woven fabrics which was made from polypropylene fibers. The non-woven fabrics was used only to investigate the potential application of silver annoparticels in medial protective textiels. The GSM of plain, knit, twill, and non-woven was 123, 154, and 230, 20, respectively. Gram-positive (*S.aureus*) and Gram-negative (*K.pneumonia*) were used for the antibacterial test.

3.2. Plant Extraction Preparation

3.2.1. *C.arvensis* (Field marigold) plant Extract

The plants were collected from the garden of the Textile Engineering Department at Cukurova University. Then the leaves are separated, washed with 95% ethanol, and dried in the shade for a few days. The dried leaves are chopped into small pieces. Five grams of the dried leaves are kept in 200 ml of water and boiled at 90 ^{0}C until the liquor becomes 100 ml. After getting back to room temperature, the solution or mixture was filtered with a Whatman no.1 filter paper. The solution was preserved at 3°C for future use.

3.2.2. FTIR of *C.arvensis* plant extract

FT/IR-6700 of JASCO has been used to determine the functional groups of phytochemicals in the *C.arvensis* plant extract. The FTIR image shows two strong peaks at the absorbance bands between 500- 4000 cm^{-1} wave number. One peak is at

3325.64 cm-1, and the other is at 1633.41 cm^{-1}. It confirms the presence of –OH and >C=C< groups. Various phytochemicals such as flavonoids, terpenoids, etc., contain hydroxyl and alkene groups as shown in figure 3.1.

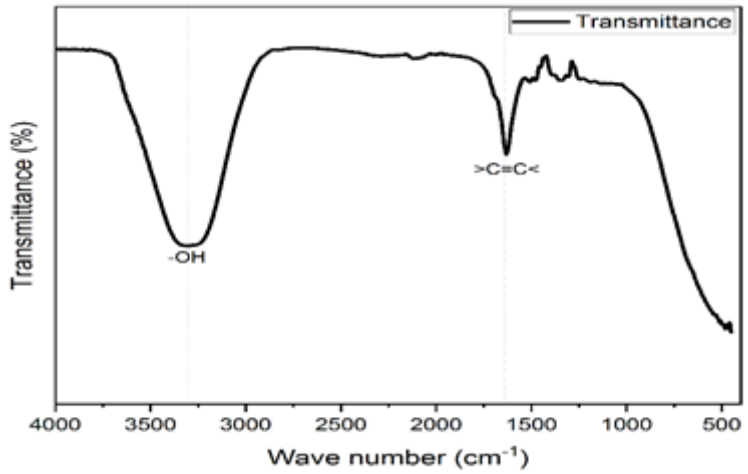


Figure 3.1. FTIR of C.arvensis plant extract

3.2.3. *C.raticulata* Peel Extract

The mandalina orange (*C.reticulata*) were collected from the Agriculture Research and Applications Shop of Cukurova University (Çukurova Üniversitesi Ziraat Fakültesi Araştirma Ve Uygulama Çiftliği). Next, the peels were dried in shadow for a few weeks to ensure no water content. Then 5 grams of this dried peel were crushed and boiled in 200 ml of distilled water until the extract volume dropped down to 100 ml. after cooling. This extract solution was kept at 3 °C for future use.

3.3. Green Synthesis

For green synthesis, a certain amount of $AgNO_3$ with certain molarity was taken, and a few drops of plant extracts were added to synthesize. Proper silver nanoparticle synthesis depends on several parameters such as certain plant extract amount, temperature, $AgNO_3$ molarity, etc.

3.3.1. Temperature for green synthesis

3.3.1.1. Different amounts of plant extract at room temperature

The $AgNO_3$ and plant extracts were tried in different ratios. However, each of the cases caused precipitation (table 3.1).

Table 3.1. Different amount of plant extract at room temperature

Sample	$AgNO_3$ (0.1 M)	Plant Extract	Ratio	Result
S-1	5 ml	5 ml	1:1	Instant precipitation (turn to black within a few minutes)
S-2	5 ml	1 ml	5:1	Precipitation in few seconds
S-3	5 ml	0.5 ml	10:1	Precipitation within a minute
S-4	5 ml	0.25 ml	20:1	Precipitation in 1.5 min
S-5	10 ml	4 ml	2.5:1	Slow color change and precipitation
S-6	5 ml	6 ml	1:1.2	Black Precipitated in few hours
S-7	5 ml	2 ml	2.5:1	Precipitated
S-8	5 ml	5 drops	1:1	Nothing happen

Any quantity (in ml) of plant extract at room temperature caused quick precipitation. But very small amount (in µl) of plant extract did not change for a few days. On the other hand, at high temperatures (such as 60 °C), the reaction occurred within a blink of an eye. Hence, the temperature is a critical parameter in silver nano synthesis as well as plant extract also plays a crucial role in nanoparticle stability. Table 3.2 and figure 3.2 explain the phenomenon in detail.

Table 3.2. Effect of temperature on AgNPs (0.1M) formation and stability

Sample name	Temp	$AgNO_3$ (0.1M)	Plant extract	Time to react	Results	Stability
H-ice	3 ^{0}C	5 ml	5 drops	2 hours	No NPs. Precipitate in 2 hours	2 hours
H-30	30 ^{0}C	5 ml	5 drops	2 hours	No. NPs. Precipitate in 2 hours	2 hours
H-40	40 ^{0}C	5 ml	5 drops	5 min	Deep red color	1 hour
H-50	50 ^{0}C	5 ml	5 drops	1 min	Deep red color	24 hour
H-60	60 C	5 ml	5 drops	40 sec	Deep red color	24 hour
H-60	60 ^{0}C	5 ml	2 drops	55 sec	Deep red color	72 hours
H-70	70 ^{0}C	5 ml	2 drops	30 sec	Deep red color	48 hours
H-80	80^{0}C	5 ml	2 drops	12 sec	Deep red color	48 hours
H-90	90 ^{0}C	5 ml	2 drops	12 sec	Deep red color	48 hours

The information in table 3.2 is log-transformed and scaled using MinMax Scaler (depicted in figure 3.2).

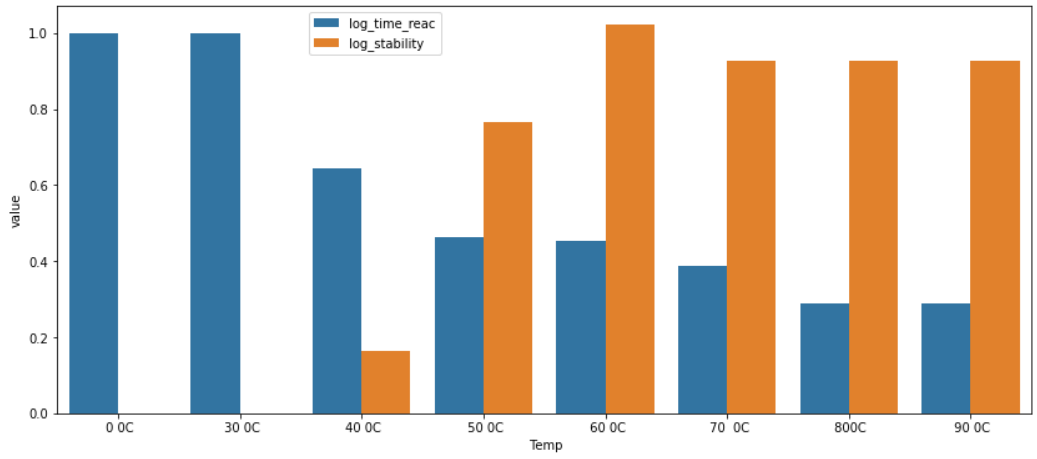


Figure 3.2. The temperature of AgNPs stability and reaction time

It is seen from figure 3.2 that the required time for reaction is decreased with temperature, but stability increases with temperature. The highest stability is found at 60 ºC. Beyond 60 °C the stability is the same, but the reaction is fast. On the other hand, lower than 40 °C fails to form nanoparticles. Hence, it needs to investigate the influence of temperature on AgNPs. For this purpose, Surface Plasmon Resonance (SPR) from UV-vis was used.

3.3.1.2. UV-vis Spectroscopy

For confirming the formation and stability of AgNPs in the solution Shimadzu UV- 1800 UV/Visible spectrophotometer is used. The wavelengths range from 300 nm to 650 nm. As a blank solution, distilled water was used (figure 3.3).

The maximum peaks at UV-vis is 421nm, which is in the range of silver nanoparticle. UV-Vis spectrophotometric analysis is used for confirmation of AgNPs formation. AgNPs produce a SPR band in the range of 350-500 nm (Ider et al. 2017). In this study a range of successfully synthesized AgNPs is 416 – 430 nm was observed, shown in figure 3.4.

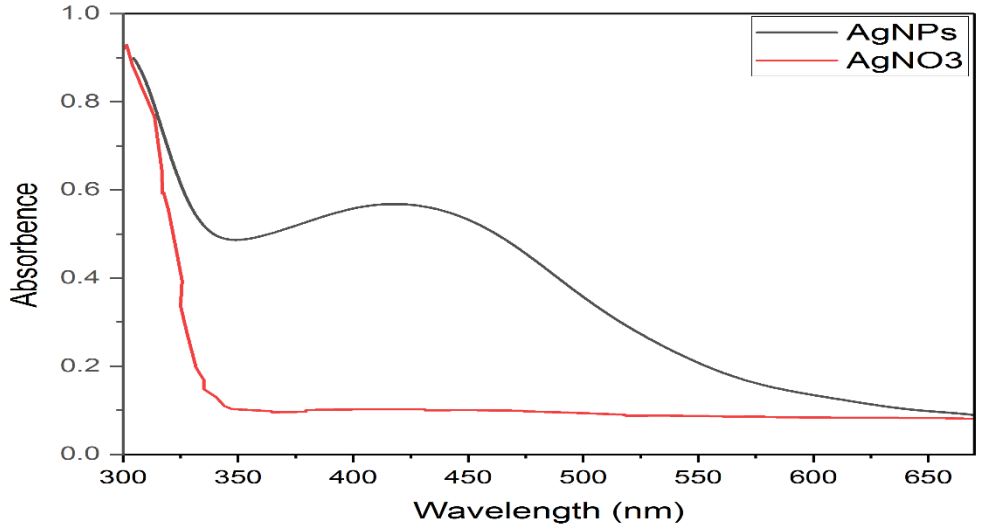


Figure 3.3. UV-vis spectrum for AgNPs

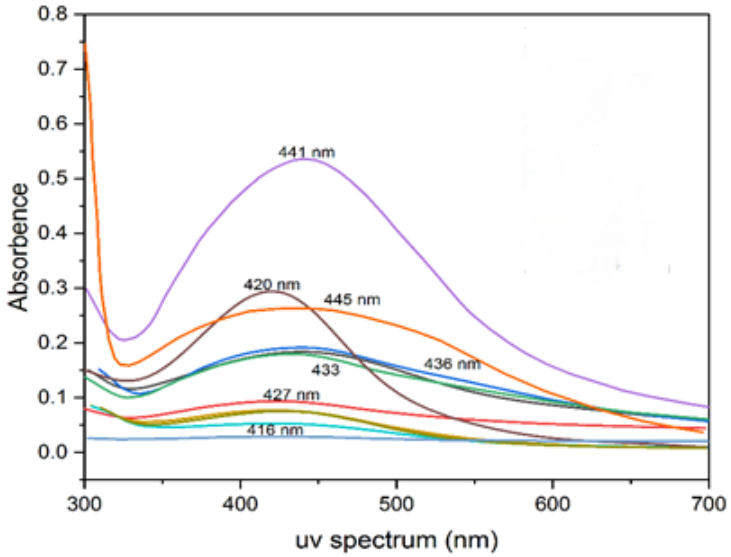


Figure 3.4. Different peak positions

3.3.2. Fabric pretreatment

Pretreatment is a crucial matter in AgNPs incorporation. The fabrics were pretreated in various ways. But the most widely used pretreatment was by using NaOH (4g/1L) for 1hour at 90 °C and then neutralizing it by boiling for another 1 hour in distilled water. For understanding the effect of various pretreatment, the samples were also pretreated with citric acid, Span-80, in different combinations.

3.4. Formulating the amount of plant extract

The previous discussion shows that plant extract should be a minuscule amount, and the temperature should be more than 40 °C for low UV-vis SPR peaks. After many trials, the equation was formulated to determine the exact amount for immersion and *in-situ* methods.

3.4.1. For the Immersion method

As 1 mole contains 6.02 x 10^{23} molecules. Hence the mole is important to quantify plant extract. But the phytochemicals amount are unknown in the plant extract solution. Hence after a lot of trials, it was identified that the logarithm function can determine the quantity for lower UV-vis spectrum (which will give smaller nanoparticle size).

Mole = $M \times V$

Plant extract quantity = Mole x (10 + $moles\ x\ \left(10 + \frac{\log V}{\log M}\right)$) + $log10\ V$ drops

1 ml = 25 drops (for the used dropper)

Hence to convert the plant extract quantity in μl it is needed to divide it by 0.025

Again, from logarithm formula:

$$\log_v M = \frac{\log_e M}{\log_e v}$$

Hence concisely, it can be written:

$$\text{Plant extract quantity} = \frac{MxV(10+log_M V)+log_{10} V}{0.025}\ \mu l \qquad (1)$$

Where M = Molarity of $AgNO_3$

V= Used volume of $AgNO_3$

According to the equation, 0.002 M of 100 ml $AgNO_3$ will require

$\frac{0.002x100(10+log_{0.002}100)+log_{10}100}{0.025}$ = 153 μl plant extract

3.4.2. For the in-situ method:

For *in-situ* synthesis, the formula is the same as above. But there, the plant extract solution should be made in a different vessel. Empirical studies show that the minimum amount of liquid to wet the fabric is 2.5 times of fabric weight.

Required volume for fabrics, $v = \frac{GSM}{10000} xLxWx2.5xdilution\ volm$ (2)

Required Plant extract = $\frac{0.002x100(10+log_{0.002}100)+log_{10}100}{0.025x1000}$ ml (3)

Here, M = Molarity of $AgNO_3$

L = sample length

W = sample width

If the dilution volume is 1 then the calculated plant extract will be directly added to the 1 ml water.

For example, to find out the required plant extract for *in-situ* synthesis of 230 GSM fabric having 10 cm x 10 cm sample size for 100 ml plant extract dilute solution for *in-situ* method,

Volume $v = \frac{230}{10000} x10x10x2.5x100 = 575$ ml

Plant extract amount $= \frac{0.001\ x575x(10+\log_{0.001}575)+\log_{10}575)}{0.025x1000} = 0.5\ ml$ in 100 ml water.

3.5. AgNPs incorporation methods

AgNPs were incorporated by 4 methods: padding (80% WPU), immersion, in-situ, sol-gel, and 3 derivative methods in-situ-pad, 2-times-padding, immersion (*in-situ*).

3.5.1. Padding

A pad-dry-cure machine was used with the pressure set to ensure 80% wet pick up. After padding, the samples are dried at 60 °C for 20 minutes and then cured at 90 °C for 10 minutes.

3.5.2. Immersion

The samples are kept in the AgNPs suspension solution for more than 10 minutes and then air-dried.

3.5.3. In-situ

It was done in 2 steps. In the first step, the fabric was immersed in an $AgNO_3$ solution, and in the second step, it was soaked in the plant extract solution. This process was done in such a way that it did not allow more wastage of plant extract and Ag^+.

3.5.4. Immersion (in-situ)

Same as the immersion method. But here, before beginning synthesis, the samples were added to the vessel immediately after adding the plant extract to the $AgNO_3$ solution so that the synthesis begins inside the fabric.

3.5.5. Two-times-padding

This is just the same as padding (80% WPU). The only difference is the padding was done 2 times. After first padding, the samples were kept in the AgNPs solution for a few minutes and then again padded at 80% wet pick up.

3.5.6. In-situ-pad

The fabrics are padded with plant extract with 80% WPU, and the fabrics are immersed in the silver nitrate ($AgNO_3$) and again padded with the same pressure.

3.5.7. Sol-gel

Sol-gel is another way to incorporate AgNPs. More than ten methods for sol-gel and AgNPs synthesis were implemented. Below some are depicted.

3.5.7.1. Sol-gel Preparation

For the sol-gel experiments, 2 types of fabric were selected: twill and knit, having 230 and 154 GSM, respectively. According to the previously discussed fabric pretreatment method, the fabrics were pretreated with NaOH. These alkaline fabrics will work as a catalyst for sol-gel formation.

For sol preparation, TEOS, Ethanol, and acid with a ratio of 5:21:1 were used. Hence, 20 ml TEOS was dissolved in 84 ml Ethanol and stir it. Then 4 ml of 0.01N HCl are added in stirring condition. This solution was aged for 24 hours for acid hydrolysis. After that, a minuscule amount of NH_4OH was added. In this way, the sol formed within a few minutes.

3.5.7.2. Applied on textiles

For incorporating AgNPs through sol-gel in fabrics, seven methods were implemented.

3.5.7.2.(1). Method -1 (In-situ- sol-gel)

For applying sol-gel film on fabrics, 2% citric acid was used as the acid solution. Sol-gel on fabric was applied by using the in-situ method. In this method, 100 ml 96% Ethanol was mixed with 23.5 ml TEOS in stirring condition. Then 4 ml of 2% citric acid (2gm citric acid in 100 ml water) was added to the solution. For acid hydrolysis, the solution was kept at room temperature overnight. Then this solution was poured on the scored fabrics. The scoured fabrics have alkalinity, and hence no need to add the extra alkaline solution to the TEOS solution. In this way, the sol-gel film will be formed on the fabrics. After drying at room temperature, the fabrics were washed several times with the tap water.

3.5.7.2.(2). Method-2 (Dip coating)

This was done in 2 steps:

Step-1 (AgNPs formation): 20 ml $AgNO_3$ (0.08 M) was heated to 60 °C and 3 ml PE are (also at 60 °C) mixed. Within a few minutes, the AgNPs were formed.

Step-2 (Sol-gel solution preparation): The fabric was treated with aged TEOS solution (TEOS + Citric Acid+ Ethanol). Then without delay, the prepared AgNPs are applied to it. Then the samples were kept in the open air to dry. Finally, they were washed with tap water. As a result, the fabric turned to violet color (figure 3.5)

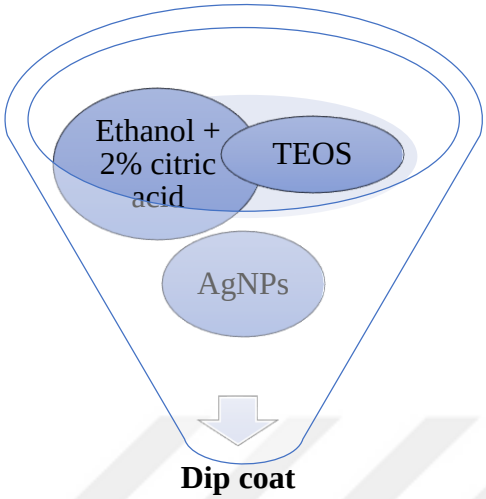


Figure 3.5. Process flow of method-2 (dip-coating)

3.5.7.2.(3). Method-3 (In-situ AgNPs synthesis in sol-gel)

TEOS-$AgNO_3$ mixture: TEOS mixture was prepared by mixing TEOS, Ethanol, and CA with the same ratio (5:21:1). $AgNO_3$ (0.08 M) was also mixed with this TEOS mixture and kept at room temperature overnight. The scored fabrics were immersed in plant extract solution. After 10 minutes TEOS-$AgNO_3$ (1:1) mixture was poured onto the fabric sample. Then the samples were kept at room temperature for simultaneous AgNPs synthesis and sol-gel formation. When the samples were dried up, it was washed with tap water. Then again, it was dried. The fabric also turned to a violet color (such as Method-2).

3.5.7.2.(4). Method-4 (Spray)

The fabric was immersed in a solution of 15 ml acid hydrolyzed TEOS and 15 ml $AgNO_3$ (0.08 M) solution. The sample was kept at 60 ^{0}C for 10 minutes. This treated fabric plant extract was sprayed on both sides of the fabrics. Latter, this fabric was kept at 60 ^{0}C. Finally, the fabric was washed with tap water. The cloth turned to golden color.

3.5.7.2.(5). Method-5 (insitu-1:1)

Scoured fabrics soaked in plant extracts solution. Then 50 ml 0.002 M $AgNO_3$ is mixed with 50 ml acid hydrolyzed TEOS solution (1:1)**.** The color of the cloth remains white.

3.5.7.2.(6). Method-6 (immersion 2:1)

100 ml of 0.001 M $AgNO_3$ was synthesized by plant extract. Then the 40 ml of these synthesized AgNPs was added to the 20 ml acid hydrolyzed TEOS solution (AgNPs: TEOS = 2:1). Subsequently, the scoured fabric was immersed in this solution. After a few minutes, the sol film with AgNPs formed. The color of the fabric also remained white.

3.5.7.2.(7). Method-7 (immersion 1:1)

Same as Method-6 but the ratio of AgNPs: sol-gel is 1:1. Just like Method-5 and Method-6, the color of the fabrics remains white.

3.6. Characterization

3.6.1. XRD

For assessing the crystalline structure of AgNPs and the sol-gel film, XRD (PANalytical, EMPYREAN XRD) was used. The AgNPs-loaded fabric was analyzed using X-ray diffraction. The minimum step size is 0.0001(2θ), and the range of 2θ is 10 to 90. The operation voltage was 40 kV and the current 40 mA with Cu anode. Finally, HighScore plus was used to match the peaks with reference silver materials.

3.6.2. SEM and EDS

For size and shape analysis and to determine the presence of Si and Ag in the fabric sample SEM and EDS of FEI (model Quanta 650) were used.

3.7. Antibacterial Test

The antibacterial tests were done according to AATCC-100 test standard using *S. aureus* (Gram-positive bacteria) and *K. Pneumoniae* (Gram-negative bacteria) with a slight modification. In this method, a 4.8 cm x 4.8 cm square fabric sample was used. First, an inoculum with 100 ml nutrient broth was incubated for 24 hours at 37 ^{0}C. The concentration of bacteria was set to 2 x10^5 cells/ ml by adding Muller Hinton nutrient broth. Then, 1 ml of this inoculum was taken by pipet, poured on each sample, and closed the vessel's lid to prevent evaporation. Subsequently, each sample was again incubated at 37 ^{0}C for 24 hours. After the incubation period, 100 ml of water as buffer solution was added to the vessel with an incubated fabric sample, and the samples were shaken for 1 minute. Then required serial dilution was performed. Next, 0.5 µl of this diluted solution was poured on a Muller Hinton Agar plate. The plates were incubated for another 24 hours. The number of living bacteria on the agar plates were counted. Finally, the following formula calculates the percentage of bacterial reduction after 24 hours incubation period:

$$\text{Reduction rate \%} = \frac{B-A}{B} x100$$

Where B = bacterial colony for the untreated sample

A = bacterial colony for AgNPs treated sample

3.8. Wash fastness

Wash fastness was done according to AATCC 61-2010 (ISO 105-C06). The fabric samples were kept in 120 ml liquor prepared with 4-gram AATCC standard

reference detergent without optical brightener. The machine was run at 40 °C for 45 minutes with 10 steel balls. In this method, one wash cycle is equivalent to 5 home laundry.

3.9. Fabric's pH test

Fabric pH is measured according to ISO 3071 and AATCC 81. In this method, 2-gram fabric samples are cut into small pieces. Then, the pH of distilled water is measured. Next, the cut sample pieces are put in 100 ml water and rotated for 2 hours at 30 rpm. Finally, the pH of this water is measured and recorded.

3.10. Data Analysis and visualization

For data analysis, statistical analysis, and visualization, several python 3.0 libraries such as Pandas, Scipy, and Seaborn were used. As IDE (Integrated Development Environment) the popular web IDE google colab was used. Besides, for scaling, mutual information calculations etc., the famous Scikit-learn machine learning library was used. Statistical tests were done by Scipy and Statsmodels libraries; for post-hoc test Scikit_posthocs library was used.

3.10.1. Data Correlation

Correlation is the measurement of the relationship and direction of the relationship between 2 variables. Compute pairwise correlations. Pearson, Kendall (for ranked data), and spearman method (for ranked data). In this study, Pearson Correlation was used. The mathematical expression of Pearson correlation (Benesty, Jingdong Chen, and Yiteng Huang 2008) is:

$$\rho(x, y) = \frac{E[xy]}{\sigma_x \sigma_y} \tag{4}$$

Where, $E[x, y]$ is cross correlation between x and y

σ_x^2 = E[x^2] and σ_y^2 = E[y^2] is the variance of signals or x and y respectively
For a sample the Pearson correlation Coefficient is:

$$r = \frac{\sum(x_i-\bar{x})(y_i-\bar{y})}{\sqrt{\sum(x_i-\bar{x})^2 \sum(y_i-\bar{y})^2}} \quad (5)$$

Where, r = correlation coefficient
x_i = values of the x-variable in a sample
$\bar{x}$ = mean of the variable of x-variable
y_i = values of the y-variable in a sample
$\bar{y}$ = mean of the variable of y-variable

3.10.2. Mutual information

Mutual information (MI) is a statistical measure of information owned by a variable about another variable. It has 2 main properties 1) it can measure any relationship (including nonlinear relationships) between random variables 2) MI is invariant under any transformations (Vergara and Estévez 2014). Equation 6 is a basic formula for mutual information (Veyrat-Charvillon and Standaert 2009).

$$p(i,j) = \sum_{ij} p(i,j) log \frac{p(i,j)}{p(i).p(j)} \quad (6)$$

In case of independent variables *p(i,j) = p(i).P(j)* and hence $log \frac{p(i).p(j)}{p(i).p(j)}$ =0, which means there is no relation between *p(i)* and *p(j)*. In other words, here, the information is zero.

4. RESULT AND DISCUSSION

During the plant extract amount determination, the influence of temperature was discussed in short. But to analyze the impact of temperature on AgNPs stability and absorbance UV-vis spectroscope was used. The previous study shows that blue shift (i,e shifting towards left) in Uv-vis SPR (Surface Plasmon Resonance) causes smaller nanoparticles and red shit (shifting to right) in Uv-vis spectrum causes larger nanoparticles (Shengtai He et al. 2001) (Darroudi et al. 2011)

4.1. Influence of Temperature on UV-Vis SPR of AgNPs

Table 4.1 shows the effect of temperature of both $AgNO_3$ and pant extract on AgNPs, 0.002 M and 100 ml silver nitrate was taken and added 4 drops (153 µl) of plant extract. All the samples were stable for more than 1 month.

Table 4.1. Effect of temperature on AgNPs UV-SPR and absorption

Sample	$AgNO_3$ (0.002M)	$AgNO_3$ Temp (^{0}C)	PE temp (^{0}C)	reaction time (min)	UV-1	Abs _1_day	UV_4 Days	Abs_4_ days
X1	100 ml	70	70	3	421	0.1829	423	0.2230
X2	100 ml	70	60	1	422	0.2187	423	0.2773
X3	100 ml	70	50	4	421	0.2647	424	0.3174
X4	100 ml	70	40	4	420	0.2505	421	0.2901
X5	100 ml	60	70	14	425	0.0912	428	0.2428
X6	100 ml	60	60	14	417	0.1205	425	0.2922
X7	100 ml	60	50	12	423	0.1298	424	0.3918
X8	100 ml	60	40	12	423	0.1599	424	0.2379
X9	100 ml	50	70	36	424	0.1034	425	0.1908
X10	100 ml	50	60	26	416	0.0764	426	0.1633
X11	100 ml	50	50	42	424	0.1334	425	0.2322
X12	100 ml	50	40	42	425	0.0884	428	0.1613
X13	100 ml	40	70	180	416	0.0523	429	0.1244
X14	100 ml	40	60	180	424	0.0533	430	0.1342
X15	100 ml	40	50	180	424	0.0683	431	0. 1658
X16	100 ml	40	40	180	424	0.0804	428	0.1686

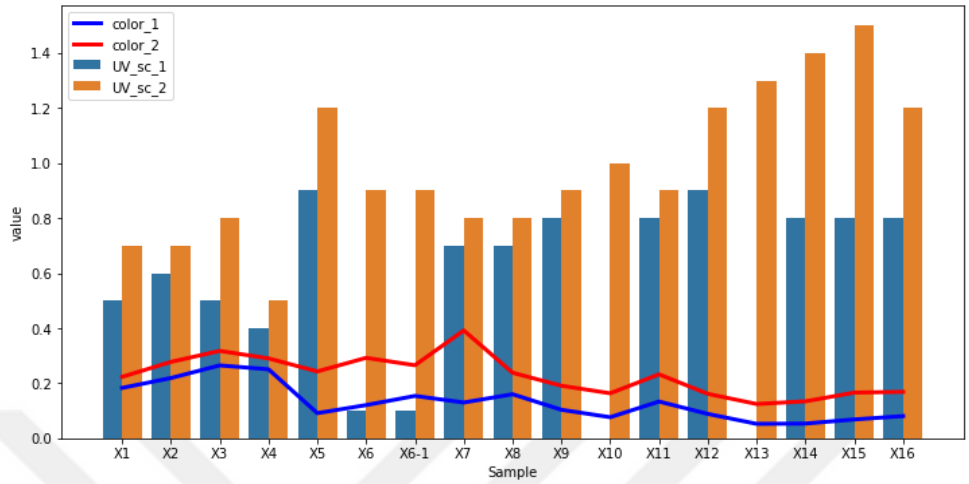


Figure 4.1. Temperature on AgNPs formation and UV spectrum

Table 4.1 and figure 4.1 show that the lower UV spectrum (nm) value is lowest (417 nm) at 60°C for both silver nitrate and plant extract. But the UV spectrum is rapidly increased in case of lower temperature (40 ^{0}C) for silver nitrate solution. Silver nitrate solution is much more than that of plant extract. But the temperature is essential in both cases. Temperature below 40°C for plant extract will not disperse or activate and consequently oxidize silver nitrate.

Sastry et al. (2008) show that high temperature will disorder $AgNO_3$ structure (Pbca) and slight thermal expansion along the c-axis. More specifically, the temperature will decrease the O1-N-O2 angle, whereas it the O2-N-O3 angle will increase non-linearly with temperature. Probably, for this reason, the low temperature cannot synthesize AgNPs. However, does the effect of temperature from 40 °C to above really significant? To know the answer, some statistical tests are done.

4.1.1. Data distribution for effect on temperature

The data distribution should be observed to determine the appropriate statistical test. Figure 4.2 shows the Q-Q plot of the data. It shows data distribution

is not normal. Moreover, the Shapiro-Wilks test and Bartlett's test reject the ANOVA assumptions. Hence non-parametric test will be more appropriate here. As there are more than 2 groups, the Kruskal-Wallis test is conducted.

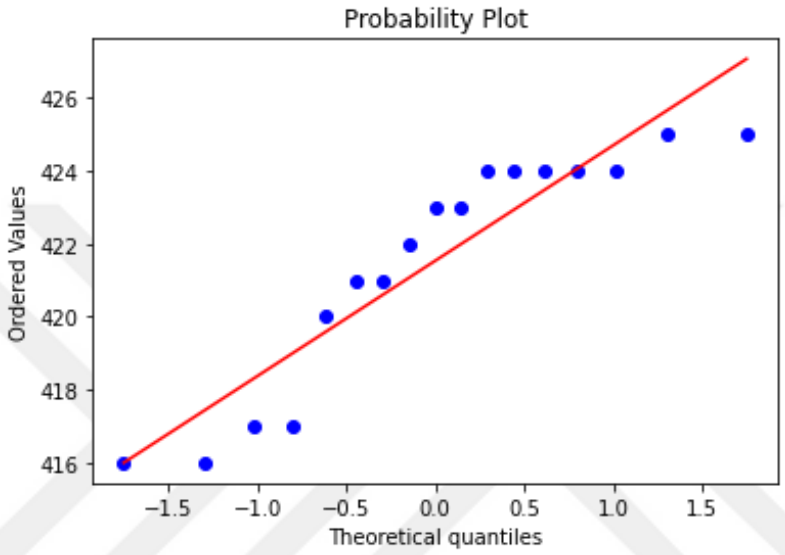


Figure 4.2. Q-Q plot of UV- spectrum for different $AgNO_3$ temperature

4.1.1.1. Shapiro-Wilks test of Normality

Table 4.2. Shapiro-Wilks Normality test

	statistics	p-value
Shapiro- Wilks test	0.84517	0.009

The null hypothesis for Shapiro- Wilks test (table 4.2) is- data is normally distributed (H0 = data are normally distributed). But, the p-value is much less than the significance value (0.05). Hence, Shapiro-Wilks test confirms that the data is not normally distributed.

4.1.1.2. Bartlett's Homogeneity test

Table 4.3. Bartlett's Homogeneity test

Variables	Statistic	p-value
$AgNO_3$ Temp	10.14	0.017

The small p-value of Bartlett's test (table 4.3) concludes that the population does not have equal variance; hence they are not homogeneous.

In the dataset, 2 independent variables have categorical subgroups. Hence Kruskal-Wallis tests are done separately. The results are in the following table 4.4:

Table 4.4. Kruskal-Wallis test

Test name	Source	df	statistic	P-value
Kruskal-Wallis test	$AgNO_3$ Temperature	3	5.04491	0.65448
	Plant extract	3	5.683	0.1280
	Temperature			

The p-value in the Kruskal-Wallis test is more than 0.05; hence null hypothesis can not be rejected. Hence, temperature has no effect on UV-vis spectrum. For confirmation- Dunn’s post hoc test is also done:

4.1.1.3. Dunn’s post hoc Test

From the Dunn’s post hoc test (table 4.5) it is clear that in all the cases, the Kruskal-Wallis test fails to reject the null hypothesis. So it cannot be concluded that temperature affects the AgNPs’ stability and size.

Table 4.5. Dunn's post hoc test

Subject	Temp	40 °C	50 °C	60 °C	70 °C
$AgNO_3$_Temp	40 °C	1.000000	0.803445	0.626095	0.302484
$AgNO_3$_Temp	50 °C	0.803445	1.000000	0.453505	0.200541
$AgNO_3$_Temp	60 °C	0.626095	0.453505	1.000000	0.548728
$AgNO_3$_Temp	70 °C	0.302484	0.200541	0.548728	1.000000
PE_Temp	40 °C	1.000000	0.886903	0.126227	0.643919
PE_Temp	50 °C	0.886903	1.000000	0.167822	0.748966
PE_Temp	60 °C	0.126227	0.167822	1.000000	0.297448
PE_Temp	70 °C	0.643919	0.748966	0.297448	1.000000

4.2. Different concentration of $AgNO_3$ on AgNPs formation

To evaluate the effect of $AgNO_3$ concentration on nanoparticle stability, different concentrations with the same volume were taken. The plant extract is determined according to the molarity and volume. The temperature for both plant extract and $AgNO_3$ were kept 60 °C.

Table 4.6. Different concentration of silver nitrate on UV-vis spectrum

$AgNO_3$ molarity	$AgNO_3$ amount	Plant extract	Time	UV-1 (nm) (day-1)	Absorption	UV-2 (nm) day-2	Stability
0.001M	100	2 drops	15 min	423	0.169	425	60 days
0.002 M	100	2 drops	10 min	417	0.072	424	60 days
0.003 M	100	2 drops	24 hrs	421	0.098	425	50 days
0.005 M	100	6 drops	50 sec	424	0.197	426	25 days
0.01 M	100	14 drops	6 min	430	0.618	430	7 days
0.1 M	100	18 drops	instant	432	0.821	Aggr. (20hrs)	20 hrs
0.1 M	20	2 drops	instant	445	0.272	No	3 hours

The first UV-Vis spectrum has been taken after 2 hours of solution preparation so that the solution has enough time to get synthesized. Table 4.6 depicts $AgNO_3$ molarity, UV spectrum, and stability interaction. For visualizing the UV spectrum, the data was scaled within 1. The stability is log-transformed as it is a log-normal distribution where some samples have much more stability than others.

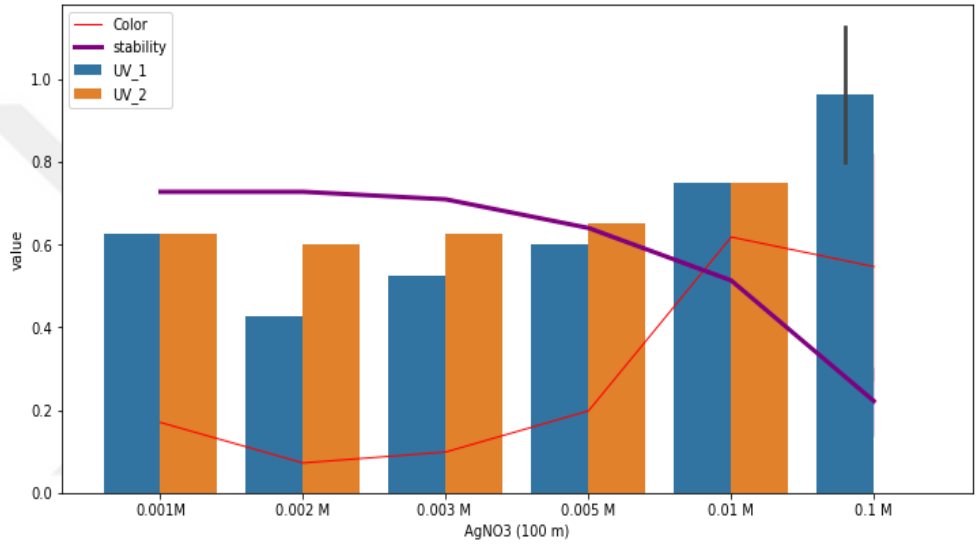


Figure 4.3. UV spectrum of $AgNO_3$ having various molarity

Figure 4.3 shows that high molarity causes high UV-spectrum and low stability and vice versa. In the case of 0.001 M, the used plant extract is excess which causes relatively high absorbance, and the UV spectrum is also comparatively high. In all other cases, it maintains the same pattern. The increase of molarity will increase the UV-Vis SPR and thus increase nanoparticle size and decrease stability. The high morality of silver nitrate is tough to make stable for several days.

4.3. The different volumes of $AgNO_3$ on AgNPs formation

$AgNO_3$ molarity is closely related to the amount. However, the influence of $AgNO_3$ volume was determined by keeping the silver nitrate molarity the same. Plant

extract cannot be kept constant as high molarity and high volume need more plant extract; otherwise, there will be no nanoparticles. Table 4.7 depicts 4 categories of $AgNO_3$ molarity (0.01, 0.1, 0.005 and 0.002) with different volumes in each category. From table 4.7 and figure 4.4, it is clear that there is no noticeable relationship between $AgNO_3$ volume with UV spectrum and stability. Rather $AgNO_3$ molarity plays the most crucial role in this aspect, as shown in figure 4.4.

Table 4.7. $AgNO_3$ volume on UV spectrum and stability

$AgNO_3$ Molarity	$AgNO_3$ amount	PE amount	Time	Temp (ºC)	UV_2 hrs	Absor bance	UV_ 24hrs	Stability (atleast)
0.01 M	25	1 drop	5 min	60	421	0.2715	429	14 days
0.01 M	50	2 drops	1800 min	60	429	0.1349	430	3 days
0.01 M	55	6 drops	Instant	60	417	0.5059	430	4 days
0.01 M	100	14 drops	6 min	50	421	0.618	429	7 days
0.1 M	20	6 drops	instant	60	445	0.272	0	3 hrs
0.1 M	10	2 drops	instant	70	431	0.6076	440	1 day
0.1 M	116	8 drops	instant	65	432	0.7604	445	20 hrs
0.005 M	155	6 drops	50 sec	60	424	0.5321	429	25 days
0.005 M	200	4 drops	2 min	60	425	0.4509	433	30 days
0.005 M	500	14 drops	5 min	60	425	0.4106	425	20 days
0.002 M	120	7 drops	3 min	50	416	0.2298	421	60 days
0.002 M	100	2 drops	15 min	70	423	0.1699	425	60 days

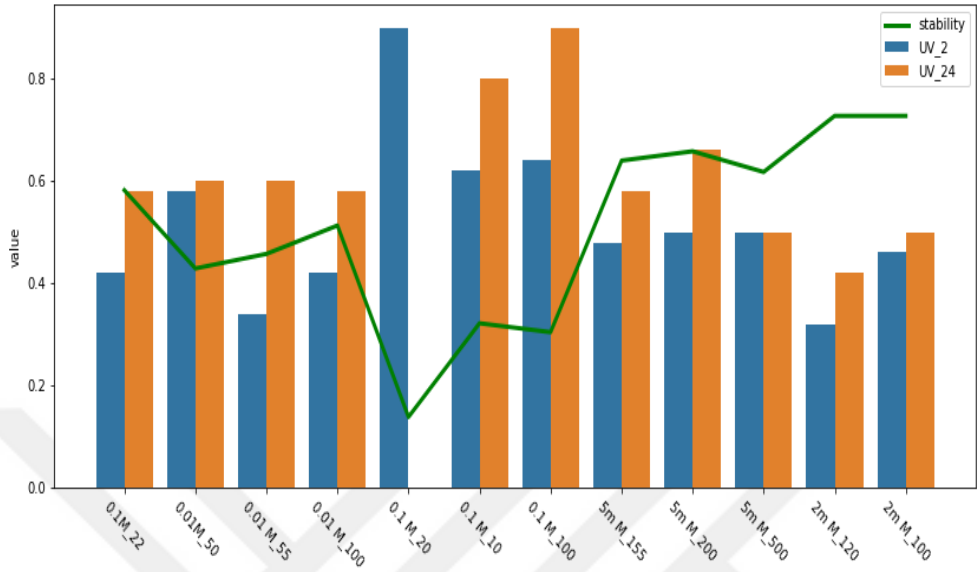


Figure 4.4. $AgNO_3$ volume on AgNPs

Basically, the influential roles are played by $AgNO_3$ molarity and plant extract amount. The high molarity tends to aggregate more quickly. Figure 4.3 depicts the relation between molarity and stability. The data is based on $AgNO_3$ molarity and the mean of stability. As there are few subgroups of $AgNO_3$ molarity, a statistical test can be applied here.

4.3.1. Data distribution

Figure 4.5 shows the Q-Q plot of the data related to $AgNO_3$ molarity and volume to stability. It shows data is normally distributed. In addition, the Shapiro-Wilks test for normality and Levene's Homogeneity test has also been conducted.

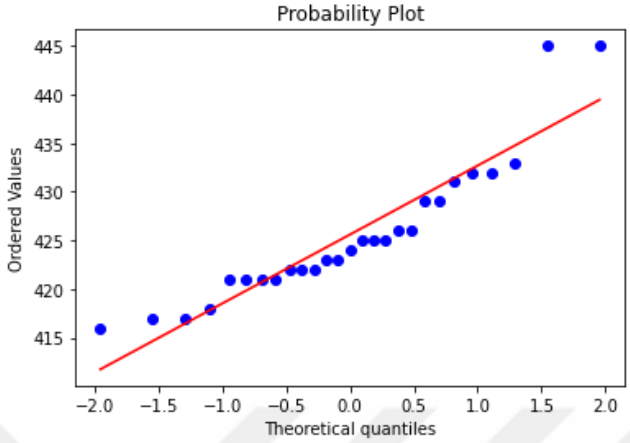


Figure 4.5. Q-Q plot of UV on the influence of $AgNO_3$ Molarity and Volume

4.3.1.1. Shapiro-Wilks test of Normality

For normality of data, Shapiro-Wilks test is done as shown in table 4.8.

Table 4.8. Shapiro-Wilks normality test for $AgNO_3$ Molarity

	Statistic	p-value
Shapiro-Wilks test	0.880	0.092

Here the p-value of the Shapiro-Wilks test is larger than the significance value, so it fails to reject the null hypothesis. Hence the UV spectrums are normally distributed.

4.3.1.2. Levene's and Bartlett's Test for homogeneity

If Levene's test is significant, ANOVA and Post Hoc should not be implemented. However, Levene's homogeneity test shows the null hypothesis (H0 = population variance are equal) cannot be rejected (table 4.9). So the population data is homoscedastic. Hence ANOVA test can be conducted.

Table 4.9. Tests for homogeneity of $AgNO_3$ molarity on UV-vis

Test name	statistics	p-value	df
Levene's Test	0.4793	0.7046	3
Bartlett's Test	5.549	0.1357	3

4.3.2. ANOVA

Hence the dataset is fit for the ANOVA test. Table 4.10 depicts the ANOVA test results. It shows in 3 cases the p-value rejects the null hypothesis. They are: the $AgNO_3$ molarity, $AgNO_3$ molarity + plant extract, and $AgNO_3$ molarity + $AgNO_3$ volume (table 4.10)

Table 4.10. ANOVA table for different variable

Parameters	**SS**	**df**	**F**	**P-value**
$AgNO_3$_Molarity	426.810870	1.0	30.405629	**0.000893**
$AgNO_3$_Volume	26.047554	1.0	1.855605	0.215341
PE	8.986223	1.0	0.640171	0.449945
$AgNO_3$_Molarity:PE	121.489024	1.0	8.654771	**0.021655**
$AgNO_3$_M:$AgNO_3$_V	121.452009	1.0	8.652134	**0.021669**
Residual	98.260624	7.0	NaN	NaN

4.3.3. TUKEY'S HSD test

Tukey's HSD test was done on all variables against the UV-vis spectrum to determine more specific interactions among variables. But all variables fail to reject the null hypothesis except the $AgNO_3$ molarity. Table 4.11 depicts Tukey's HSD test on $AgNO_3$ molarity to UV-vis spectrum.

Table 4.11. TUKEY's HSD test on influence of $AgNO_3$ Molarity on UV-vis SPR

Multiple Comparison of Means - Tukey HSD, FWER=0.05

group1	group2	Mean diff	p-adj	lower	upper	reject
0.002	0.005	4.0	0.7539	-8.9235	16.9235	False
0.002	0.01	1.3333	0.9	-10.7555	13.4221	False
0.002	**0.1**	**15.3333**	**0.0209**	**2.4099**	**28.2568**	**True**
0.005	0.01	-2.6667	0.8983	-14.7555	9.4221	False
0.005	0.1	11.3333	0.089	-1.5901	24.2568	False
0.01	**0.1**	**14.0**	**0.0239**	**1.9112**	**26.0888**	**True**

Hence, it can be concluded that $AgNO_3$ concentration can only affect the UV-Vis spectrum (figure 4.6). Other parameters such as $AgNO_3$ amount, plant extract, etc., can influence other factors.

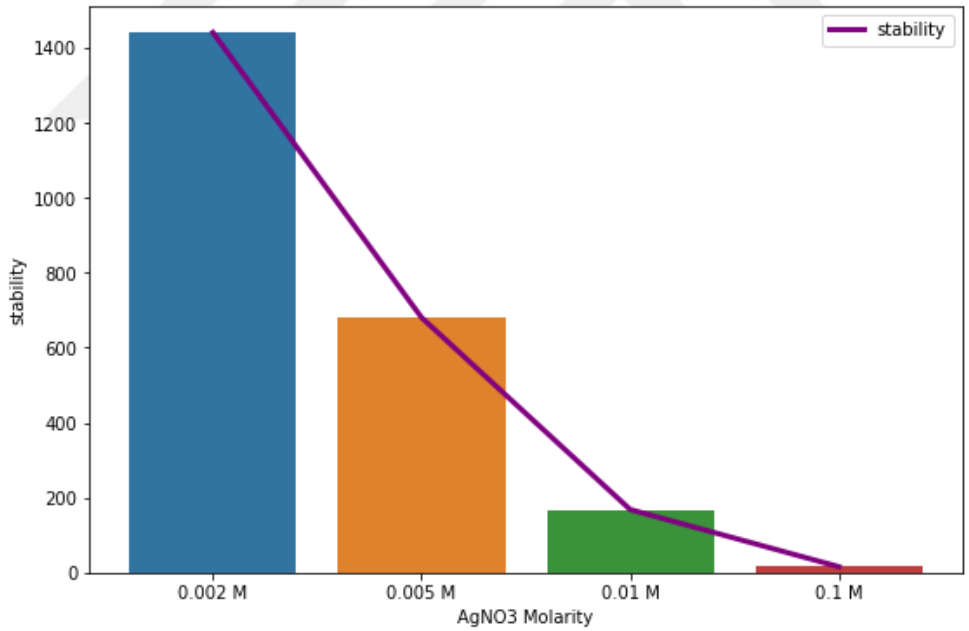


Figure 4.6. $AgNO_3$ molarity on AgNPs stability

4.4. Amount of Plant Extracts on AgNps formation:

From the above experiments, it is easily understood that plant extract is another crucial factor for AgNPs. From the ANOVA test (table 4.10), it is easily understood that plant extract has a significant effect in combination with $AgNO_3$ molarity. Hence, to determine the influence of plant extract on the UV-vis spectrum, different amounts of plant extract ranging from 2 to 26 drops with constant molarity have experimented. The data have been visualized by scaling in figure 4.7. It shows higher amount of plant extract causes a higher UV spectrum and lesser reaction time. Besides, the absorption value is also proportional to the plant extract. In table 4.12, with the plant extract 5 ml of water had been added to each experiment. Both the $AgNO_3$ solution and plant extract are very low; hence the reaction is also super slow. The UV-vis was taken after 6 days.

Table 4.12. Effect of different plant extract on AgNPs

code	$AgNO_3$ (100 ml)	Temp (both) (^0C)	Plant extract (drops)	Water added to PE (ml)	Reaction time	UV (nm)	Color
K1	0.001 M	70	2	5	48 hours	425	0.01699
K2	0.001 M	70	4	5	24 hours	426	0.0528
K3	0.001 M	70	6	5	24 hours	436	0.1867
K4	0.001 M	70	8	5	24 hours	437	0.1687
K5	0.001 M	70	26	5	5 min	441	0.5437
C1	0.002 M	60	2	0	10 min	417	0.072
C2	0.002 M	60	4	0	7 min	421	0.1538
C3	0.002 M	60	5	0	6 min	423	0.1092
C4	0.002 M	60	6	0	5 min	425	0.194
C5	0.002 M	60	7	0	4 min	433	0.2464
M1	0.002 M	60	1	2	24 hours	423	0.1178
M2	0.003 M	60	3	2	5 min	426	0.1928
M3	0.003 M	60	4	2	2 min	429	0.2343
M4	0.003 M	60	2	0	24 hours	421	0.0985
M5	0.003 M	60	2	5	4 min	429	0.1779

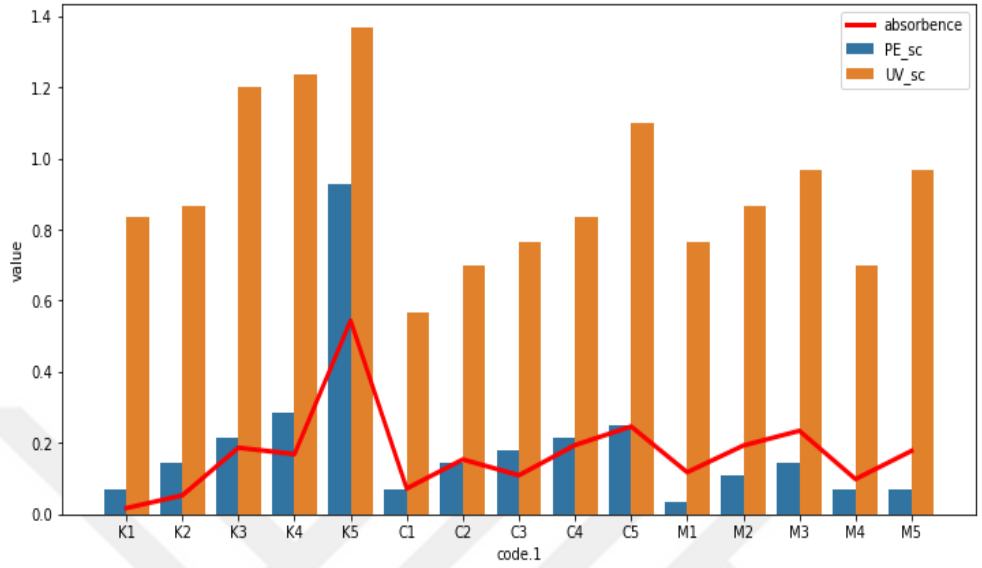


Figure 4.7. Plant Extract on UV spectrum

From figure 4.7 it is seen in almost all the cases that the amount of plant extract is proportional to the UV-Vis spectrum. The higher the plant extract, the higher the UV-vis spectrum. The exceptions are in samples M4 and M5. The added 5 ml water causes it to the 2 drops of plant extract in the M5 sample. The added water will help in dispersing the phytochemicals more, and hence the plant extract will treat like 5 ml (containing much lower phytochemicals than that of 5 ml plant extract). The absorbance (visual color) is also proportional to the UV spectrum.

The $AgNO_3$ molarity, amount, and respective plant extract amount are highly interrelated, and it is impossible to infer any quantitative relation among them, keeping all other variables constant. For example, plant extract and $AgNO_3$ molarity can not be kept constant simultaneously.

4.5. Green Synthesis Mechanism

When a few drops of plant extract are added to the $AgNO_3$ solution, three tasks happen simultaneously, reduction, nucleation, and stabilization figure 4.8.

a) Reduction:

The co-enzymes present in the phytochemicals, such as $NADP^+$ or NAD^+, carry hydrogen atoms (H) and electrons. The $NADP^+/NAD^+$ accepts two electrons (since H has 2 electrons) and is converted to NADPH/NADH. Later the NADPH/NADH supplies two electrons to the silver nitrate (Guilger-Casagrande and Lima 2019) (Anil Kumar et al. 2007). In the same way, co-enzyme-dependent nitrate enzymes also reduce silver ions (Kalimuthu et al. 2008) (Gudikandula, Vadapally, and Singara Charya 2017).

$$NAD^+ + 2H^+ \rightarrow NADH - 2e^-$$
$$2Ag^+ + 2e^- \rightarrow 2Ag^0$$

b) Nucleation:

The formed Ag^0 atoms are needed to nucleate to form nanoparticles. Nanoparticles are associated with the formation of a new volume, and the new surface will create free energy. This free energy initiates the nucleation process. For spherical particles, the free energy shift is as follows: -

$$\Delta G = \frac{-4}{V}\pi r^3 k_b T ln(S) + 4\pi r^2 \gamma$$

Where, V= molecular volume; r = radius of nuclei, kb = Boltzmann constant, S= saturation ratio, γ = surface free energy per unit surface area (Burda et al. 2005).
The free energy shift decreases when the particle size gets bigger than the critical size and forms a stable particle (nanoparticles).

c) Limiting Aggregation (Stabilization):

The particle formation initiates a drop in the solution concentration, and when it drops below the critical level, the molecular addition starts postponing the

nucleation. For uniform size distribution, short nucleation is desirable (Burda et al. 2005). Here, the smaller particles begin to grow swiftly due to their high free energy (Peng, Wickham, and Alivisatos 1998). Hence, the aggregation will make the particles bigger unless it is not stopped. Consequently, the comparatively large particles will grow up, and minute particles will be smaller and eventually disappear through Ostwald ripening (S. Li et al. 2007). So, aggregation must have to prevent. In this case, the functional groups (-OH, >C=C<) of *C.arvensis* extract will attach to the nanoparticle (as polar head) and cause the limiting aggregation or stabilization (Makarov et al. 2014).

In this way, the obtained green synthesis AgNPs are spherical. However, in some cases, the shape can be cubic or square. The mechanism of cubic shape is similar, but here, the thermodynamic equilibrium or Gibbs free energy by the added NaOH in fabric pretreatment will lead the shape to cubic. Figure 4.9 shows the mechanism of *in-situ*.

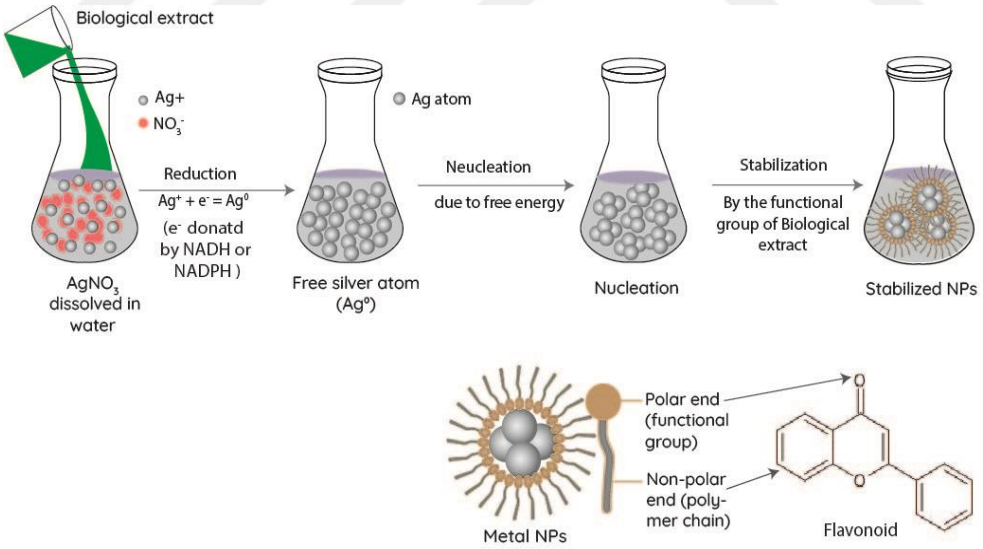


Figure 4.8. Green synthesis mechanism (T. Ahmed and Ogulata 2021)

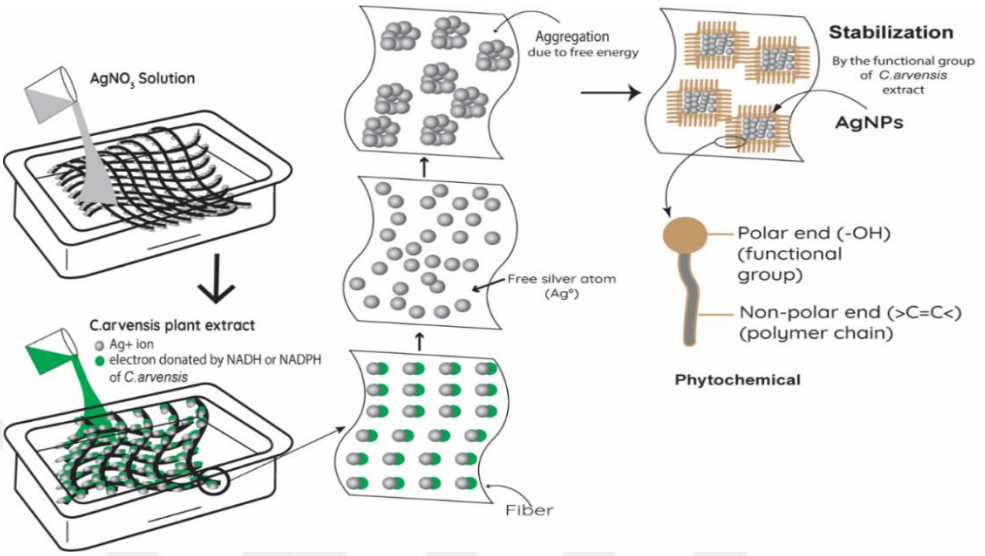


Figure 4.9. Green synthesis mechanism (in-situ method)

4.6. Sol-gel Mechanism

The sol-gel preparation depends on multiple factors. The most important two are acid hydrolysis time (ageing) and pH.

4.6.1. Influence of pH

Venkateswara Rao and Bhagat (2004) hypothesized gelation would take at least 3 days without any alkaline. But in this study, no gel, even after a couple of months, had been formed. However, adding a very little amount (1 or 2 drops) of alkaline (such as NaOH or NH_4OH) will cause gelation within a few minutes. Importantly, if the alkaline solution is added before acid hydrolysis, the acid and alkali will react, and there will be no gel.

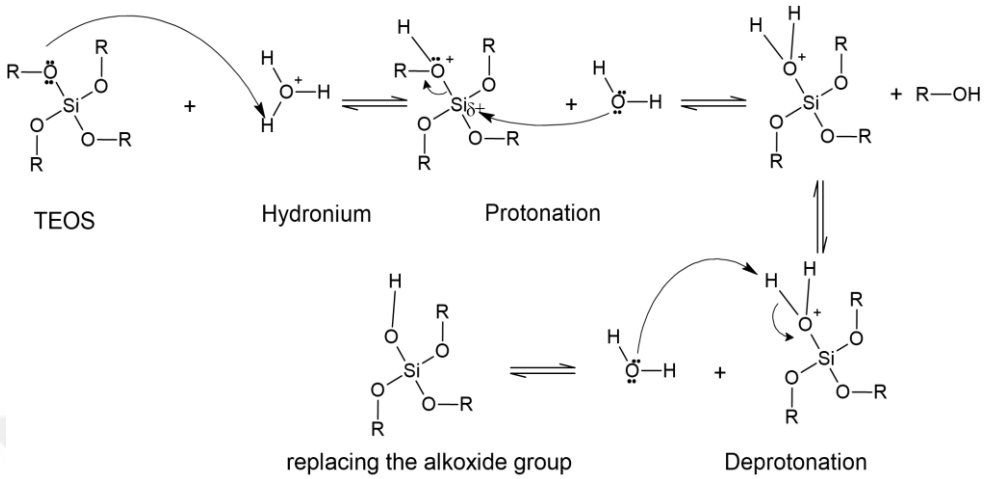


Figure 4.10. Acid hydrolysis of TEOS

Figure 4.10 shows the acid hydrolysis of TEOS. The added acid will cause hydronium ion (H_3O^+), which will protonate the alkoxide groups (-OR). Due to this protonation, the alcohol (R-OH) group will be released as the -OH leaving group, and simultaneously partially positive silicon group will attract the water molecule. Then it will deprotonate, leaving a silanol group (Si-OH). Finally, the entire alkoxide groups (-OR) will be replaced by the hydroxyl groups (-OH). These alkoxide groups are pretty stable and will not attach to each other without any alkaline catalyst. As soon as an alkaline solution is added, the condensation process starts (figure 4.11).

In figure 4.11, the –OH groups of alkaline solution (NH_4OH or NaOH) will take proton and leave the nucleophilic O^-. On the other hand, the pi-electron resonance of oxygen (O) causes a partial positive ion in silicon ($Si_{\delta+}$) and makes it an ideal electrophile. Hence, O^- will be bonded with this silicon. A complex and highly cross-linked polymer (i, e gel) will be formed. pH normally ranged from 1-5, it promotes a controllable gelation (Hernández-Barrios et al. 2017). According to this investigation, after acid hydrolysis (ageing) the pH is around 3. When adding alkali, reach the pH of about 8.9, and then the gel will be formed within 8 min.

However, this time may vary based on the TEOS concentration and other factors such as aging time, temperature, etc.

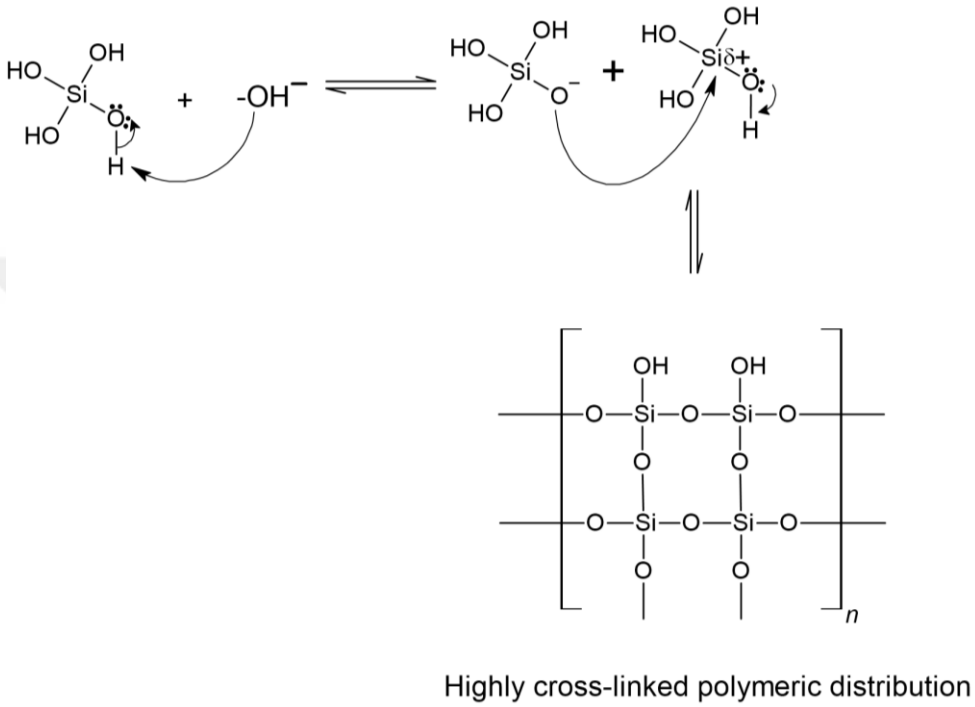


Figure 4.11. Condensation after acid hydrolysis

4.6.2. Influence of acid hydrolysis time

The TEOS and Ethanol solution must be hydrolyzed with an acidic solution. This reaction is slow and needs a long time. The time was investigated at different temperatures. For this purpose, the TEOS, Ethanol, and acid solution were mixed together and kept at three different temperatures 3 ^{o}C, room temperature (25 ^{o}C), and 60 ^{o}C. In each 2 hours interval, a few drops of NH_4OH was added to 5 ml TEOS solution to set pH 8.5 and mixed with a propeller stirrer to observe colloidal gel and gel formation. Table 4.13 and figure 4.12 depict the result.

Hence, it can be concluded that temperature can speed up the gel formation process. Low temperatures will need more time to form a gel. For example, at 60 °C,

the acid reaction time should be more than 5.30 hours. In case of room temperature, this duration should be more than 6.30 hours, and for 3 °C this duration should be more than 8 hours. However, this gelation may be affected by the concentration of TEOS, alkaline, etc.

Table 4.13. Influence of time on esterification and sol-gel formation

Sample	TEOS (ml)	Acid reaction temperature (^{0}C)	Acid reaction Time (hours)	Result	Gelification Time (min)
1	5	3	2	Nothing	-
2	5	Room temp	2	Nothing	-
3	5	60	2	Nothing	-
4	5	3	4.50	Nothing	-
5	5	*Room temp*	*4.50*	*Colloidal gel (20 min)*	*20*
6	5	*60*	*4.50*	*Colloidal gel (20 min)*	*20*
7	5	3	5.50	Nothing	-
8	5	Room temp	5.50	Nothing	-
9	5	**60**	**5.50**	**Gel in 13 min**	**13**
10	5	3	6.50	No *Colloidal gel*	-
11	5	**Room temp**	**6.50**	**Gel (15 min)**	**15**
12	5	3	*7.50*	*Colloidal gel (20 min)*	*20*
13	5	**3**	**8**	**Gel (15 min)**	**15**

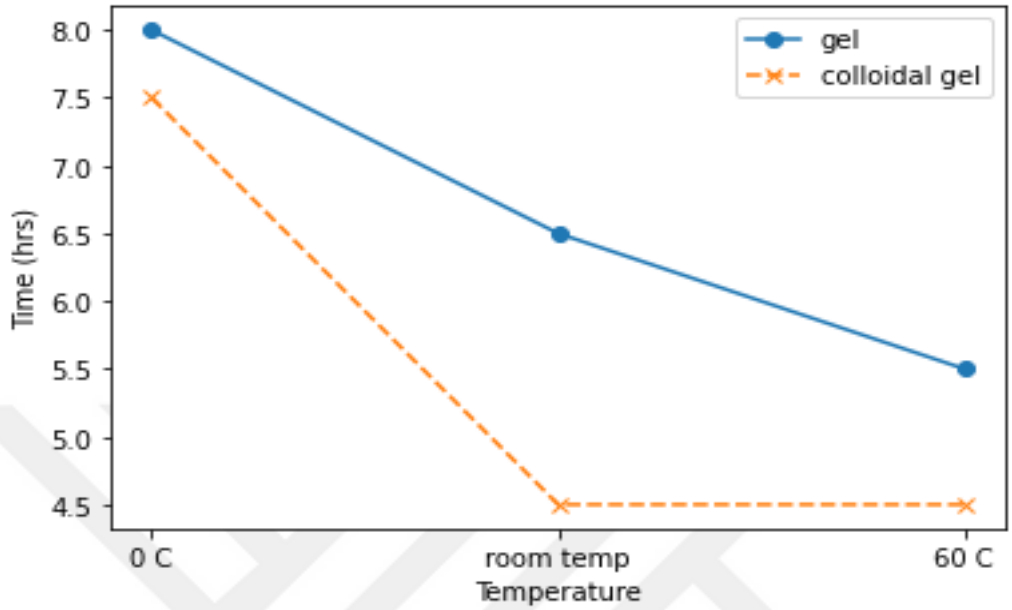


Figure 4.12. Time required for gel and colloidal gel

4.6.3. Influence of temperature on gelation

To understand the effect of temperature on gel formation. First, the TEOS and acidic solution are allowed to get acid hydrolyzed. Then 7 drops of NH_4OH are added to the hydrolyzed solution and kept in three different conditions (0 ^{0}C, Room temperature, and 60 ^{0}C). The results are depicted in table 4.14.

Table 4.14. Temperature has effect on sol-gel formation of hydrolyzed solution

TEOS (ml)	Ethanol (ml)	Acid (m)	Acid reaction time (hrs)	Reaction Temperature	Alkali (drops)	Gelification time (min)
20	84	4	18.	3 ^{o}C	7	30
20	84	4	18	60 ^{o}C	7	30
20	84	4	18	Room temp	7	30

The temperature does not affect gel formation. In addition, because the condensation reaction is comparatively quicker, the molecular mobility will not be affected more in this reaction.

4.7. XRD of Green synthesized AgNPs

XRD tests are done for the different samples prepared with other methods (immersion, in-situ, and pad-dry-cure). All the sample shows different patterns in a close look. The XRD pattern of AgNPs showed several intense peaks at different 2-theta values ranging from 20 to 80 (as shown in Figures 4.13, 4.14). According to our calculation, the crystallinity of AgNPs in the sample is about 74%. The figure depicts various lattice parameters (miller index) (hkl). The crystals from figure 4.13 are indexed as hexagonal and orthorhombic crystal systems (ICSD: 161580- AgI and ICSD: 30516- CAgNO- Silver Fulminate). On the other hand, figure 4.14 is indexed as only an orthorhombic crystal system (ICSD: 30516- CAgNO). The average crystal size is 6.60 nm which is calculated by the Scherrer equation where K= 0.90 and λ = 1.540598 (CuKα).

$$D = \frac{K\lambda}{\beta cos\theta}$$

The d-spacing is calculated using the Braggs law:

$$\lambda = 2dsin\theta$$

The lattice constants (a,b,c) are different in most of the crystals, the lattice constants were calculated by using the following formula.

$$\frac{1}{{d_{hkl}}^2} = \frac{h^2}{a^2} + \frac{k^2}{b^2} + \frac{l^2}{c^2}$$

The calculated lattice parameters are very close to the reference (Table 4.15).

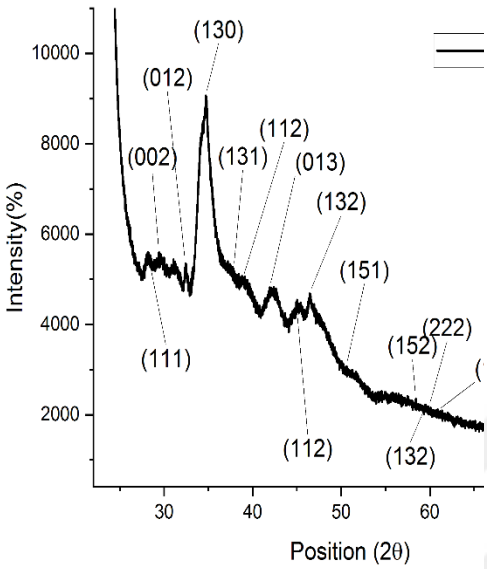


Figure 4.13. XRD of spherical shaped AgNPs

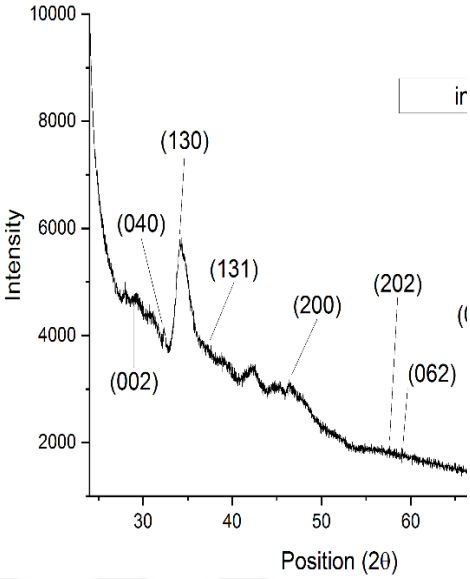


Figure 4.14. XRD of squared shaped AgNPs

From figures 4.13 and 4.14, it is clear that a spherical shape has many close-packed crystals, whereas a squared shape has a large number of loosely packed crystals. The loosely packed crystal will have more free energy, and hence they will orient more robustly. Additionally, the little bit of added alkaline condition will produce some small nanoparticles, which will be attached to the main nanoparticles. In this way, they will form a cubic shape. Hence, the cubic shape will be a little bit bigger than the spherical.

Table 4.15. XRD parameters for C.arvensis synthesized AgNPs

2*θ*	(hkl)	Micro strain	Lattice a	*Ref. of lattice a*	Lattice b	*Ref. of lattice b*	Lattice c	*Ref. of lattice c*
22.4	(012)	0.026			10.75	*10.722*		
28.7	(111)	0.005						
30.7	(002)	0.033					5.804	*5.851*
34.0	(130)	0.033	3.88	*3.86*				

4.8. XRD of AgNPs incorporated with Sol-gel method

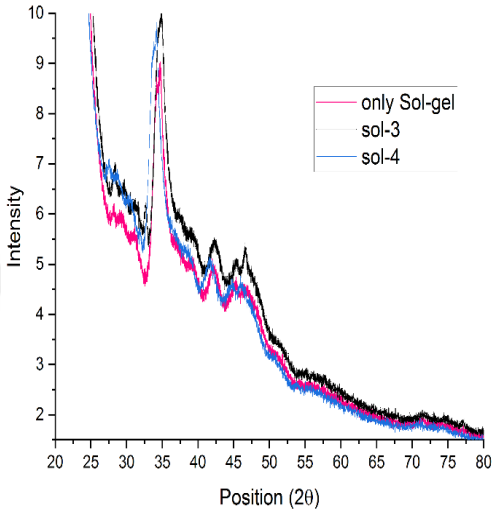


Figure 4.15. XRD comparison of only sol-gel, sol:AgNPs= 1:2, and sol:AgNPs = 1:1

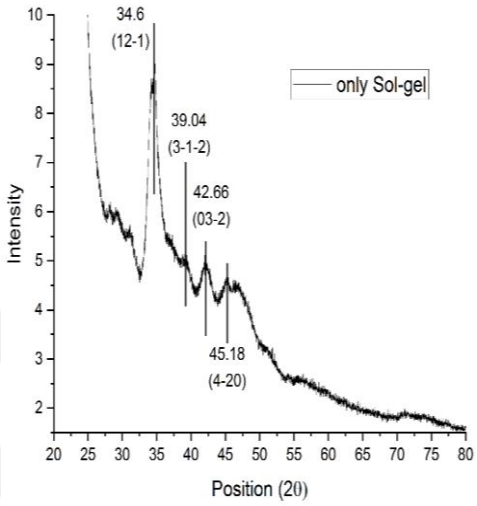


Figure 4.16. XRD of only sol-gel

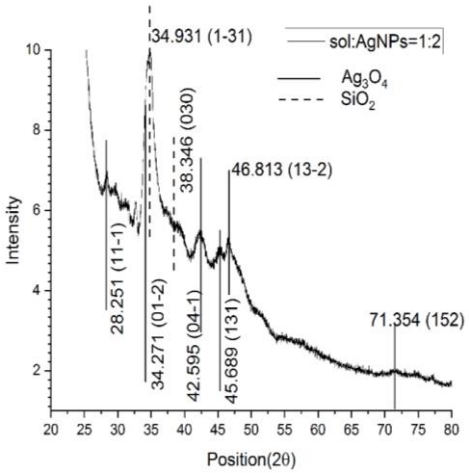


Figure 4.17. XRD of sol:AgNPs = 1:2

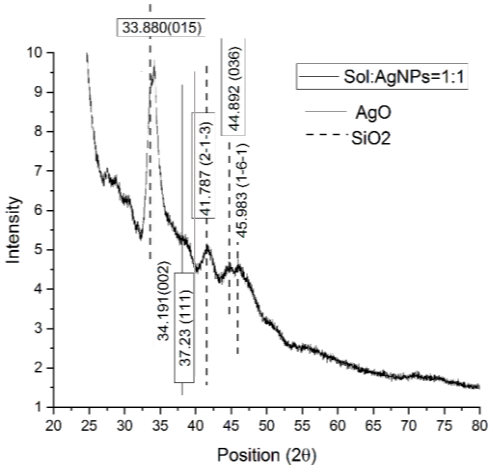


Figure 4.18. XRD of sol:AgNPs = 1:1

The XRD graphs show the comparison of the peaks of only sol-gel and AgNPs-sol combinations. Figure 4.15 shows the comparison of 3 different sol-gel-AgNPs proportions. It shows that there is no apparent difference in the 3 graphs. However, it is distinguishable in a close look. Figure 4.16 (only sol-gel or sol: AgNPs = 1:0) shows 4 intense peaks at different 2 theta positions ranging from 20 to 80. The peaks match with ICSD: 170544 (SiO_2) which are 34.6, 39.04, 42.66, 45.18 having (hkl) value of (12-1), (3-1-2), (0 3-2), (4-20). Figure 4.17 shows 8 peaks; among them, 6 are matched with Ag_3O_4 (ICSD: 59225) and 2 with SiO_2 (ICSD: 170544). The Ag_3O_4 peaks are 28.251 (11-1), 34.271 (01-2), 42.595 (04-1), 45.689 (131), and 71.354 (152), where the digits inside the parenthesis indicate (hkl) values. On the other hand, SiO_2 peaks are 34.931 (1-31), and 38.346 (030). Figure 4.18 shows 6 peaks; among them, 4 peaks match with SiO_2 (ICSD: 170544) 33.880 (015), 41.787(2-1-3), 44.982(036), 45.983 (1-6-1), and rest 2 peaks 34.91 (002), 37.23(111) match with AgO. From figure 4.17 and 4.18 it can be understood that the sol: AgNPs = 1:2 has more portion of Ag than sol: AgNPs = 1:1.

4.9. SEM-image of Green Synthesized AgNPs

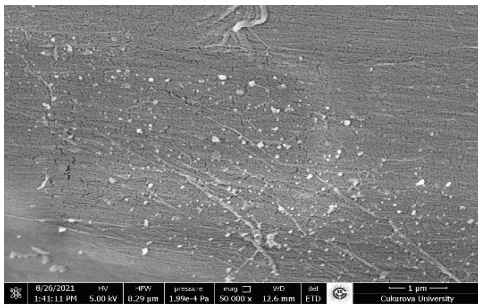


Figure 4.19. in-9mM-0.10-p

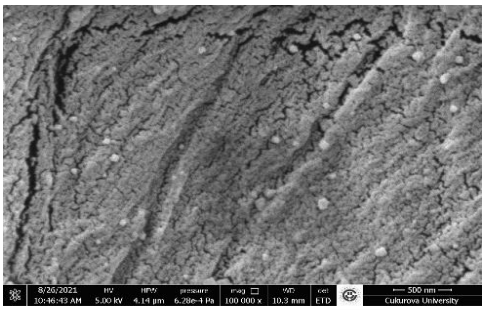


Figure 4.20. imn-2mM-.04-p

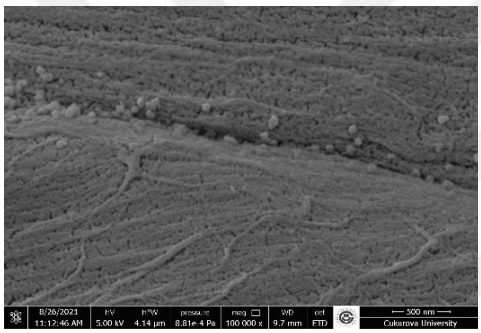


Figure 4.21. imn-2mM-.03-p

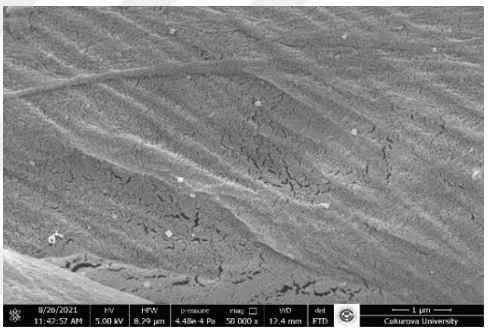


Figure 4.22. in-2mM-.04-k

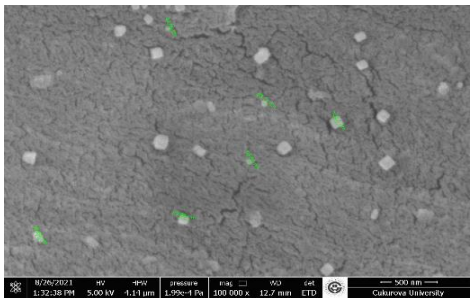


Figure 4.23. in-2mM-.04-p

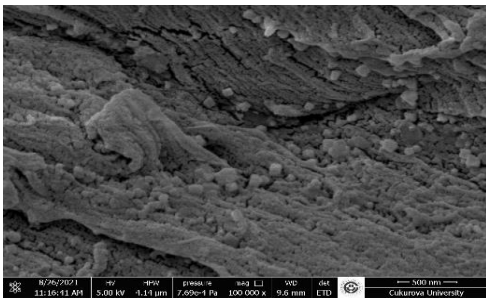


Figure 4.24. im-2mM-.04-p

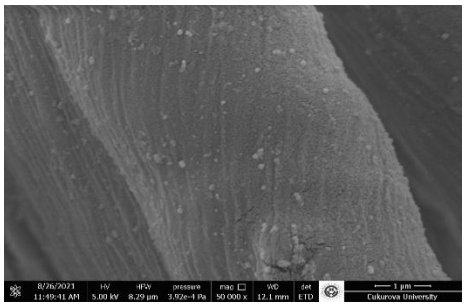


Figure 4.25. in-2mM-.04-t

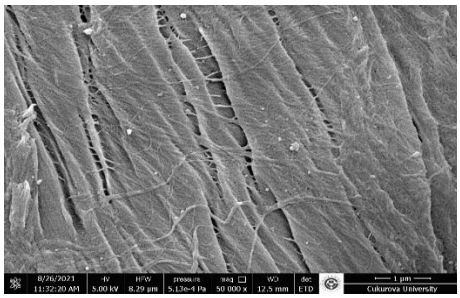


Figure 4.26. imn-2mM-.04-wk

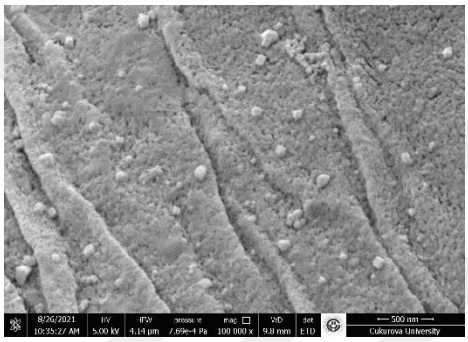


Figure 4.27. pad-2mM-.04-x4

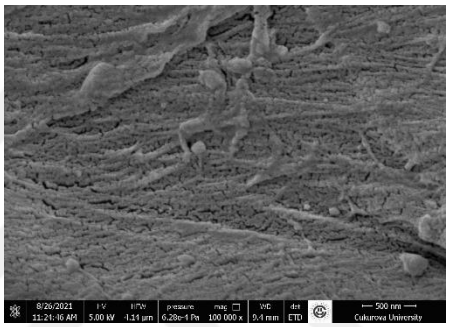


Figure 4.28. pad-2mM-.04-x8

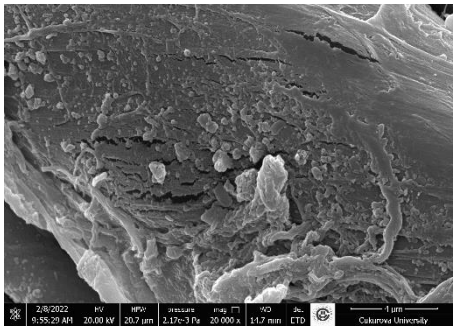


Figure 4.29. in-2mM-2.6-F3

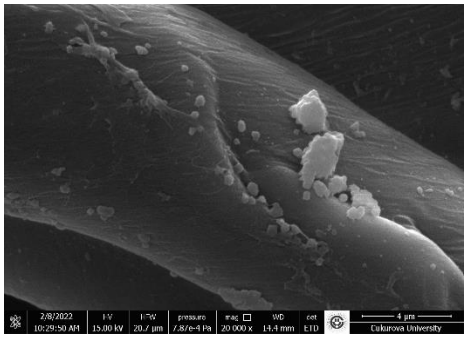


Figure 4.30. in-1mM-.52-or-t

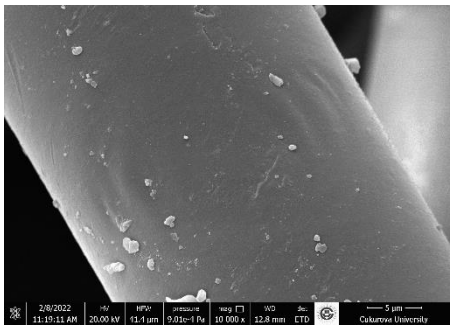


Figure 4.31. in-2mM-2.6-nw-sc

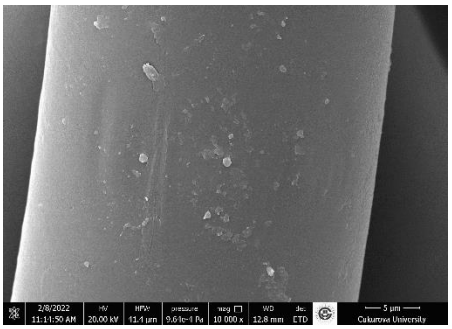


Figure 4.32. ip-1mM-2.6-nw-r

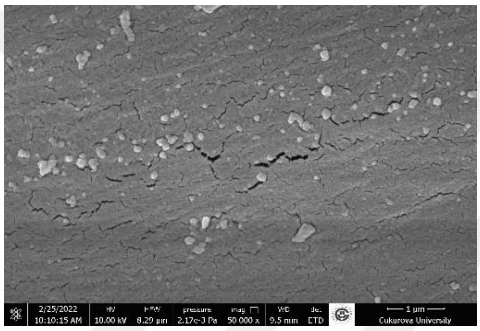


Figure 4.33. in-2mM-2.6-F1

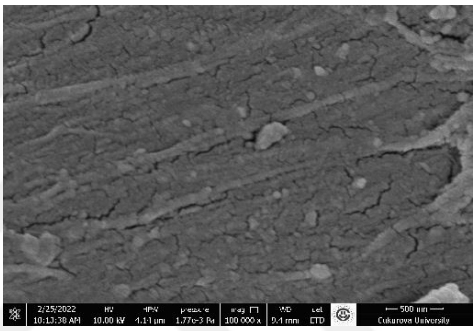


Figure 4.34. p2x-1mM-.03-F2

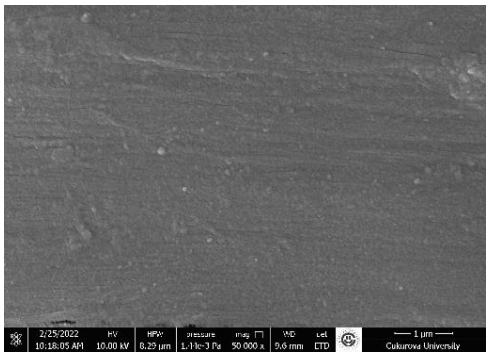


Figure 4.35. p2x-1mM-.03-F3

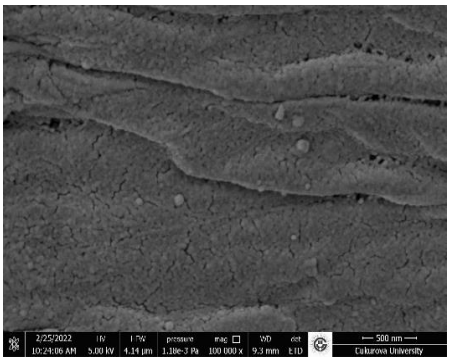


Figure 4.36. im-1mM-.04-F4

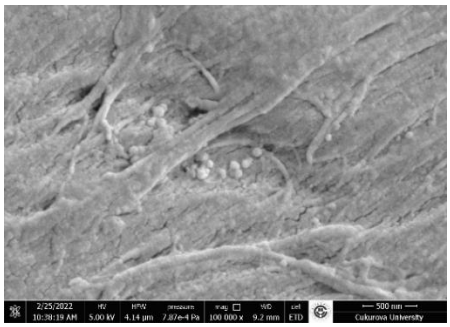


Figure 4.37. p2x-1mM-.03-F5

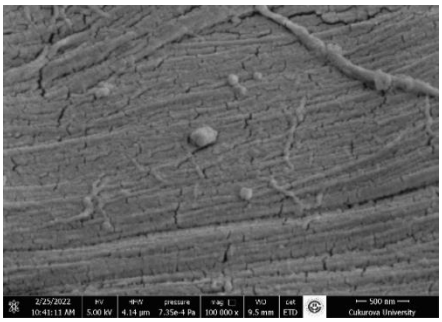


Figure 4.38. p2x-2mM-.04-wk

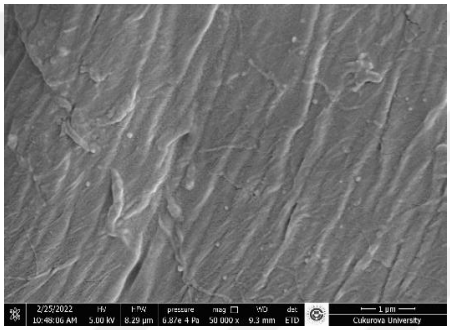


Figure 4.39. p2x-1mM-.03-F7

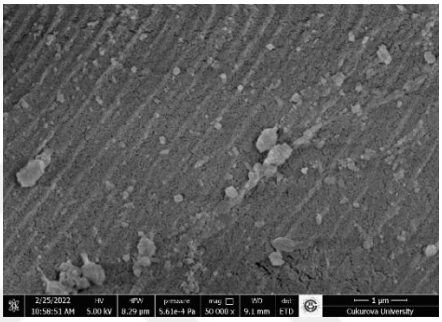


Figure 4.40. in-1mM-1.04-t

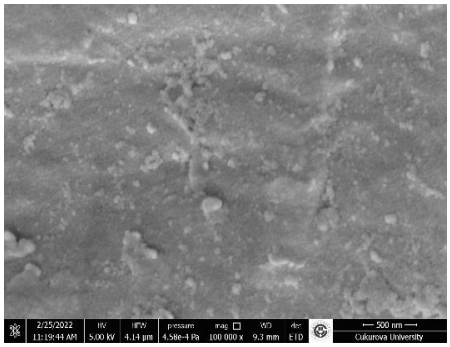


Figure 4.41. in-.05M-2.6-tm

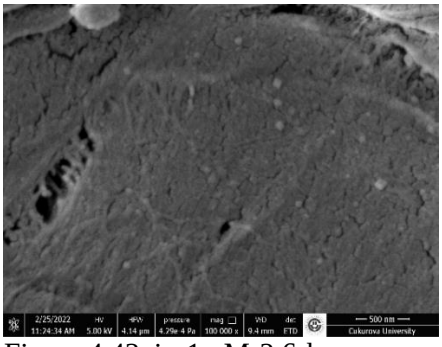


Figure 4.42. ip-1mM-2.6-k-r

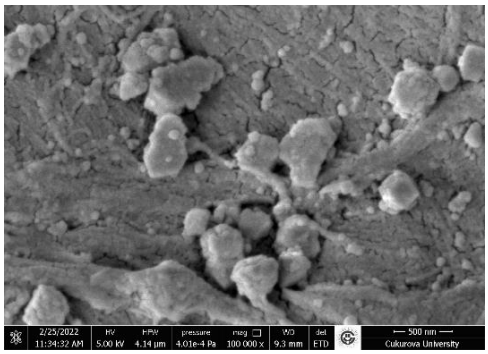


Figure 4.43. ip-1mM-2.6-sk

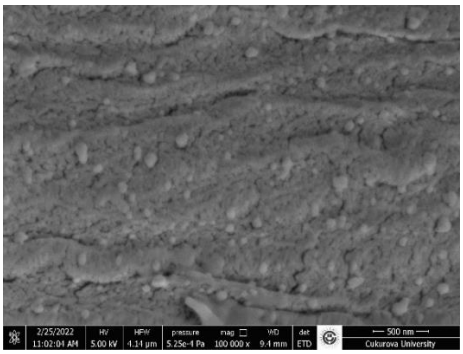


Figure 4.44. in-2mM-.03-or-t

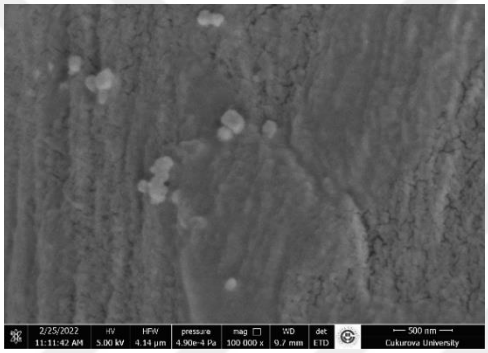


Figure 4.45. pad-2mM-.04-wash

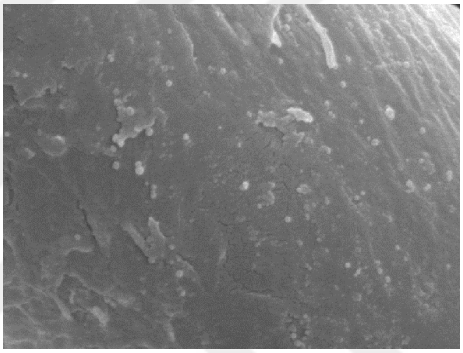


Figure 4.46. im-2mM-.03-or-rt

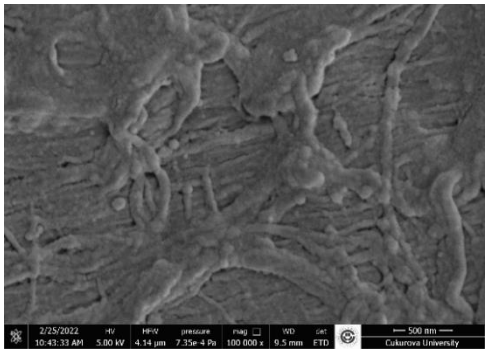


Figure 4.47. p2x-2mM-2.6-F6

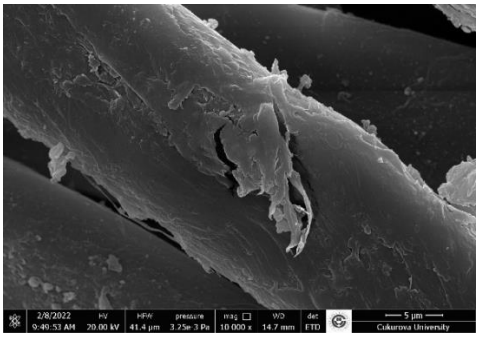


Figure 4.48. in-2mM-2.6-F1-d

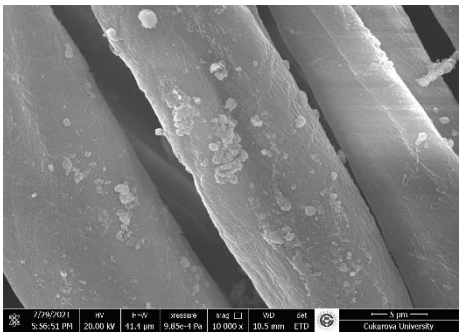


Figure 4.49. in-0.1M-0.1-t

4.10. EDS of AgNPs

The EDS spectrum (figure 4.50, 4.51, 4.52) has different peaks for Ag, C, O the EDAX profile shows Ag peaks which confirm that the AgNPs were formed in the reaction medium. Further, at around 3 keV, there are some peaks that are typically caused by the absorption of silver nanocrystals due to Surface Plasmon Resonance of AgNPs (Magudapathy et al. 2001). The C and O elements indicate the carbonyl group's presence (=C=O) in *C.arvensis* plant extract. Other strong peaks are from Au due to the gold plating of the sample before SEM sample preparation. The K and L beside the metal elements represent the shell of the metal.

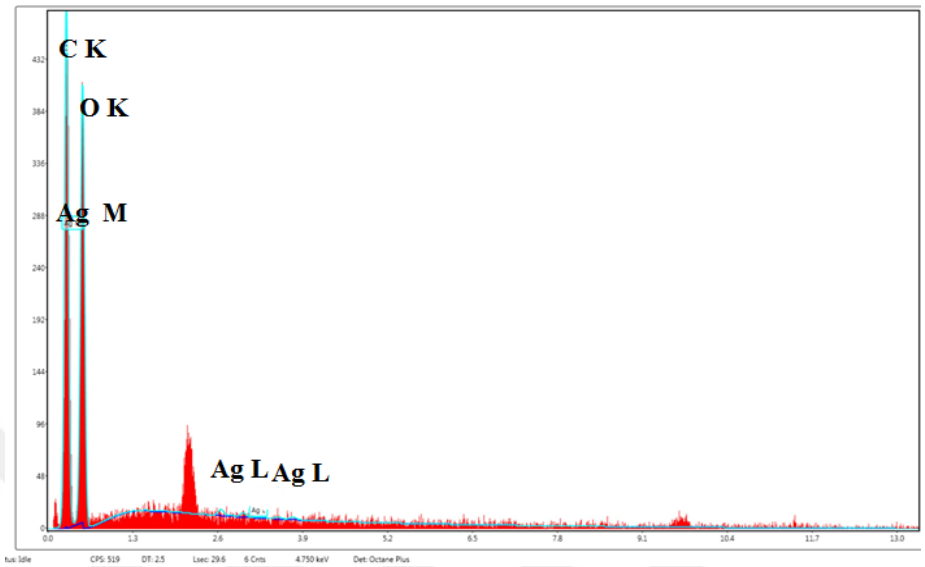


Figure 4.50. EDS of green synthesized AgNPs

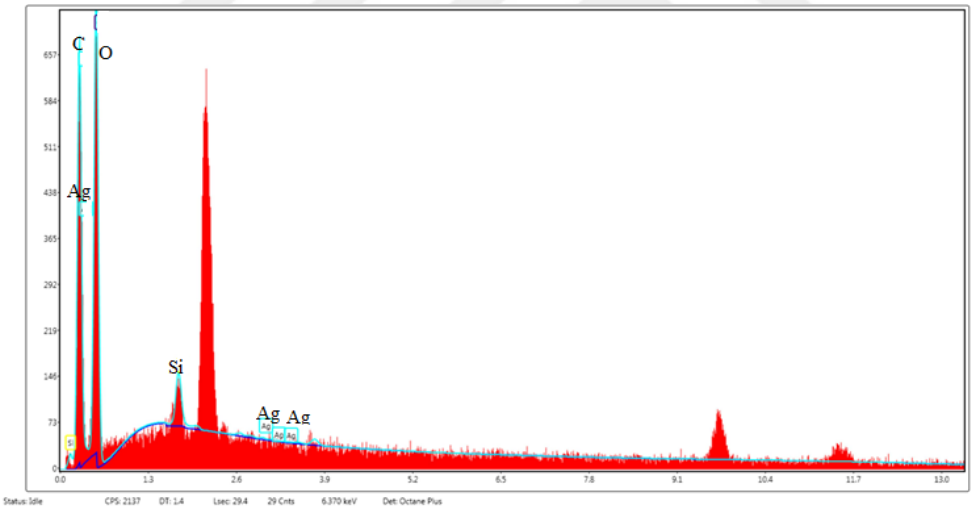


Figure 4.51. Sol-gel (Sol: AgNPs = 1:2)

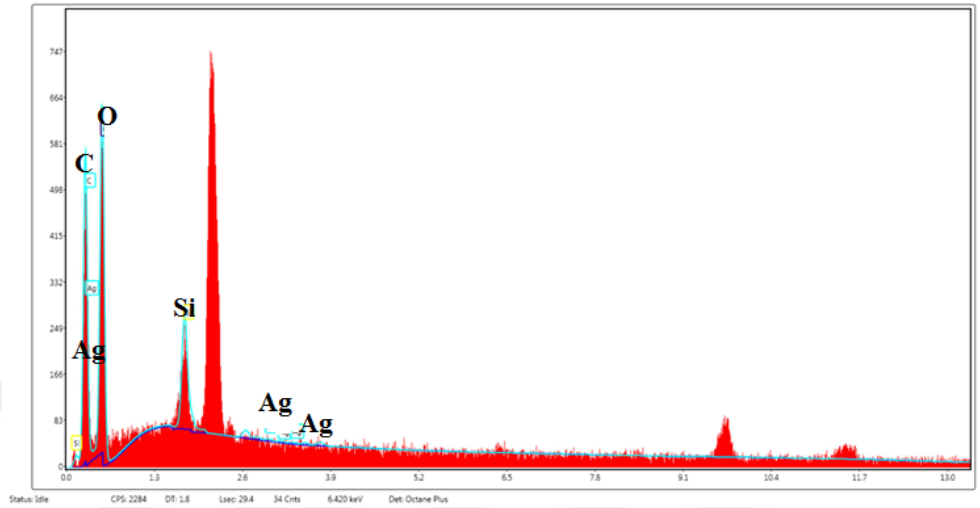


Figure 4.52. Sol-gel (Sol: AgNPs = 1:1)

The EDS images in figure 4.51 and figure 4.52 for both sol: AgNPs = 1:2 and 1:1 show the presence of Si and Ag. Besides, the presence of other metals is from the surroundings. The EDS spectrum has different peaks for Ag, C, O, and Si. The EDS profile shows Ag peaks which confirms that AgNPs and Sol-gel film. The C and O elements indicate the presence of carbon and oxygen present in cotton fabrics and plant extracts. Other strong peaks are Au, which occurred due to the gold plating of the sample.

4.11. AgNPs number, shape and size of different samples

Figure 4.53 shows the number of silver nanoparticles produced, their shape distribution, and size distribution. It shows that highest number of AgNPs come from *in-.05M-2.6-tm* (figure 4.41), *in-2mM-2.6-F3* (figure 4.29), *in-9mM-0.10-p* (figure 4.19). On contrary, the largest size nanoparticles come from the *p2x-2mM-2.6-F6* (figure 4.47), *in-2mM-2.6-F1-d* (figure 4.48), *in-0.1M-0.1-t* (figure 4.49) and so on.

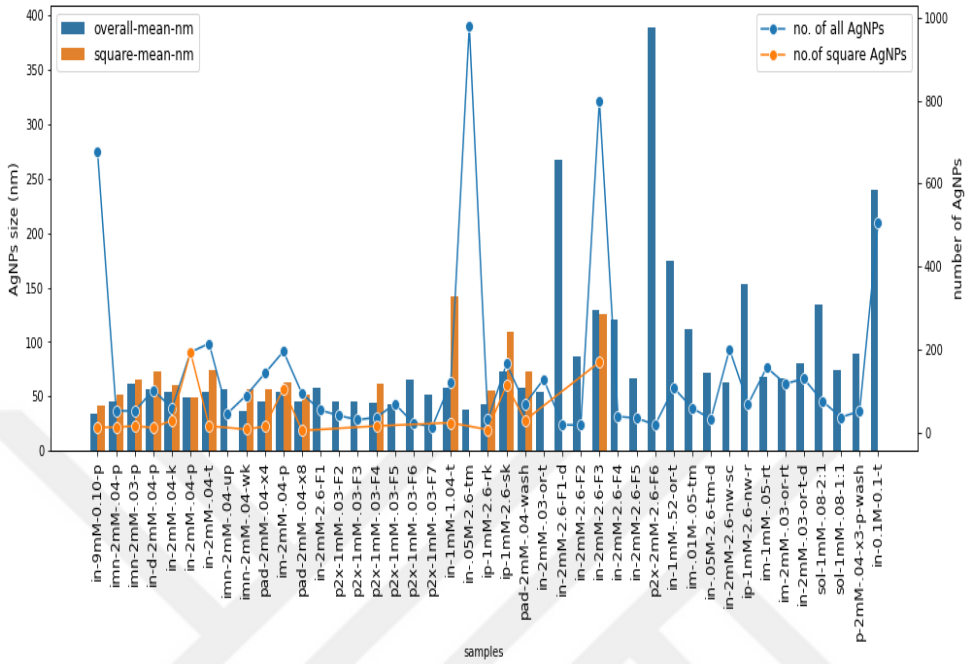


Figure 4.53. Overall information about synthesized AgNPs

A high concentration and high plant extract amount will produce a high number of AgNPs, whereas a low concentration of $AgNO_3$ with a high plant extract amount or vice versa will produce a large particle size. This will happen due to quick aggregation. On the other hand, the minimum particle sizes are obtained from *in-9mM-0.10-p* (figure 4.19), *imn-2mM-.04-p* (figure 4.20), and *in-.05 M-2.6-tm* (figure 4.41). Hence, it needs an optimal amount of plant extract against a specific concentration of silver nitrate ($AgNO_3$). Table 4.16 illustrates the details.

Table 4.16. Various factors on AgNPs size

Sl	Sample	No. of AgNPs	Mean (nm)	Treatment	PE-ratio	$AgNO_3$ _M	PE:M	$AgNO_3$ _Vol	Fabric	pH	Method
1	in-1mM-.52-or-t	107	174.8	NaOH	0.52	0.001	520	100	twill	8.3	insitu
2	in-2mM-2.6-F3	800	129.2	Span-80	2.6	0.002	1300	100	plain	6	insitu
3	in-2mM-2.6-F2	17	86.9	CA	2.6	0.002	1300	100	plain	1.7	insitu
4	ip-1mM-2.6-sk	165	73	NaOH	2.6	0.001	2600	200	knit	8.1	insitu-pad
5	p2x-1mM-.03-F6	22	65.7	NaOH, S-80	0.033	0.002	16.5	100	plain	4.2	pad 2x
6	imn-2mM-.03-p	51	61.3	NaOH	0.03	0.002	15	200	plain	7.2	immersion
7	in-2mM-2.6-F1	53	58.5	NaOH	2.6	0.002	1300	400	plain	8	insitu
8	in-1mM-1.04-t	120	58.1	NaOH	1.04	0.001	1040	100	twill	8.3	insitu
9	pad-2mM-.04-wh	68	57.9	detergent	0.04	0.002	20	100	plain	7.2	pad80%
10	in-d-2mM-.04-p	102	56.7	NaOH	0.067	0.002	33.5	50	plain	7.2	insitu
11	imn-2mM-.04-up	46	56.4	NaOH	0.04	0.002	20	100	plain	6.5	Immersion
12	in-2mM-.04-t	214	54.6	NaOH	0.04	0.002	20	100	twill	7.9	insitu
13	im-2mM-.04-p	195	54.4	NaOH	0.04	0.002	20	100	plain	7.2	pad100%
14	in-2mM-.03-or-t	128	54	NaOH	0.03	0.002	15	100	twill	8.3	insitu
15	in-2mM-.04-k	58	54	NaOH	0.04	0.002	20	100	knit	7.4	insitu
16	p2x-1mM-.03-F7	13	52	NaOH, CA, Span-80	0.0325	0.002	16.25	100	knit	5.5	pad 2x
17	in-2mM-.04-p	193	49.7	NaOH	0.04	0.002	20	100	plain	7.2	insitu

18	p2x-1mM-.03-F2	40	46	CA	0.0325	0.002	16.25	100	knit	1.7	pad 2x
19	pad-2mM-.04-x8	93	45.9	NaOH	0.04	0.002	20	100	knit	7.4	pad80%
20	imn-2mM-.04-p	52	45.7	NaOH	0.4	0.002	200	100	plain	7.2	immersion
21	pad-2mM-.04-x4	142	45.7	NaOH	0.04	0.002	20	100	twill	7.9	pad80%
22	p2x-1mM-.03-F3	30	45	NI	0.0325	0.002	16.25	100	plain	6	pad 2x
23	p2x-1mM-.03-F4	36	44.3	NaOH, CA	0.0325	0.002	16.25	100	knit	6.7	pad 2x
24	p2x-1mM-.03-F5	68	42.6	CA, NI	0.0325	0.002	16.25	100	knit	4.2	pad 2x
25	ip-1mM-2.6-k-r	30	42.4	no	2.6	0.001	2600	200	knit	6.5	pad100%
26	in-.05M-2.6-tm	980	37.7	Bleached	2.6	0.05	52	25	twill	6.5	insitu
27	imn-2mM-.04-wk	89	36.6	NaOH	0.04	0.002	20	100	knit	7.4	Immersion
28	in-9mM-0.10-p	675	33.9	NaOH	0.1	0.009	11.11	110	plain	7.2	insitu

4. RESULT AND DISCUSSION Toufique AHMED

4.11.1. Pearson Correlation of AgNPs synthesis

To know the other factors related to the AgNPs production. The machine learning libraries Pandas and Scikit were used to determine correlations as shown in figure 4.54 and mutual information as shown in figure 4.55. But Pearson correlation and Mutual information only work on numerical data. Hence, the next section will discuss the categorical variables (such as methods, treatment, etc.).

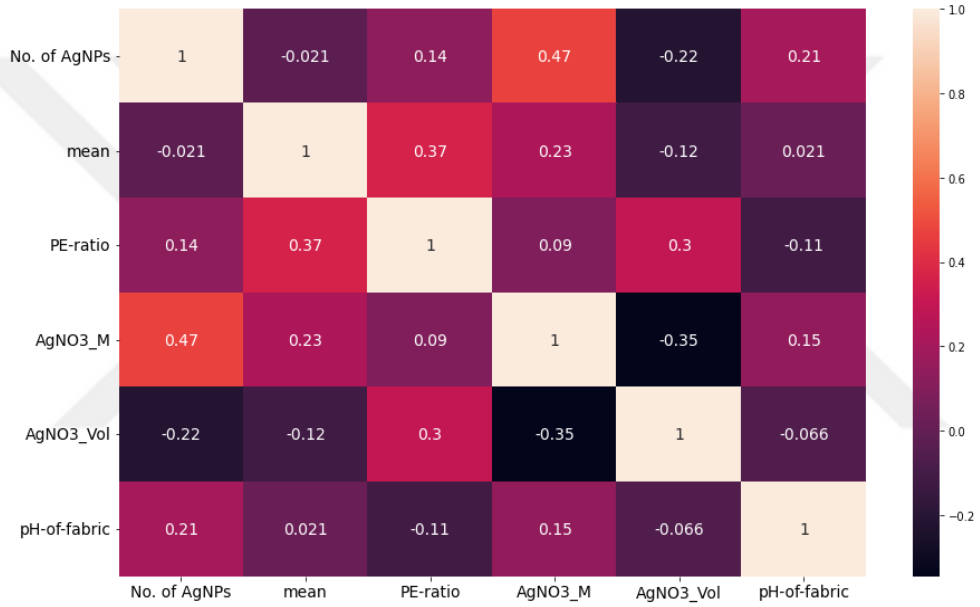


Figure 4.54. Pearson correlation of different factors related to AgNPs number

From the correlation in figure 4.54, it is seen that the mean size of AgNPs is strongly correlated to $AgNO_3$ molarity, plant extract ratio, $AgNO_3$ volume (negatively). For more specific relations, mutual information scores were used for this process.

4.11.2. Mutual information

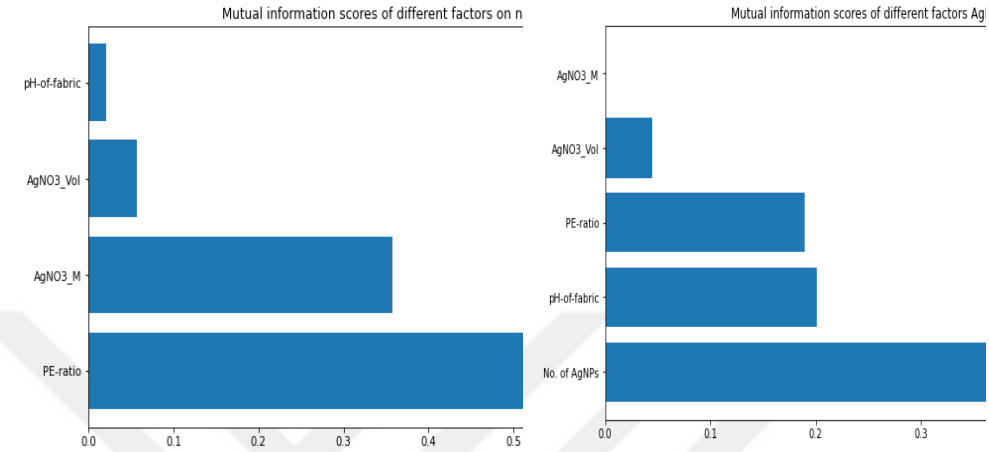


Figure 4.55. Mutual information of different factors on the number of AgNPs (left) and mean-size (right)

Mutual information (figure 4.55) also reveals that the plant extract ratio in water is the most influential factor in $AgNO_3$ number, followed by $AgNO_3$ molarity and volume. On the contrary, AgNps mean size is greatly dependent on the number of AgNPs, the pH of fabric, and then plant extract.

4.11.3. Plant Extract on AgNPs size

Figure 4.56 shows that increasing plant extract will also increase the mean size. But the error bars indicate that there are factors other than a plant extract. Additionally, 0.4 and 1.04 plant extract ratio in figure 4.56 shows a decrease in mean size. Hence, to explain this phenomenon, table 4.16 should be considered.

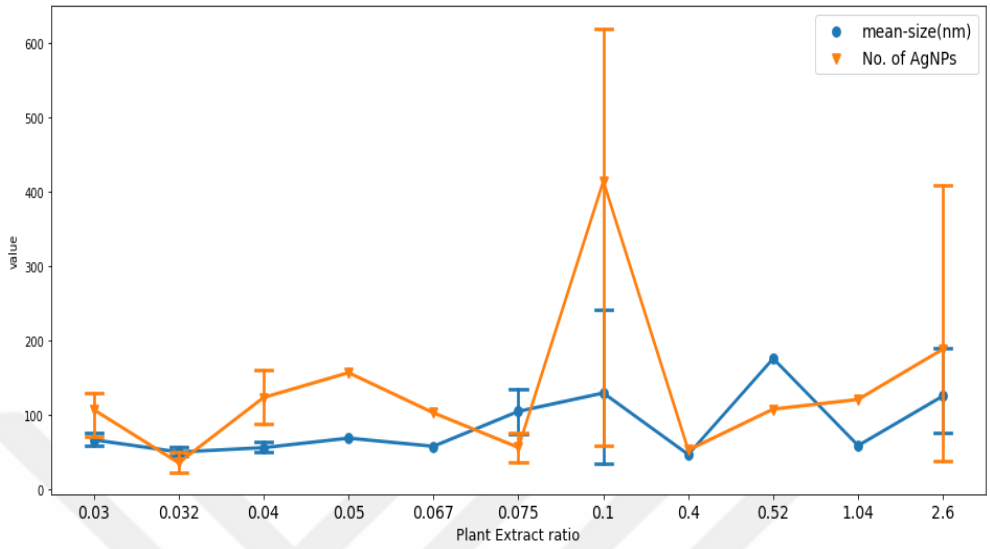


Figure 4.56. Plant Extract on AgNPs size and AgNPs number

Table 4.16 shows that the major influencer of AgNPs size is plant extracts to $AgNO_3$ Molar ratio (PE: $AgNO_3$_M) and NaOH treatment (or pH). The high plant extract to molarity ratio and high pH will cause large nanoparticles. Other factors (such as method, $AgNO_3$ Molarity, etc.) are not so important here. An exception to this explanation is (*p2x-1mM-.03-F6* /sl no 5: it should produce smaller particles) where the fabric is pretreated with NaOH and non-ionic detergent; hence the pH falls to 4.2.

Another important thing is that the AgNPs number is directly related to NaOH. Therefore, high pH normally will cause a higher number of AgNPs. Hence, to get prolific and smaller AgNPs, it needs to maintain plant extract to $AgNO_3$ molarity ratio around or below 20 and NaOH treated with a proper neutralization so that pH level should be around 7.8.

4.11.4. Influence of $AgNO_3$ Molarity

It is a common belief that high $AgNO_3$ molarity will produce an increased number of AgNPs. But this study shows that plant extract amount (reducer) is more important than silver nitrate concentration- the more plant extracts, the more silver nanoparticles. However, there is an intricate relationship between $AgNO_3$ Molarity and plant extract amount. The inadequate amount will not synthesize a high number of silver nanoparticles. But, on the other hand, the excessive amount of plant extract will cause particle aggregation and results in big particle size (as shown in *in-2mM-2.6-F3* in Table 4.18).

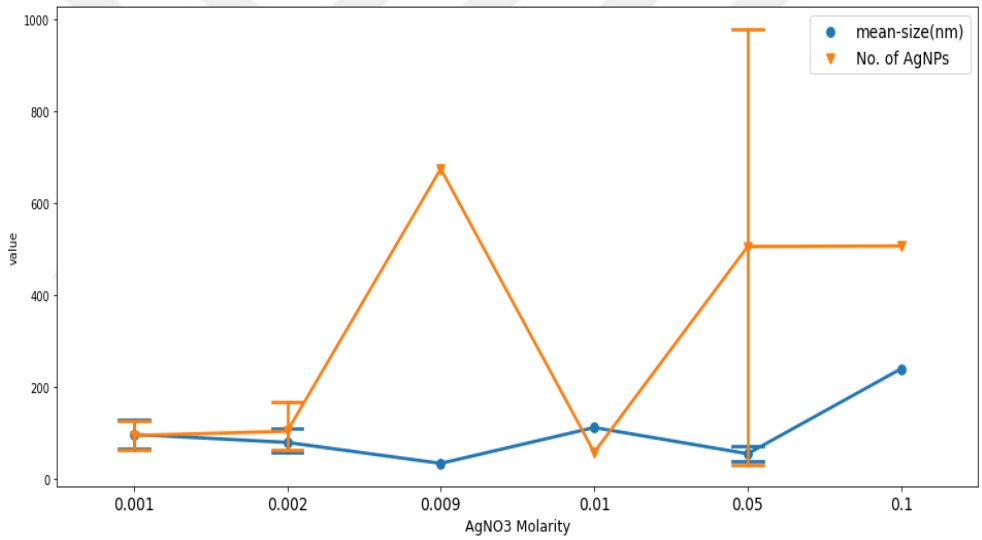


Figure 4.57. $AgNO_3$ molarity, AgNPs number and AgNPs mean size relation

From figure 4.57, $AgNO_3$ molarity is not always related to high AgNPs size. For example, high molarity (0.05 M) cause lower AgNPs size. The large error bar also indicate the unreliable results. Again, low $AgNO_3$ molarity (2mM) produce high AgNPs size (such as in-2mM-2.6-F1, *in-2mM-2.6-F3*, *p2x-1mM-.03-F6* in table 4.16).

4.11.5. Influence of $AgNO_3$ Volume

Figure 4.58 depicts the influence of $AgNO_3$ volume on AgNPs' size and number. It reveals high volume of $AgNO_3$ will produce smaller AgNPs, but the number may depend on other factors such as plant extract amount, pH of fabrics, etc.

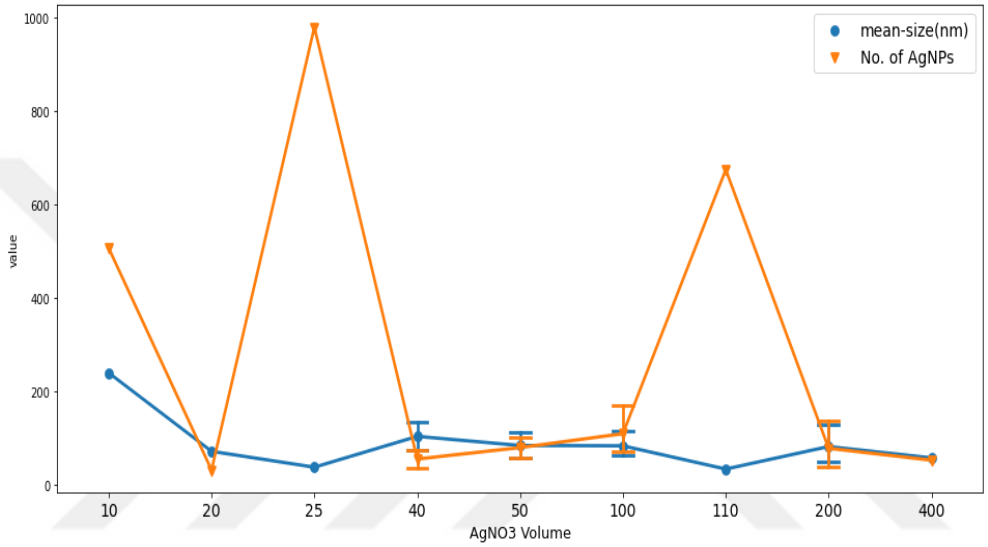


Figure 4.58. $AgNO_3$ volume on AgNPs size

4.11.6. Fabric pH on AgNPs size and number

Figure 4.59 shows that when pH increases from the neutral position, the mean size and number increase, but at low pH, the number of AgNPs is lower. The pH is a powerful influencer in AgNPs synthesis. But, it works in combination with plant extract, $AgNO_3$ molarity, volume, etc.

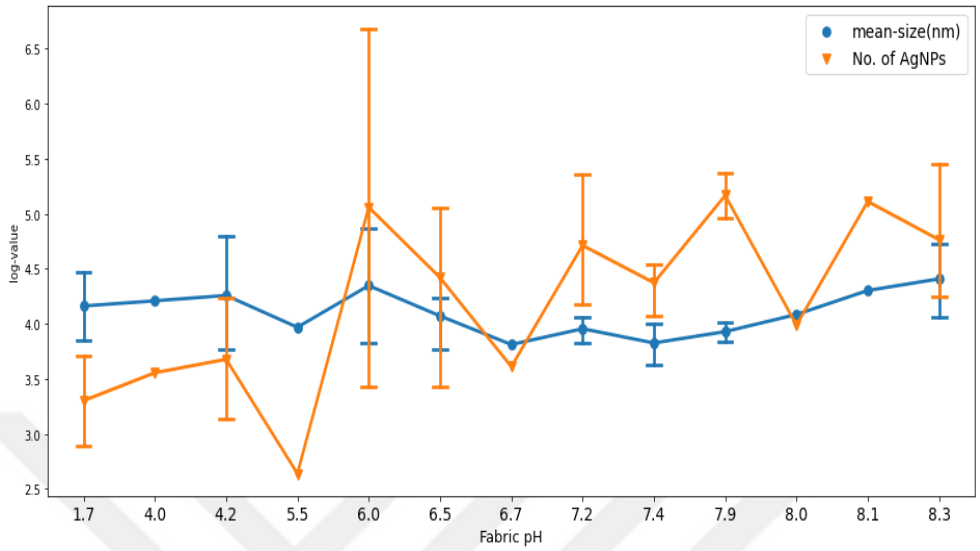


Figure 4.59. pH of fabric on AgNPs mean size and number

4.11.7. Different methods on AgNps size and number

To determine the influence of various AgNPs incorporation methods, all other parameters (such as Molarity, volume, plant extract, etc. should be constant, as these can influence the AgNPs size to a great extent. The description is depicted in table 4.17 and figure 4.60.

Table 4.17. Effect of Methods with constant molarity, volume

Sample	No. of AgNPs	mean	shape	Treat-ment	PE-ratio	Fabric	pH	method
UV-424	94	30.5	irregular	No	0.04	plain	6.5	drop
UV-431	266	39.4	irregular	No	0.04	plain	6.5	drop
UV-426	270	40.3	irregular	No	0.04	plain	6.5	drop
pad-2mM-.04-x4	142	45.6	irregular	NaOH	0.04	twill	7.9	Padding
pad-2mM-.04-x8	93	45.8	irregular	NaOH	0.04	knit	7.4	Padding
in-2mM-.04-p	193	49.6	square	NaOH	0.04	plain	7.2	insitu
in-2mM-.04-k	58	53.9	square	NaOH	0.04	knit	7.4	insitu
im-2mM-.04-p	195	54.3	square	NaOH	0.04	plain	7.2	immersion
in-2mM-.04-t	214	54.5	irregular	NaOH	0.04	twill	7.9	insitu
imn-2mM-.04-up	46	56.3	irregular	NaOH	0.04	plain	7.2	Immersion
Importance of post washing								
imn-2mM-.04-wk	89	36	irregular	NaOH	0.04	knit	7.4	Immersion
imn-2mM-.04-up	46	56.3	irregular	NaOH	0.04	plain	7.2	Immersion

Table 4.17 and figure 4.60 show that simply dropping a few drops of AgNPs on fabric will produce the smallest AgNPs mean size. On the contrary, the in-situ method produces bigger AgNPs. However, the AgNPs size does not solely depend on a single parameter; rather, there are complicated relationships among other parameters. According to the AgNPs size the methods order is: drop < immersion (in-situ) < 2-times padding < padding < immersion < sol< *in-situ* < *in-situ*-pad.

There will be very little interaction between AgNPs colloid and cellulosic fiber in the dropping method. Hence the particle aggregation is very low. On the other hand, the *in-situ* and immersion method will have few more opportunities to react with cellulose, plant extract, fabric pretreatment materials, etc. Hence, the particle size will be bigger. Again, the padding method squeezes out some AgNPs, pretreatment, plant extract, and AgNPs, and there will be less scope to aggregate.

Again, another important matter is: a normal washing (with tap water or distilled water) dried AgNPs loaded textile materials will cause much smaller AgNPs (e.g., 36 nm), whereas without washing will have much bigger nanoparticles (e.g.> 56nm). The probable reason behind this, the washing will remove the aggregated unfixed nanoparticles and may supply some more –OH groups by activating the cellulose, pretreatment materials, etc.

4.11.8. Different methods on AgNPs amounts

Figure 4.60 shows the immersion method will synthesize the lowest amount of AgNPs, whereas simple dropping AgNPs colloidal solution will produce the highest number of AgNPs. This is because the immersion method will precipitate a lot of AgNPs due to the reaction between Ag^{+}, reducing material, and pretreatment agents. Hence, there will be a much lower number of AgNPs in this method. The padding method will also squeeze out about 20% materials (for 80% pad-dry), and hence the synthesized AgNPs will be lower.

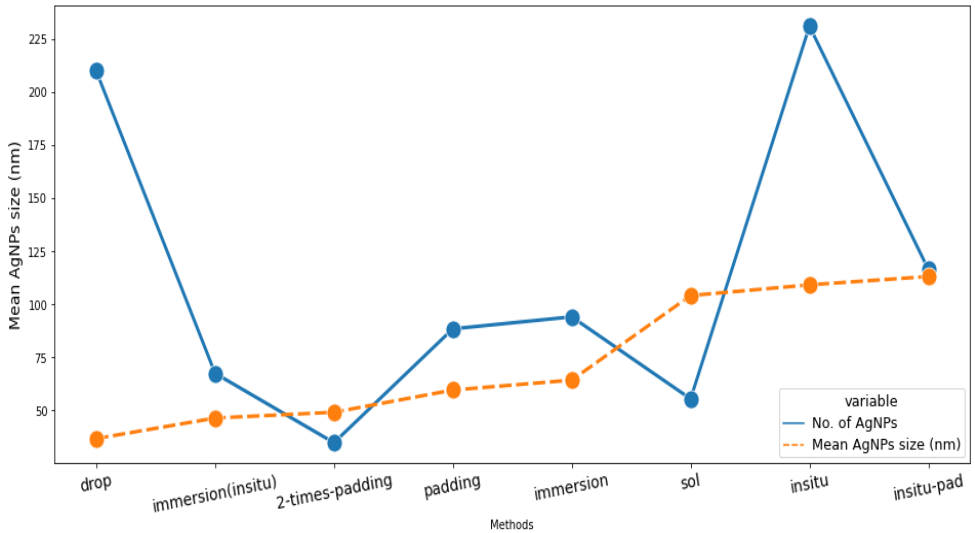


Figure 4.60. Effect of Methods where Molarity-2mM, volume 100ml, plant extract 0.04 on plain fabrics

4.12. Comparison of square and spherical AgNPs:

In the whole study, mainly 2 types of AgNPs are found. One is irregular cum spherical, and another one is square or cubic. Figure 4.61 depicts the distribution of AgNPs shapes. In 3- samples, there is the vast majority of square or cubic shapes (*in-d-2mM-.04-p*, *in-2mM-.04-k*, *im-2mM-.04*). The shaping mechanism is vague, and very few previous works are available. However, it is tried to explain it.

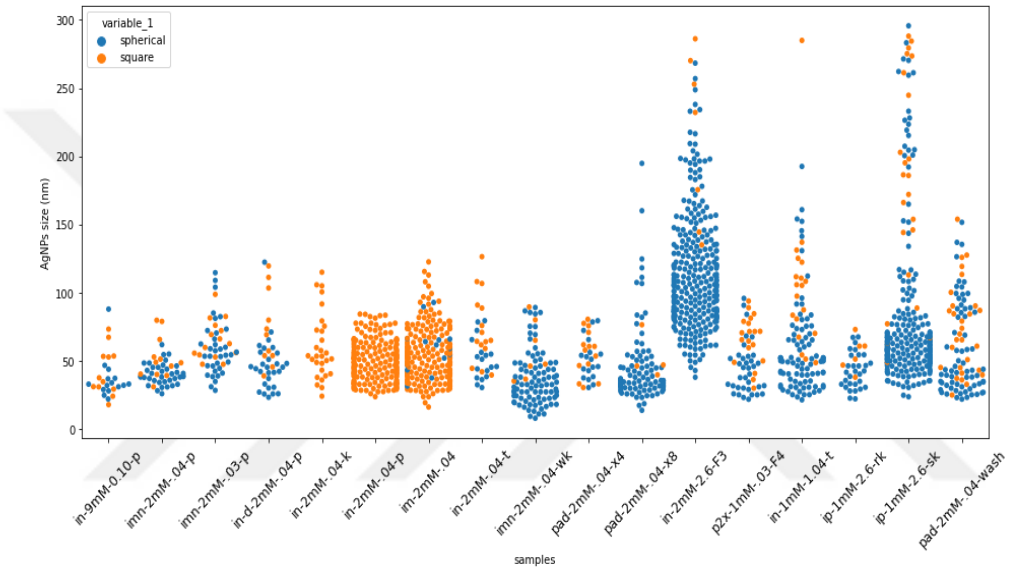


Figure 4.61. Distribution of AgNPs spherical and square shapes

4.13. Mechanism of shape

4.13.1. Growth

At the beginning of AgNPs synthesis, spherical AgNPs formed, and then the residual Ag^{+} was reduced by NaOH (from pretreatment of fabric) to produce smaller AgNPs. Later the newly created small nanoparticles attached to the typical AgNPs produced an irregular shape. This hypothesis is a close match to the work of (Dong et al. 2010).

The nanoparticles are very irregular at high pH due to the fast reaction rate (Dong et al. 2009). On the other hand, decreasing pH will synthesize spherical

nanoparticles according to the Lamer model (Dong et al. 2009). Similarly, the spherical shapes are obtained in Citric acid added fabrics and orange peel extract (such as figure 4.37 *p2x-1mM-.03-F5* (CA, NI), figure 4.39: *p2x-1mM-.03-F7* (NaOH, CA, NI), figure 4.44 *in-2mM-.03-or-t* (orange extract), figure 4.46 *im-2mM-.03-or-rt* (orange extract).

4.13.2. Crystallinity

The closed packed (111) crystal surface has the lowest free energy, and the loosely packed (110) has the largest surface free energy (Luo, Hu, and Xiao 2008). Again if the driving force is weak, then nanoparticles will be spherical. On the other hand, if the driving force is strong, it will be very irregular, like dendrites. Additionally, the driving force determines the growth rate, and again, the growth rate is influenced by the surface energy differences in different cryptographic directions, leading to anisotropy (Meng, Tang, and Vongehr 2010). The driving force is obtained from Gibbs free energy (GFE). GFE can be calculated from the following equations where the pressure is zero, and the temperature is T (Luo, Hu, and Xiao 2008).

$$g(T) = u(T) - Ts(T) \tag{7}$$

Where $u(T)$ is the internal energy/ atom and $s(T)$ is the specific entropy.

$$G^{total} = G^{bulk} + G^{surface} = Ng(T) + \gamma(T)A_s \tag{8}$$

T = predetermined reference temperature

G^{bulk}= sum of volm free energy

$G^{surface}$ = surface free energy

$g(T)$ = Gibbs free energy per atom

If the particle is spherical, then the specific surface areas will be:

$$A_s = \frac{6NV_{at}(T)}{D} \quad (9)$$

Where,

N = total number of atoms in the particle

A_s = Specific surface area

Where V_{at} = volume/ atom

The medium-level GFE will cause loosely packed crystals because of the leeway of thermodynamic equilibrium. The loosely packed crystals tend to form well-shaped cubic AgNPs due to its high Surface-free energy. On the other hand, high-level GFE will cause closed-packed crystals. For example, the spherical nanoparticles' XRD images show many closed-packed (111) crystals. On the other hand, the loosely packed (110) crystals are available in cubic-shaped nanoparticles. However, if the driving force is very high, irregular shapes will be formed. A similar explanation was provided by (Meng, Tang, and Vongehr 2010).

4.14. Various parameters on AgNPs shape

4.14.1. The pH of fabric:

If the pH of the fabric is between 7.1 to 7.9, the fabric will be leeway from the thermodynamic equilibrium. The driving force (GFE) from this system's non-thermodynamic equilibrium will form an orthorhombic crystal system with a loose pack. The loose pack crystal's high surface free energy (SFE) will orient them in a cubic shape. However, in acidic conditions, the total energy (GFE + SFE) will be weak, so spherical AgNPs will form.

4.14.2. Incorporation methods

The pH influence the low GSM fabrics for all methods except padding (80% WPU). Because padding will squeeze out a substantial amount of pretreatment materials, the created thermodynamic non-equilibrium will be destroyed and there will be very low number of square shapes. On the contrary, the roller pressure will squeeze out some pretreatment materials (NaOH) from high GSM fabric. However, there will still be substantial to create the desired thermodynamic inequivalent (pH near 7.5). This hypothesis is supported by pad-2mM-.04-x8-k (knit) and pad-2mM-.04-x4-t (twill). Both samples are 80% padded but knit fails to produce many cube shapes, whereas the twill created many cube shapes.

Again 2-times-padding will also produce big irregular shape AgNPs. This is because the first-time padding will activate the –OH group, and some will be lost due to squeezing. The next time padding will aggregate the Ag^{+} quickly by the activated –OH groups. Due to the pressure imbalance (of non-equilibrium thermodynamics), the particles will be large and cubic. However, when the pressure gets in equilibrium, there will be small AgNPs as shown in figure – 4.43(*ip-1mM-2.6-sk).*

4.14.3. Plant Extract on the shape

In the case of *im-2mM-.04-p* (immersion) sample, the added plant extract is slightly less (plant extract ratio= 0.03) than in-2mM-.04-p (plant extract ratio =0.04); hence the created nanoparticles are slightly bigger. On the other hand, the same solution is used in the immersion (in-situ) method; this method produces many spherical nanoparticles and a few cubic shapes. Because, before synthesis, the -OH groups react with the Ag^{+} and oxidize then as Ag_2O precipitation. This waste a large number of capping and reducing agent. Hence the mean size increase. Same reason for *imn-2mM-.04-wk* (figure 4.26). For this reason, the *immersion* (*in-situ*) method will fail to synthesize cube nanoparticles. If the fabric pH is high (pH 8.3) and added

plant extract (*C.arvensis*) is also high, then a large amount of plant extract will mitigate the pH (since the pH of *C.arvensis* is about 5.0), but still it is far from the desired pH level (between 7.2 to 7.5), for this reason there will be some cubic shape and large number of irregular AgNPs (figure 4.40: in-1mM-1.04-t). If the fabric has no NaOH but Span80 treatment the fabric will be very surface active and attracts the newly formed AgNPs. Many AgNPs coalesce and form big irregular shapes (figure 4.29: *in-2mM-2.6-F3*). Finally, it was found that the orange peel extract (*C.reticulata*) will cause spherical shapes in all situations due to its acidic nature.

Table 4.18. Square or cubic shaped AgNPs formation

sample	No. of AgNPs	mean	shape	treatment	square count	sq-mean (nm)	PE-ratio	$AgNO_3$_M	$AgNO_3$_Vol	Fabric	pH	method
in-2mM-.04-p	193	49.65	square	NaOH	193	49.65	0.04	0.002	100	plain	7.2	insitu
in-2mM-2.6-F3	800	129	irregular	NI	169	125.65	2.6	0.002	100	plain	6	insitu
ip-1mM-2.6-sk	165	72.9	big-sq-smal-sp	NaOH	114	109.62	2.6	0.001	100	knit	8.1	insitu-pad
im-2mM-.04-p	195	54.32	cubic	NaOH	105	62.53	0.03	0.002	200	plain	7.2	immersion
in-2mM-.04-k	58	53.92	square	NaOH	29	60.06	0.04	0.002	100	knit	7.4	insitu
pad-2mM-.04-ws	68	57.82	irre-clean	detergent	29	73.32	0.04	0.002	100	plain	7.2	padding
in-1mM-1.04-t	120	58.08	irregular	NaOH	23	141.95	1.04	0.001	100	twill	8.3	insitu
imn-2mM-.03-p	51	61.28	irregular	NaOH	15	65.27	0.03	0.002	200	plain	7.2	Immersion (insitu)
in-2mM-.04-t	214	54.52	irregular	NaOH	15	73.62	0.04	0.002	100	twill	7.9	insitu
pad-2mM-.04-x4	142	45.60	irregular	NaOH	14	56.17	0.04	0.002	100	twill	7.9	Padding
imn-2mM-.04-p	52	45.65	irregular	NaOH	12	51.64	0.4	0.002	100	plain	7.2	immersion
in-9mM-0.10-p	675	33.88	irregular	NaOH	12	41.86	0.1	0.009	110	plain	7.2	Insitu
in-d-2mM-.04-p	102	56.64	irregular	NaOH	11	73.04	0.07	0.002	50	plain	7.2	Insitu
imn-2mM-.04-wk	89	36.50	irregular	NaOH	7	56.93	0.04	0.002	100	knit	7.4	Immersion (insitu)
ip-1mM-2.6-k-r	30	42.32	irregular	no	6	54.87	2.6	0.001	200	knit	6.5	insitu-pad
pad-2mM-.04-x8	93	45.89	irregular	NaOH	4	52.10	0.04	0.002	100	knit	7.4	padding
p2x-**1mM-.03-F5**	68	42.50	spherical	CA, NI	0	0	0.03	0.002	100	knit	4.2	Pad 2 times
in-2mM-2.6-F5	34	66.29	spherical	CA, NI	0	0	2.6	0.002	100	plain	4.0	insitu

4.15. Antibacterial Performance

The antibacterial tests are done according to the AATCC-100 standard. For wash fastness, AATCC 61-2010 was followed, where 1 cycle is equivalent to 5 home wash. The results are illustrated in table 4.19

Table 4.19. Main factors of antibacterial activity

Sample	Treatment	PE-ratio	PE source	AgNO3 _M	Fabric	Method	Living-bacteria
in-1mM-.52-or-t	NaOH	0.52	orange	0.001	twill	insitu	17
im-1mM-.05-rt	no	0.05	c.arvensis	0.001	twill	pad100%	7
im-2mM-.03-or-rt	no	0.03	orange	0.002	twill	pad100%	7
in-.01M-.09-rt	no	0.09	c.arvensis	0.01	twill	insitu	5
in-2mM-2.6-nw-sc	NaOH, NI	0.04	c.arvensis	0.002	non-woven	insitu	4
in-.02M-.19-rt	no	0.19	c.arvensis	0.02	twill	insitu	4
im-1mM-.04-F1-t	**NaOH**	**0.04**	**c.arvensis**	**0.001**	**twill**	**pad100%**	**2**
ip-1mM-2.6-nw-sc	NaOH	2.6	c.arvensis	0.001	non-woven	insitu-pad	2
im-1mM-.04-F4-t	**NaOH, CA**	**0.04**	**c.arvensis**	**0.001**	**twill**	**pad100%**	**1**
im-2mM-.03-or-t-2	NaOH	0.03	orange	0.002	twill	pad100%	1
in-1mM-.13-or-t	NaOH	0.13	orange	0.001	twill	insitu	2
ip-1mM-2.6-t-m	NaOH	2.6	c.arvensis	0.001	twill	insitu-pad	1
ip-1mM-2.6-k-r	no	2.6	c.arvensis	0.001	knit	Insitu-pad	1
im-2mM-.03-or-t-3	NaOH, CA	0.03	orange	0.002	twill	pad100%	0
in-2mM-.03-F1-p	**NaOH**	**0.03**	**c.arvensis**	**0.002**	**plain**	**pad2x**	**0**
p2x-1mM-.03-F2-k	CA	0.03	c.arvensis	0.002	knit	pad 2x	0
p2x-1mM-.03-F3-p	NI	0.03	c.arvensis	0.002	plain	pad 2x	0
p2x-1mM-.03-F4-k	**NaOH, CA**	**0.03**	**c.arvensis**	**0.002**	**knit**	**pad 2x**	**0**
p2x-1mM-.03-F5-k	CA, NI	0.03	c.arvensis	0.002	knit	pad 2x	0
p2x-2mM-.03-F6-p	NaOH, NI	0.03	c.arvensis	0.002	plain	pad 2x	0
p2x-1mM-.03-F7-k	NaOH, CA, NI	0.03	c.arvensis	0.002	knit	pad 2x	0
in-2mM-.03-or-t	NaOH	0.03	orange	0.002	twill	insitu	0
in-1mM-1.04-t	NaOH	**1.04**	**c.arvensis**	**0.001**	**twill**	**insitu**	0
in-1mM-.13-t	NaOH	0.13	c.arvensis	0.001	twill	insitu	0
ip-1mM-2.6-k	NaOH	2.6	c.arvensis	0.001	knit	insitu-pad	0

Interestingly, the sample *ip-1mM-2.6-k-r* high very good antibacterial performance although being knit fabric without any pretreatment (table 4.19). But the method used here is *in-situ- pad.* During *padding*, the fabric gets in contact with NaOH from the pad-dry-roller (due to the previous padding). Hence, it produces some square nanoparticles *and* shows excellent antibacterial properties. However, the *in-situ-pad* is not a good method for a high antibacterial wash activity. On the contrary, sol-methods, and methods with low plant extract show poor antibacterial activity, especially after 5 home washes.

4.15.1. Antibacterial Mechanism

The impeccable mechanism of how the silver ion damage the bacteria is still undiscovered. However, several models are there as follows can explain it (Figure 4.62).

4.15.2. Adhesion to the microbes

The AgNPs attract the microbes basically for electrostatic attraction and acid-base theory. After attaching to the microbes, AgNPs create pits on the microbial membrane (Figure 4.62).

4.15.2.1. Electrostatic interaction

Almost all the bacterial cell membranes (either gram-positive or gram-negative) are negatively charged (at neutral pH) because of the abundance of carboxyl and phosphate groups than that of the positive amino groups (Baszkin and Norde 1999) (Abbaszadegan et al. 2015). Hence, the positively charged metal nanoparticles will have an electrostatic attraction to microbes (T. Ahmed and Ogulata 2021).

4.15.2.2. Acid-basic theory

It is an established theory that soft-acid has a strong affinity for soft-basic and vice versa (TSE and HO 1975). Silver is a soft acid (Dillard and Tappel 1986), and the sulphur or phosphorus compounds are the soft-base (House and House 2016). The membrane of bacteria is composed of sulphur and phosphorus-containing proteins resulting in a strong interaction between silver and bacterial membrane (Morones et al. 2005). In line with this, the DNA of bacteria also contains phosphorus (0.1 fg) (Km, M, and S 1996), which reacts with the silver (soft-acid) and annihilates the bacterial DNA activities.

4.15.3. Pit formation and penetration

AgNPs damage the bacterial cell wall. Consequently, an enormous number of AgNPs accumulate on the cell wall and formulate some 'pits' on it and later infiltrate. The enormous number of AgNPs inside the bacteria corroborates the hypothesis (Morones et al. 2005). In this way, the significantly damaged cell wall results in cell death (Sondi and Salopek-Sondi 2004).

4.15.4. Inside the cell

After forming pits on the microbial membrane, the numerous AgNPs enter the cell and interact with the organelles. In this way, they produce cytotoxicity and free radicals.

4.15.5. Cytotoxicity

The AgNPs penetrate the microbial cell smoothly on account of their superfine size and large surface area. It discharges silver ions (Ag^{+}) while in the cytoplasm by reacting with it (You et al. 2012) (S.-H. Kim et al. 2011). The silver ions (Ag+) interact with the thiol group of the microbial protein and consequently destroy its activities. This action breaks the molecular structure of bacteria (Mowafi

et al. 2017) (Feng et al. 2000). Furthermore, AgNPs facilitate superoxide generation through the univalent reduction of Oxygen neighbouring to the microbial organelles like mitochondria. Hence, both the silver ions and AgNPs contribute to cytotoxicity in different ways (You et al. 2012).

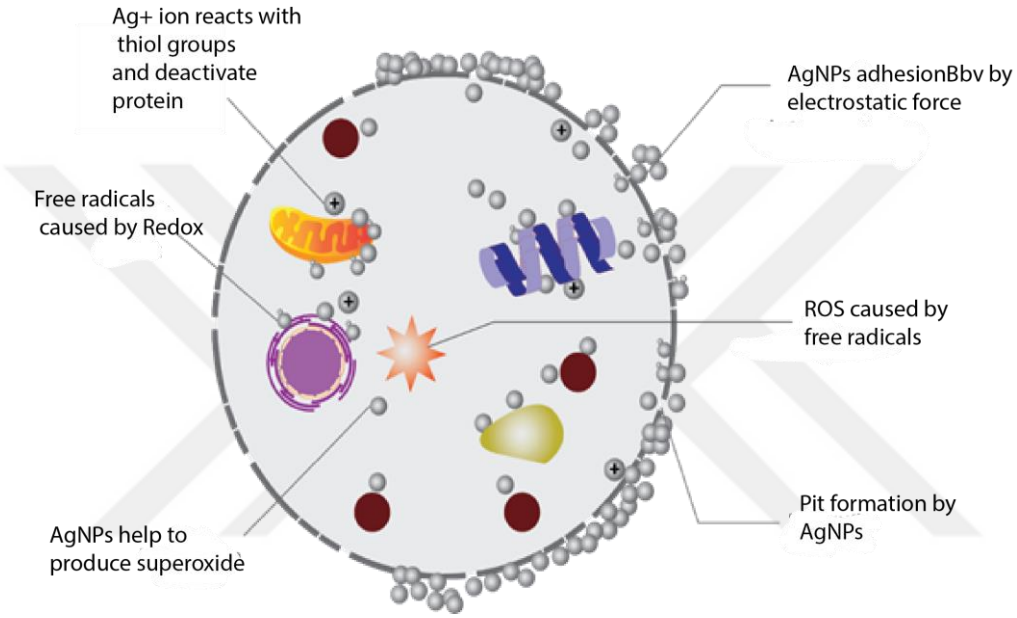


Figure 4.62. Antimicrobial action of AgNPs

4.15.6. Free radical generation

Once penetrating the bacterial membrane, silver ions and silver nanoparticles interact with the protein, lipid, DNA, and others (Liao, Li, and Tjong 2019). Metal nanoparticles can effortlessly accept or receive electrons based on the oxidation state (Ramamurthy et al. 2013). Therefore it smoothly generates free radicals through redox reaction resulting in Reactive Oxygen Species (ROS) (Quinteros et al. 2016). Free radicals are unstable atoms having an unpaired electron. Uncontrolled generations of free radicals and subsequently oxidative stress impairs the membrane lipids, protein, and DNA (Mendis et al. 2005) (Neal 2008). ROS predominately generated in mitochondria, ribosomes, lysosomes, and others.

Through interaction with silver nanoparticles and silver ions (Soenen et al. 2011). It is supposed to be the most influential constituent of the antimicrobial action of AgNPs (J. S. Kim et al. 2007). Hence it is termed nanoparticle toxicity (Sahu and Casciano 2009).

Besides, reactive oxygen derivatives like OH^-, superoxide radical anion (O_2), and peroxyl radicals (ROO) inhibit microbes. On the other hand, O_2 is also a crucial medium for annihilating microbes. Moreover, ROS affects various microbes in several ways. For instance, gram-negative bacteria have more resistance against O_2 than gram-positive bacteria. Additionally, the virus can protect the inhibition action of O_2 (Pellieux et al. 2000).

4.16. Correlating factors of antibacterial performance

Figure 4.63 is the Pearson correlation of different parameters with bacterial survival. It reveals that the survival bacteria is highly correlated with mean size, plant extract, and $AgNO_3$ volume. The mean size (nm) is 56% correlated with bacteria. The Pearson correlation also reveals the negative relationship between the number of AgNPs and $AgNO_3$ molarity. Because if the number of AgNPs increases, bacteria will decrease, and the molarity increases, then the AgNPs number will also be increased. (AgNPs number has 74% correction with $AgNO_3$ molarity).

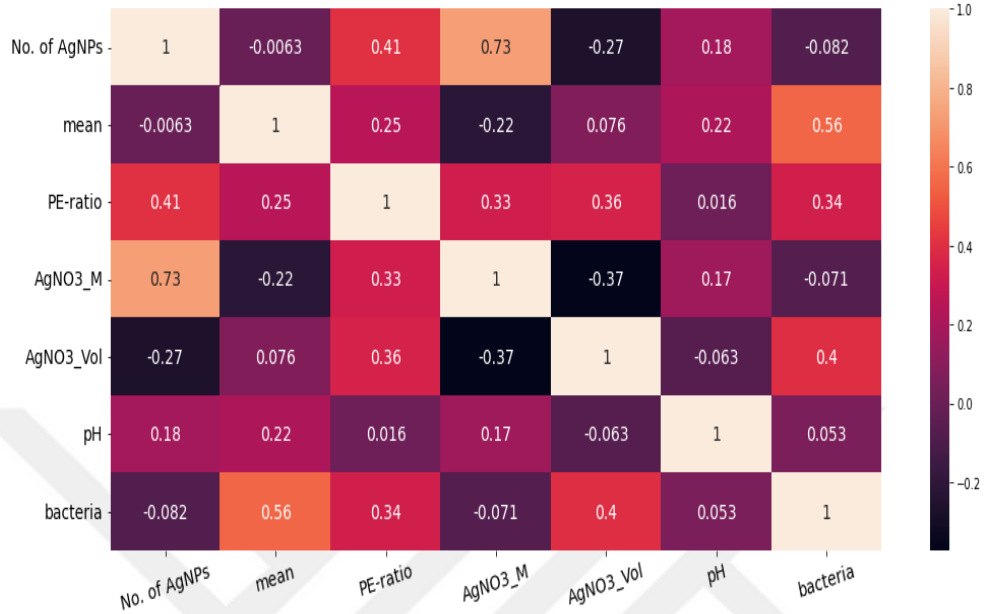


Figure 4.63. AgNPs size and antibacterial performance

A similar type of results was obtained from mutual information (MI) plot (figure 4.64).

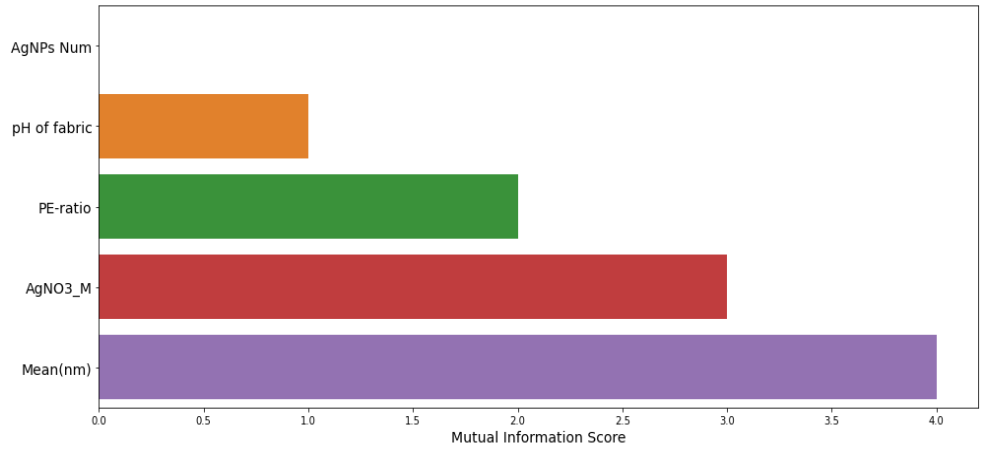


Figure 4.64. Mutual Information for antibacterial activity

Figure 4.64 shows the mutual information of different parameters to antibacterial activity. It shows mean size of AgNPs has the highest relation to bacteria.

4.16.1. AgNPs mean size on antibacterial activity

To better understand the influence of the mean size of AgNPs, the living bacteria and mean size are plotted in figure 4.65. For visualization, the data was scaled using MinMaxScaler with a range of (0, 2) using Scikit learn library.

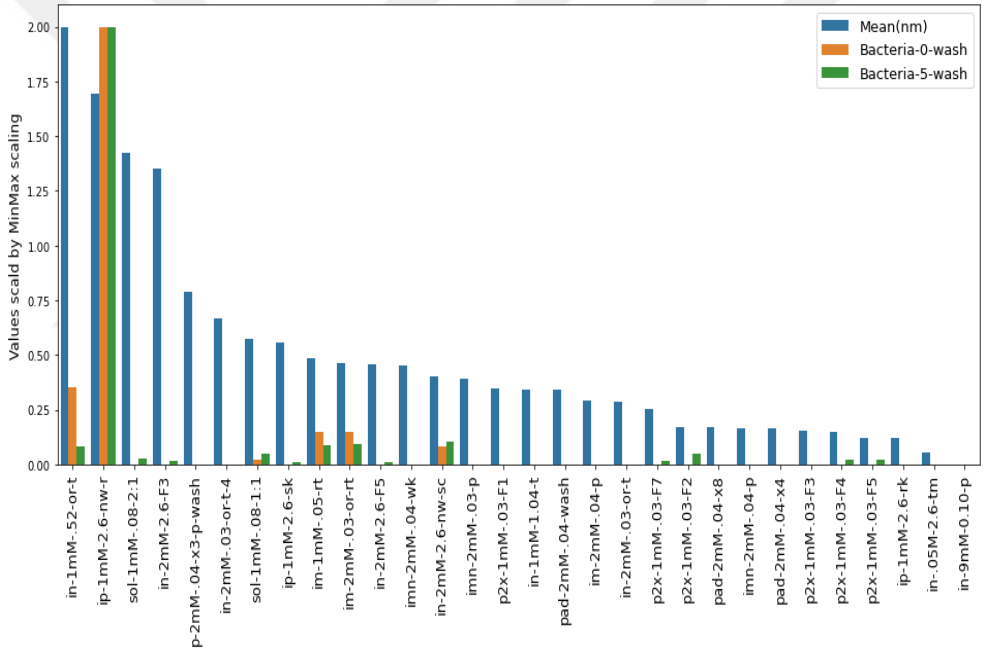


Figure 4.65. AgNPs mean size (nm) vs. number of survival bacteria

Figure 4.65 shows that the large mean value in maximum cases will cause less antibacterial activity. However, there may be other more influencing factors than mean size. For example, non-pretreated twill, non-woven, will have very low antibacterial action and wash fastness.

4.16.2. $AgNO_3$ Molarity on Antibacterial performance:

$AgNO_3$ molarity typically produces many AgNPs hence there will be high anti-bacterial activity. But high molarity also needs precise control over plant extract to synthesize a large number of AgNPs with small size. Figure 4.66 shows 0.001 M is better than 0.01 M. Though there is a strong influence of plant extract and fabric pretreatment relating to the $AgNO_3$ molarity.

Dibrov et al. (2002) demonstrated that a low concentration of Ag^+ induces an enormous proton leakage on the microbes' membrane, causes a collapse of proton motive force, and eventually kills the microbes. This study also concords with them; it also finds low concentration is more antibacterial. However, high molarity will need a very precise amount of plant extract and good pretreatment to have good antibacterial activity.

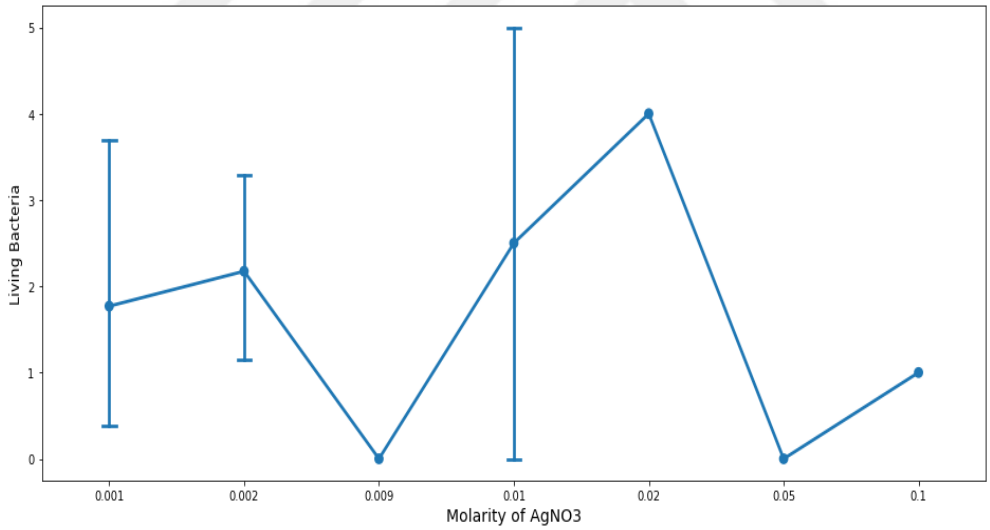


Figure 4.66. Influence of $AgNO_3$ molarity on antibacterial property

4.16.3. Plant extract amount on antibacterial performance

Figure 4.67 and Table 4.20 illustrate the influence of plant extract on antibacterial activity. Plant extract is one of the most influential factors in AgNPs

synthesis and antibacterial activities. But there is no decisive relation to the antibacterial property. Instead, it is interrelated by multiple factors such as fabric type, $AgNO_3$ molarity, etc. Figure 4.67 shows that the highest plant extract ratio (2.6) will also have the highest survival bacteria. However, the error bar reveals that this illustration is unreliable; hence, table 4.20 needs to be analyzed. It shows that the highest bacteria are caused by non-woven fabrics, the fabric with no pre-treatment, and TEOS treatment. Besides, the plant extract source is also important; e.g., orange peel needs a minuscule amount; otherwise, it will aggregate AgNPs (as shown in table 4.16: *in-1mM-.52-or-t* has mean NP size = 175 nm) and cause less amount of AgNPs and hence have a lower efficiency. So, in general, it can be said that *c.arvensis* plant extract will increase the antibacterial activity.

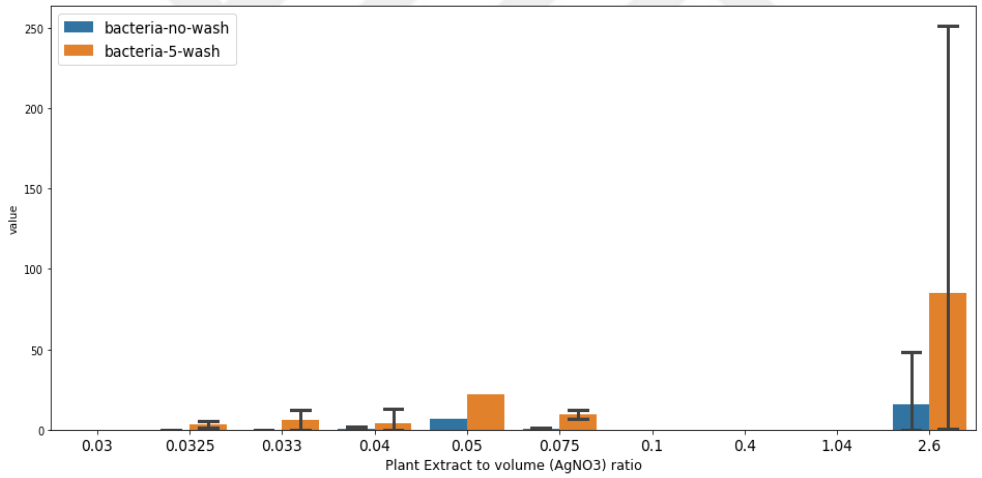


Figure 4.67. Influence of Plant extract on antibacterial activity

Table 4.20. Influence of plant extract on antibacterial performance

sample	PE-ratio	Treatment	Fabric	bacteria-no-wash	bacteria-5-wash
ip-1mM-2.6-nw-r	2.6	no	non-woven	96	500
im-1mM-.05-rt	0.05	no	Twill	7	22
in-2mM-2.6-nw-sc	0.04	NaOH, NI	non-woven	4	26
sol-1mM-.08-1:1	0.075	TEOS	Twill	1	12
p2x-1mM-.03-F7	0.0325	NaOH, CA, NI	Knit	0	4
in-.05M-2.6-tm	2.6	mercerized	Twill	0	0
ip-1mM-2.6-rk	2.6	no	Knit	0	0
p2x-1mM-.03-F5	0.0325	CA, NI	Knit	0	5
p2x-1mM-.03-F4	0.0325	NaOH, CA	Knit	0	6
p2x-1mM-.03-F3	0.0325	NI	Plain	0	0
pad-2mM-.04-x4	0.04	NaOH	Twill	0	0
imn-2mM-.04-p	0.4	NaOH	Plain	0	0
pad-2mM-.04-x8	0.04	NaOH	Knit	0	0
p2x-1mM-.03-F2	0.033	CA	Knit	0	12
pad-2mM-.04-wash	0.04	detergent	Plain	0	0
im-2mM-.04-p	0.04	NaOH	Plain	0	0
sol-1mM-.08-2:1	0.075	TEOS	Twill	0	7
in-1mM-1.04-t	1.04	NaOH	Twill	0	0
p2x-1mM-.03-F1	0.033	NaOH	Plain	0	0
imn-2mM-.03-p	0.03	NaOH	Plain	0	0
imn-2mM-.04-F5	0.0325	NaOH, NI	Plain	0	0
in-2mM-2.6-F5	2.6	NaOH, NI	Plain	0	2
ip-1mM-2.6-sk	2.6	NaOH	Knit	0	3
p-2mM-.04-x3-p-wash	0.04	detergent	Plain	0	0
in-2mM-2.6-F3	2.6	NI	Plain	0	4
in-9mM-0.10-p	0.1	NaOH	Plain	0	0

4.16.4. Influence of pH

Figure 4.68 reveals the influence of fabric-pH on antibacterial activity. It is clear that when the fabric pH is near the neutral (i,e if there is no pretreatment), the bacteria colony will be many. However, there is no direct correlation between pH and antibacterial effect. It may come into action with plant extract, $AgNO_3$ molarity.

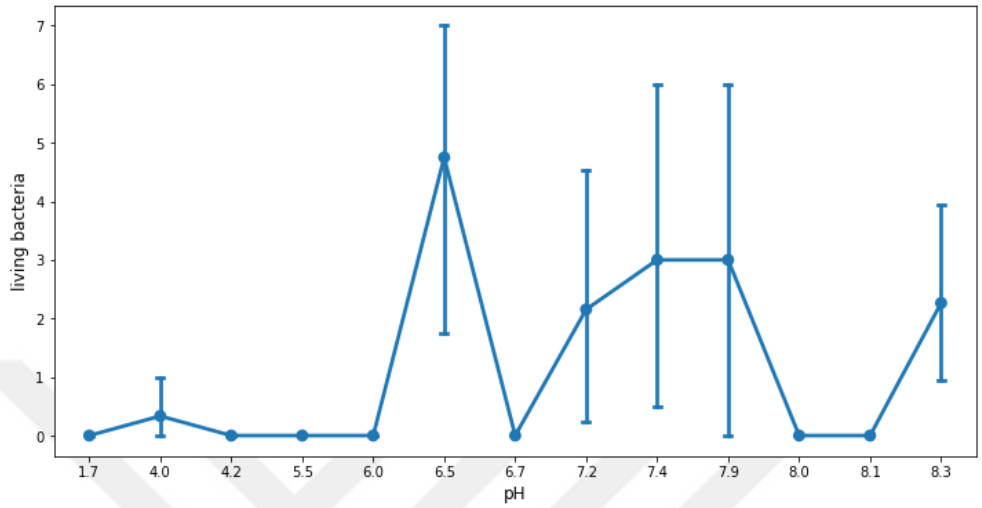


Figure 4.68. Influence of pH on antibacterial

4.16.5. Influence of $AgNO_3$ Volume on antibacterial activity

It shows higher volume will have much more antibacterial properties because a higher $AgNO_3$ volume will increase the dispersion of Ag^+ ions and plant extract accordingly (figure 4.69). It seems 25 ml worked a little better because the concentration of $AgNO_3$ was higher, the fabric was twill (high GSM), and plant extract was also enough to synthesize it. Hence, the Ag+ ions will be dispersed in the bulky fabric, and enough plant extract will synthesize it sufficiently.

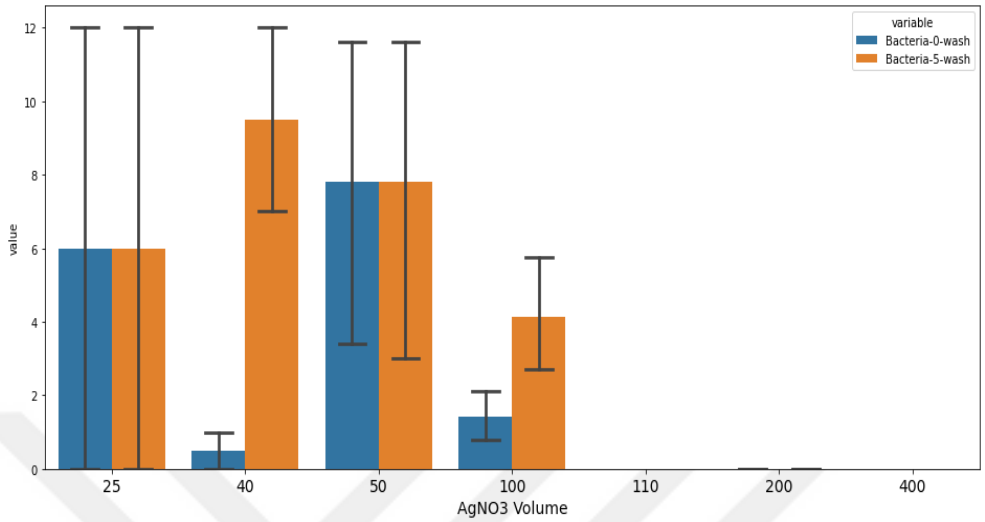


Figure 4.69. Influence of $AgNO_3$ volume on antibacterial activity

Table 4.21. $AgNO_3$ volume on antibacterial activity (only the worst 10 rows)

$AgNO_3$_Vol (ml)	$AgNO_3$_M	PE-ratio	Fabric	Treatment	Bactria-0-wash	bacteria-5-wash
25	0.050	2.6	twill	Mercerized	0	0
25	0.002	0.16	twill	NaOH	12	12
40	0.001	0.075	twill	TEOS	1	12
40	0.001	0.075	twill	TEOS	0	7
50	0.010	0.10	twill	Mercerized	0	0
50	0.002	0.067	twill	NaOH	5	5
50	0.002	0.067	plain	NaOH	10	12
50	0.002	0.067	tnit	NaOH	12	15
50	0.002	0.067	plain	NaOH	11	12
100	0.001	2.6	knit	NaOH	0	6

4.16.6. Different fabrics on antibacterial performance

Figure 4.70 represents the influence of fabric types on antibacterial performance. It shows plain fabrics have the highest antibacterial efficiency, whereas the non-woven ones have the lowest.

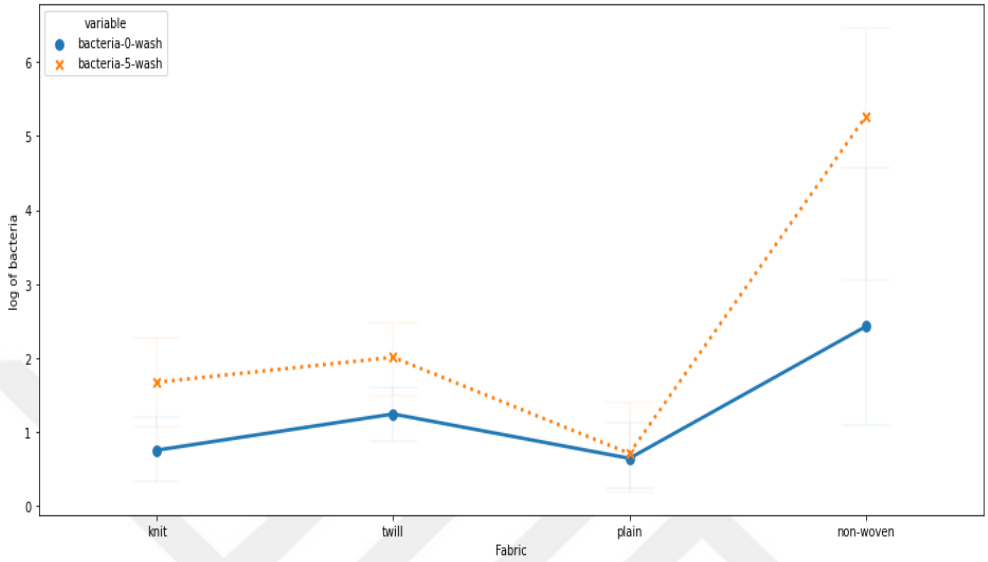


Figure 4.70. Influence of fabric types on antibacterial performance

The non-woven fabrics show the lowest antibacterial reduction. The twill fabric (GSM 230) shows lower antibacterial efficiency than low GSM fabrics (knit and plain). For example, *ip-1mM-2.6-k* (knit) and *ip-1mM-2.6-t-m* (twill) have same parameter except fabric type. It shows that knit performs much better than twill, with 0 and 1 living bacteria, respectively. Because the twill fabric needs a large number of silver nanoparticles, the large number of AgNPs may be achieved by using a high $AgNO_3$ concentration or a high amount of plant extract in case of a lower concentration of $AgNO_3$ (for example, among *im-1mM-.04-F1-t (twill)*, *im-1mM-.04-F4-t (twill)* and *in-1mM-**1.04**-t (twill)*: all have the same $AgNO_3$ concentration, but the first two did not have 100% reduction, whereas the 3rd sample showed 100% reduction due to high plant extract. This is because the twill fabric absorbs the $AgNO_3$ quickly, and the low amount of plant extract is not enough to synthesize; hence, it needs more plant extract. *In-situ-pad* methods in table 4.16 support this hypothesis. In the *in-situ-pad,* the fabric is padded after immersing in plant extract

solution. The pressure of the pad will squeeze out a substantial amount of plant extract, and hence the residing amount of plant extract will be less than that if required.

For this reason, even having high plant extract, the *in-situ-pad* method did not work well in the case of twill fabrics (*ip-1mM-2.6-t-m*). In contrast, the exact amount and same *in-situ-pad* method (*ip-1mM-2.6-k*) with knit fabrics show excellent antibacterial efficiency. Due to its bulkiness, twill fabric will squeeze out more plant extract than that of knit fabrics. Besides, it causes inter-fiber friction in washing more. For this reason, the twill fabric has a critical level regarding plant extract quantity; below this level, it will have poor antibacterial efficiency.

4.16.7. Different methods of antibacterial performance

The antibacterial activity of fabrics depends on various factors, and the factors are interrelated. Hence a superior method regarding the antibacterial activity can not be selected. For example, when keeping the most influential parameters (fabric pretreatment, fabric type, plant source etc.) and then applying a statistical point plot against the logarithm of living bacteria. The *in-situ* method is found to be the worst one. This is incorrect as previously discussed that the pant extract amount must be in proportion with the silver nitrate molarity to get good antibacterial performance; otherwise, there will be less antibacterial performance. Again, it was also tried to keep the silver nitrate concentration the same, but the plant extract amount also depends mainly on fabric type (for example, twill fabric will need more plant extract). Hence it should be analyzed manually. All methods are found to perform very well. However, they may differ regarding wash fastness.

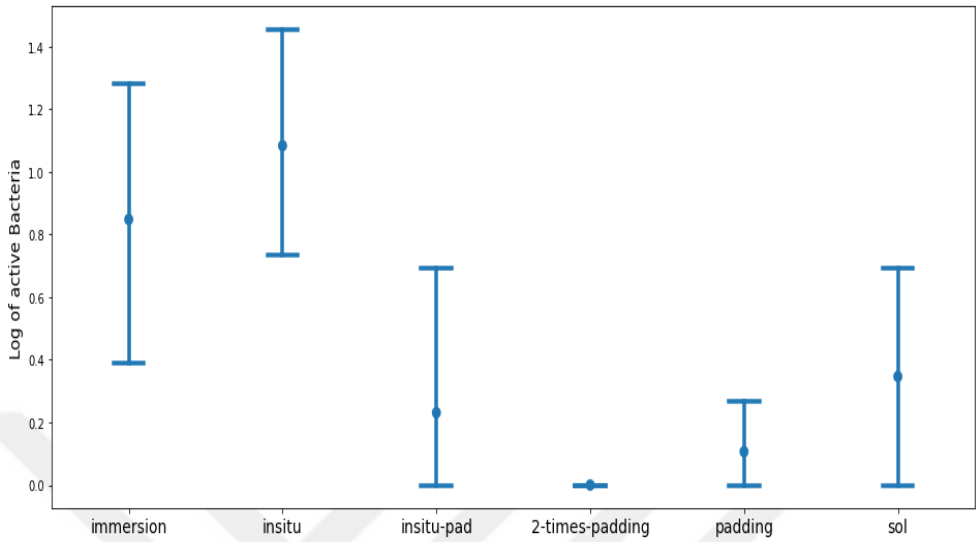


Figure 4.71. Comparison of different AgNPs incorporation methods

Figure 4.71 shows that the 2-times-padding performs best, followed by padding (80% wet pick up). The worst method here is *in-situ* because, as previously mentioned that the AgNPs get aggregated in the *in-situ* method, and the AgNPs size based on methods is **padding < immersion< in-situ**. Which is also analogous to the antibacterial activity i,e padding > immersion >insitu. However, it must have to acknowledge that the method's performance are sometimes immensely biased by other parameters such as fabric type, fabric pretreatment, plant extract amount etc.

The best performing 2-times-padding method was investigated deeply against other methods as in table 4.22. Here almost all parameters were kept the same except the incorporation method. It shows that almost all the samples show 100% reduction at no-wash, but after 5 washes, maximum samples lost antibacterial efficiency. And after 20 washes, all other method fails to annihilate bacteria except the 2-times-padding method (table 4.22).

Table 4.22. The 2-times-padding against other methods for wash fastness

Sample	Treatment	PE-ratio	$AgNO_3$_M	Fabric	Method	bacteria-0-wash	bact-5-wash	Bact-20-wash (Eff.%)
in-1mM-1.04-t	NaOH	1.04	1mM	twill	insitu	0	0	250 (58%)
in-1mM-.13-t	NaOH	0.13	1mM	twill	insitu	0	1	0%
ip-1mM-2.6-k	NaOH	2.6	1mM	knit	insitu-pad	0	3	0%
p2x-1mM-.03-p-F1	NaOH	0.033	1mM	plain	2-times-pad	0	0	17 (97%)
in-1mM-.52-t	NaOH	0.52	1mM	twill	insitu	5	21	0%

4.16.8. Wash fastness

Almost all pretreated fabrics show a 100% reduction. But the non-pretreated fabrics have low bacterial reduction.

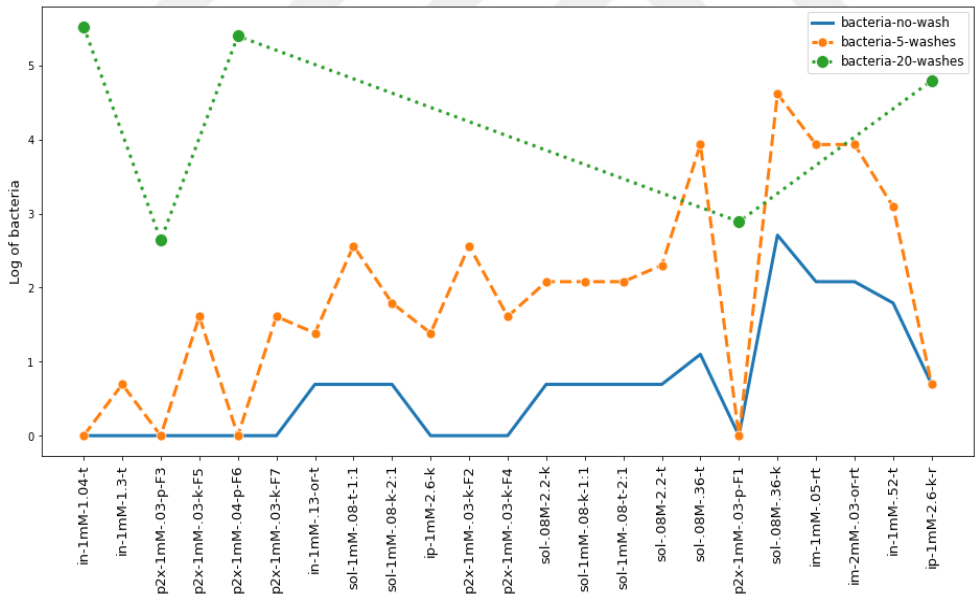


Figure 4.72. Antibacterial and wash fastness

Table 4.23. Antibacterial activity and wash fastness of different samples

Sample	Treatment	PE-ratio	$AgNO_3$_M	Fabric	Method	Bacteria-0-wash	Bact-5-wash	Bact-20-wash (Eff.%)
untreated	-	-	-	plain	-	600	-	-
in-1mM-1.04-t	NaOH	1.04	1mM	twill	insitu	0	0	250(58%)
in-1mM-.13-t	NaOH	0.13	1mM	twill	insitu	0	1	
p2x-1mM-.03-p-F3	NI	0.03	1mM	plain	pad2x	0	0	13 (98%)
p2x-1mM-.03-k-F5	CA, NI	0.03	1mM	knit	pad2x	0	4	
p2x-1mM-.04-p-F6	NaOH, NI	0.03	1mM	plain	pad2x	0	0	240(63%)
p2x-1mM-.03-k-F7	NaOH, CA, NI	0.03	1mM	knit	pad2x	0	4	
in-1mM-.13-or-t	NaOH	0.13	1mM	twill	insitu	1	3	
sol-1mM-.08-t-1:1	TEOS(1:1)	0.07	1mM	twill	sol	1	12	
sol-1mM-.08-k-2:1	TEOS(2:1)	0.07	1mM	knit	sol	1	5	
ip-1mM-2.6-k	NaOH	2.6	1mM	knit	insitu-pad	0	3	
p2x-1mM-.03-k-F2	CA	0.03	1mM	knit	pad2x	0	12	
p2x-1mM-.03-k-F4	NaOH, CA	0.03	1mM	knit	pad2x	0	4	
sol-.08M-2.2-k	TEOS(1:1)	2.23	0.08	knit	sol	1	7	
sol-1mM-.08-k-1:1	TEOS(1:1)	0.07	1mM	knit	sol	1	7	
sol-1mM-.08-t-2:1	TEOS(2:1)	0.07	1mM	twill	sol	1	7	
sol-.08M-2.2-t	TEOS(1:1)	2.23	0.08	twill	sol	1	9	
sol-.08M-.36-t	TEOS(1:1)	0.36	0.08	twill	sol	2	50	
p2x-1mM-.03-p-F1	NaOH	0.03	1mM	plain	pad2x	0	0	17 (97%)
sol-.08M-.36-k	TEOS(1:1)	0.36	0.08	knit	sol	14	100	
im-1mM-.05-rt	no	0.05	1mM	twill	immersion	7	50	
im-2mM-.03-or-rt	no	0.03	2mM	twill	immersion	7	50	
in-1mM-.52-t	NaOH	0.52	1mM	twill	insitu	5	21	
ip-1mM-2.6-k-r	no	2.6	1mM	knit	insitu-pad	1	1	120 (80%)

Figure 4.72 shows the antibacterial efficiency of 0-wash, 5-washes, and 20-washes. It reveals that 5 samples show 100% bacterial reduction after 5 washes. However, after 20-washes, they lost efficiency to a great extent. The best wash fastness performers are *p2x-1mM-.03-p-F1* and *p2x-1mM-.03-p-F3*, showing 98%

and 97% antibacterial efficiency even after 20-washes (Table 4.23). Hence, according to table 4.19, pretreatment is a vital issue for antibacterial efficiency.

4.16.9. Importance of fabric pre-treatment

To determine the influence of fabric pretreatment, the fabrics were pre-treated in 7 different ways as in the following table 4.24. Then 2 times padding at 80% wet pick up with 0.001M AgNPs with 0.03 plant extract ratio (i,e 3 drops/100 ml water) was applied. To keep the sample free from other influences, the same liquor, same fabric (knit), and environmental conditions were used.

Table 4.24. Antibacterial activity of fabric having no pretreatment

Sample	PE-ratio	$AgNO_3$_M	$AgNO_3$_Vol	method	living-bacteria	%Reduction	bacteria-ater-wash	%Red-uction
im-1mM-.05-rt	0.05	0.001	100	Immersion	7	96	22	89
im-2mM-.03-or-rt	0.03	0.002	100	immersion	7	96	20	90
in-.01M-.09-rt	0.09	0.01	100	insitu	5	98.91	10	97
in-.02M-.19-rt	0.19	0.02	75	insitu	4	99	5	98
ip-1mM-2.6-k-r	2.6	0.001	200	insitu-pad	0	100	0	100

In table 4.24, the fabrics were not pretreated. Hence the bacterial reduction is low. But the *ip-1mM-2.6-k-r* sample has shown a 100% reduction due to its high amount of plant extract. Besides, it was influenced by the NaOH from the padding roller. As pre-treatment is a very important factor of wash fastness of antibacterial textiles. The pretreatment process more meticulously investigated. For this purpose, several fabrics are prepared by adding different pretreatment chemicals. Table 4.25 shows that simple scouring and simply adding Span-80 has the best antibacterial wash fastness. It shows that the inter-reaction of chemicals is not appropriate for excellent wash fastness.

Table 4.25. Effect of different pretreatment on Antibacterial wash fastness

Sample	Pretreatment		Wash					Fastness
	Chemical	Amount	0	5	10	15	20	
F1	NaOH	4gm/L	100%	100%	100%	99%(2)	95%(17)	Strong
F2	Citric Acid (CA)	2gm/L	100%	98%(6)	80%(115)	60%(220)	0%	Medium
F3	Span-80	0.5 ml/1L	100%	100%	100%	98%(8)	98%(13)	Excellent
F4	NaOH+ CA	As per F1, F2	100%	100%	92%	65%	0%	Medium
F5	NaOH, CA, Span-80	As per F1,F3	100%	99%(4)	55%(250)	0%	0%	Very Poor
F6	NaOH, Span-80	As per F1, F3	100%	100%	92%(44)	46% (298)	63%(240)	Good
F7	NaoH, CA, Span-80	As per F1, F2, F3	100%	99%(2)	88%(63)	20%(440)	0%	Poor

4.17. An interesting phenomenon of AgNPs treated cloth and time

Strange behavior of AgNPs loaded cloth was found. The AgNPs incorporated cloth was left in the open air in the laboratory. Any experiment was not done within 5 months of preparation due to the Covid-19 pandemic. After then, the AgNPs incorporated samples were tested for antibacterial action. But, it showed very poorly, in some cases, negative antibacterial results in all the samples. After trying in various ways, finally, it was discovered that this happened due to the presence of Ag^+ all over the fabrics along with AgNPs. The Ag^+ was attached with moisture from the surroundings and formed zero-valent nanoparticles. The plenty of zero-valent silver compounds produced a nanofilm over the fabrics. Due to this film, the samples exhibit no antibacterial property (Lok et al. 2007). However, when it was washed for more than 5 home wash or 1 mechanical wash with 10 steel balls (According to AATCC 61-2010 method), about 100% antibacterial performance was obtained back. Because the detergent will destroy the zero-valent nanofilm, and again the antibacterial Ag^+ enriched AgNPs will come out. This behavior is termed the *time-effect*.

The zero-valent compound is massively formed by the presence of excess NaOH on the surface (due to the padding roller). It matches with (Xue and Mirkin

2007), who claimed the high pH would remove more Ag^+ ions by forming a passive layer of AgOH.

Table 4.26. Time effect on various samples

Sample	PE-ratio	$AgNO_3$ Mol.	$AgNO_3$ Vol	Fabric	pH	Method	Bacteria -no- wash	Bacteria (after wash)
p-2mM-.04-x3-p	0.04	0.002	100	plain	7.2	pad80%	1800	0
p-2mM-.04-x1-t	0.04	0.002	100	twill	8.3	pad80%	1300	11
p-2mM-.04-x4-p	0.04	0.002	100	plain	7.2	pad80%	1300	0
p-2mM-.04-x1-k	0.04	0.002	100	knit	7.4	pad80%	1200	1
p-2mM-.04-x1-p	0.04	0.002	100	plain	7.2	pad80%	1200	1
p-2mM-.04-x3-k	0.04	0.002	100	knit	7.4	pad80%	1200	0
p-2mM-.04-x3-t	0.04	0.002	100	twill	8.3	pad80%	900	6
in-2mM-.06-t	**0.06**	**0.002**	**100**	**twill**	**8.3**	**insitu**	**636**	**8**
p-2mM-.04-x4-t	0.04	0.002	100	twill	7.9	pad80%	630	1
p-2mM-.04-x4-k	0.04	0.002	100	knit	7.4	pad80%	630	0
p-2mM-.04-x4-t	0.04	0.002	100	twill	8.3	pad80%	600	1
in-2mM-.16-t	**0.16**	**0.002**	**25**	**twill**	**8.3**	**insitu**	**570**	**12**
in-2mM-.04-t	0.04	0.002	100	twill	7.9	insitu	570	6
in-0.1M-0.1-t	**0.1**	**0.1**	**10**	**twill**	**8.3**	**insitu**	**540**	1
in-2mM-.06-k	0.06	0.002	100	knit	7.4	insitu	430	4
imn-2mM-.04-wk	**0.04**	**0.002**	**100**	**knit**	**7.4**	**immersion**	**430**	4
in-2mM-.04-k	0.04	0.002	100	knit	7.4	insitu	430	4
imm-2mM-.04-p	0.04	0.002	100	plain	7.2	immersion	277	0
im-2mM-.03-p	**0.03**	**0.002**	**100**	**plain**	**7.2**	**pad100%**	**170**	0
pad-2mM-.04-x8	0.04	0.002	100	knit	7.4	pad80%	158	0
in-2mM-.06-p	0.06	0.002	100	plain	7.2	insitu	114	4
in-2mM-.04-p	0.04	0.002	100	plain	7.2	insitu	114	1
imn-2mM-.04-up	**0.04**	**0.002**	**100**	**plain**	**7.2**	**immersion**	**114**	**1**
in-9mM-0.10-p	**0.1**	**0.009**	**110**	**plain**	**7.2**	**insitu**	**80**	**0**
in-d-2mM-.04-p	0.067	0.002	50	plain	7.2	insitu	16	12
in-2mM-.067-k	0.067	0.002	50	knit	7.4	insitu	16	12
in-2mM-.067-p	0.067	0.002	50	plain	7.2	insitu	10	10
imn-2mM-.03-p	**0.03**	**0.002**	**200**	**plain**	**7.2**	**Imm-insitu**	**7**	0
in-2mM-.067-t	0.067	0.002	50	twill	8.3	insitu	6	5

However, it cannot be claimed that AgOH is formed here, as AgOH will convert to Ag_2O, which has antibacterial activity. But in this case, the zero-valent AgNPs film has no antibacterial activity.

4.17.1. Plant extract on time effect

Table 4.26 shows- that increasing plant extract will decrease bacterial growth. As shown in figure 4.73. However, there are few exceptions, 0.03 plant extract ratio is supposed to be more prone to growing bacteria. But in practice there is less bacteria (for pad100% (imm-2mM-.03-p) it grows 170, whether immersion-in-situ (imn-2mM-.03-p) grows only 7 bacteria. Here 200 ml $AgNO_3$ volume (0.002 M) was used. The high volume of $AgNO_3$ will disperse the Ag^+ more, whether plant extract being little will be enough for highly diluted $AgNO_3$ due to dispersion.

Moreover, the immersion in the *in-situ* state will cause some loss of fabric pH and precipitate some Ag^+ as Ag_2O. Hence there will be a very low number of loosely bound Ag^+ ions on the AgNPs surface. As a result, the "time-effect" will not be so active here due to the lack of Ag^+ ions.

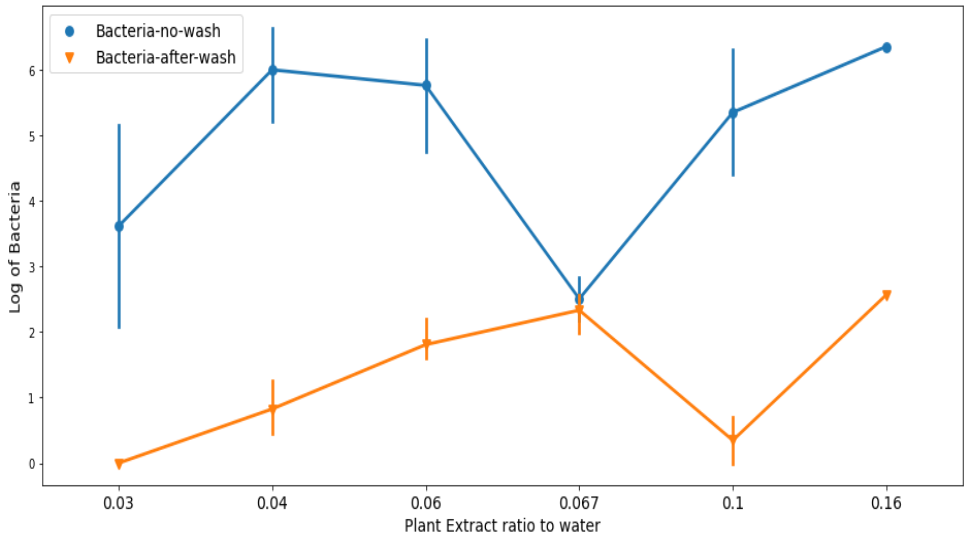


Figure 4.73. Influence of plant extract on time effect

The exact opposite happened in the case of the low volume of $AgNO_3$ but high concentric plant extract ratio. The high concentration of plant extract in the sample *in-0.1M-0.1-t* and *in-2mM-.16-t* have 540 and 570 bacteria, respectively. In these cases, the remaining NaOH will not be decreased due to the low amount of $AgNO_3$ volume 10 and 25, respectively, which will react later with the atmosphere and produce the specified zero-valent AgNPs.

4.17.2. $AgNO_3$ Volume on time effect

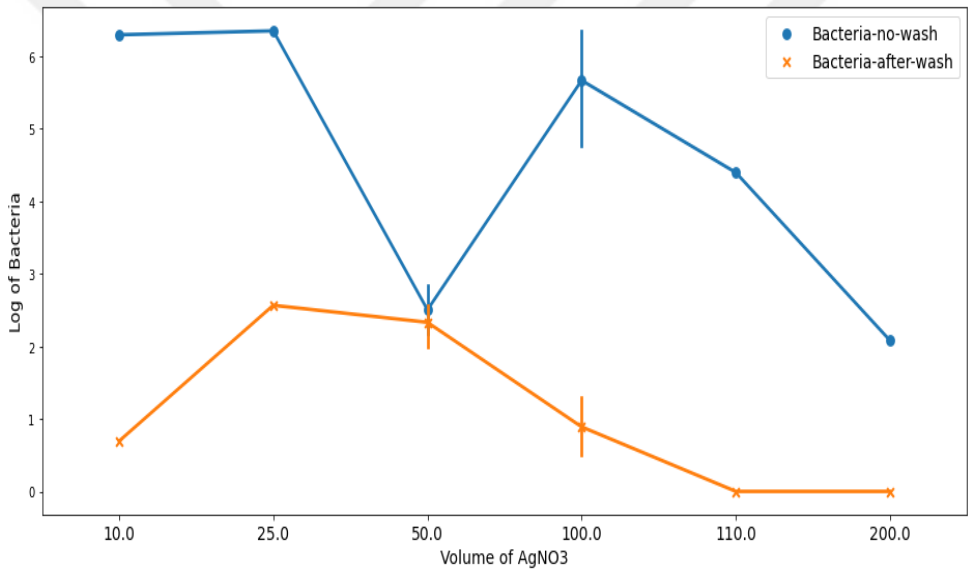


Figure 4.74. $AgNO_3$ volume on time effect

Figure 4.74 shows that the $AgNO_3$ volume has a very influential effect on the "time-effect". The high volume of $AgNO_3$ will have a low *time-effect* and excellent recovery. The antibacterial activity of AgNPs depends largely on AgNPs dispersion which is easy for high volume (Lok et al. 2007).

4.17.3. Various methods on time effect

The effect of various methods is depicted in figure 4.75. Among all the methods, the padding method loses antibacterial property to a greater extent with time, whereas the immersion and the in-situ method will not tent.

This padding method will squeeze out a lot of plant extract along with AgNPs, but the chemisorbed Ag^+ will be on the fabric surface. Moreover, the surface of the fabric will be more alkaline due to the squeezed out adhered NaOH on the roller. This hypothesis is supported by the (table 4.26: *imn-2mM-.04-wk : bacteria-430*) where the AgNPs incorporated fabric is washed with water, and hence it removes some more unfixed plant extract, not the chemisorbed Ag^+ ion due to the tightly adsorbed on AgNPs and cellulose (Lok et al. 2007) which lead to zero-valent AgNPs by time. On the contrary, the same sample was kept unwashed (table 4.26: imn-2mM-.04-up: bacteria-114), and the obtained bacterial colony here is only 114. The remaining plant extract will keep the chemisorbed Ag^+ ions on the AgNPs surface and suppress the zero-valent AgNPs. The oxidized AgNPs have antibacterial activity, but the zero-valent AgNPs don't have (Lok et al. 2007).

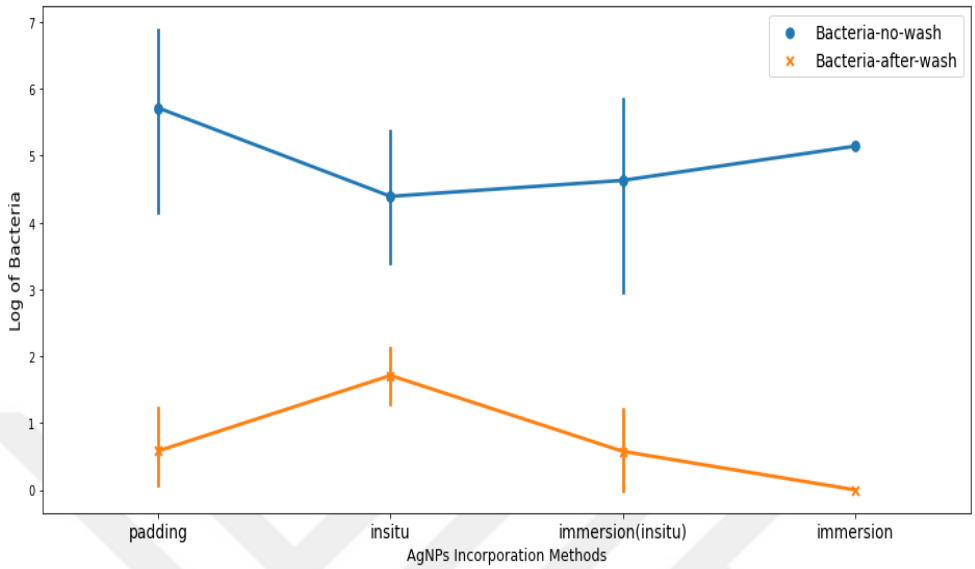


Figure 4.75. Different AgNPs incorporation methods on time effect

Among different incorporation methods on the *time-effect*, padding and immersion are affected mainly by the time-effect. But both recover up to 100%. Because here, the synthesized AgNPs are incorporated into the fabrics. Padding will squeeze out 20%. On the other hand, immersion will not squeeze out at all. On the contrary, *in-situ* and *immersion (in-situ)* methods will synthesize AgNPs inside the fabrics. It can be hypothesized that the *in-situ* synthesized AgNPs do not have much chemisorbed Ag^{+} as the synthesis happens inside the fibers.

On the other hand, AgNPs synthesized in the vessel and later incorporated inside the fabrics- will have more chemisorbed Ag^{+} ions. For this reason, the padding method works the best regarding the antibacterial activity. And previously, it was discussed that the Ag^{+} ions get converted to zero-valent AgNPs and lose their antibacterial property.

4.17.4. Fabric pH on time effect

The fabric pH also has an influential effect on antibacterial property loss with time. The results are in figure 4.76. It shows high pH will allow more bacterial growth with time (i, e loss of antibacterial activity) and have a good recovery until pH 7.9. Beyond pH 7.9, there will be more zero-valent AgNPs, and hence it will need more wash to remove all zero-valent AgNPs.

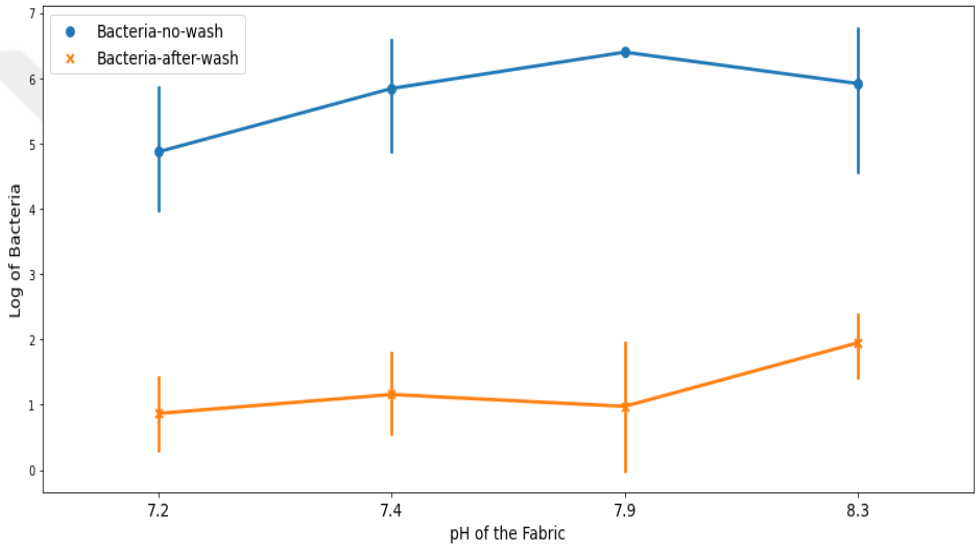


Figure 4.76. pH on time effect on AgNPs loaded fabrics

5. CONCLUSION AND RECOMMENDATIONS

5.1. Conclusion

This study included antibacterial textiles preparation with AgNPs in detail. An equation for determining plant extract for both ex-situ and in-situ methods was formulated to ensure minimum AgNPs size. Then AgNPs were incorporated into different types of fabrics using various methods. A new kind of problem of decreasing antibacterial properties with time has been observed. It is termed *time-effect*, where the AgNPs lose their antibacterial property with time, but it is recoverable by washing. This phenomenon is believed to be the conversion of chemisorbed Ag^+ ions to zero-valent AgNPs. However, it was not possible to ensure the formed zero-valent AgNPs and their antibacterial recovery mechanism.

Antibacterial textiles are getting a crying need in the future due to climate change and global pandemics such as Covid-19. The earth is getting warmer, and people will be affected by the various diseases related to the humid and hot conditions. In these cases, people may protect themselves by using antibacterial textiles. For example, the athlete's foot is caused by a fungal attack, and it might be prevented by using antibacterial incorporated soaks. Likewise, intimate clothes can also be pretreated using AgNPs. AgNPs being of a lower amount can work well as well as it will also not do so much harm to the environment and skin. The potential harm can also be tremendously minimized by decreasing the molarity of $AgNO_3$ with an excellent reducing agent. The used *C.arvensis* plant extract is also a good synthesizer. Moreover, an excellent pretreatment could also prevent the Ag^+ from leaching a lot.

5.2. Recommendations

Based on the studies, several recommendations can be made to have cheaper and more effective antimicrobial textiles for multidisciplinary applications.

1. More in-depth study is needed here to explain the shaping mechanism. This study explained using thermodynamic equilibrium, surface-free energy, crystallinity, and Gibbs free energy. But it should be studied more profoundly, and there may be some relation with electro-chemistry.
2. This study found pretreatment is a crucial factor for antibacterial textiles. Seven different samples were prepared with three different pretreatment agents, but the pretreatment agents were mixed simultaneously in the same vessel. It should be applied separately- after applying one pretreatment, it should be dried fully and then applied to the second pretreatment and then fully dried. In this way, the pretreatment chemicals will not react with each other outside fabrics.
3. It was also found lowest $AgNO_3$ molarity works better. However, up to 0.001 M was experimented with, which gave excellent results. It is recommended to experiment with as lesser molarity as possible. Besides, studies on strength loss and odor generation of AgNPs incorporated fabrics should be done.
4. Another important outcome of this study is that *C.arvensis* is better than *C.reticulata* in its antibacterial property. It should be investigated peruse. The presence of phytochemicals should be determined. The presence of exact alkene compounds should be determined.
5. This study used only two species of plants. More organic species should be tried to produce differently shaped nanoparticles.

6. The use of high molarity is often undesirable due to the cost and toxicity to the ecosystem. Details comparative study should be done to find out an appropriate plant species and plant extract amount that can provide the best antibacterial results.
7. This study primarily focuses on antibacterial activity. It should be extended to prevent odor, fabric color, and strength loss.
8. The implementation parts should be extended from regular clothes to medical and agricultural textiles.
9. The inhabitants of winter countries often suffer from various fungal diseases in this foot due to putting on socks. It is envisaged that this study may solve the problems by implementing synthesized silver nanoparticles into the socks to have a good antibacterial property.
10. Other nanoparticles from different metals such as Zinc, Iron, Manganese, Magnesium, Copper, Aluminum, etc., should be synthesized for cheaper antimicrobial textiles.

REFERENCES

Abbaszadegan, A, Y Ghahramani, A Gholami, B Hemmateenejad, S Dorostkar, M Nabavizadeh and H Sharghi. 2015. The Effect of Charge at the Surface of Silver Nanoparticles on Antimicrobial Activity against Gram-Positive and Gram-Negative Bacteria: A Preliminary Study. Research Article. *Journal of Nanomaterials*. Hindawi. doi:https://doi.org/10.1155/2015/720654.

Abou-Okeil, A, AM Sheta, A Amr and MA Ali. 2012. Wound Dressing Based on Nonwoven Viscose Fabrics. *Carbohydrate Polymers* 90 (1): 658–666. doi:10.1016/j.carbpol.2012.05.093.

Abramov, OV, A Gedanken, Y Koltypin, N Perkas, I Perelshtein, E Joyce and TJ Mason. 2009. Pilot Scale Sonochemical Coating of Nanoparticles onto Textiles to Produce Biocidal Fabrics. *Surface and Coatings Technology* 204 (5): 718–722. doi:10.1016/j.surfcoat.2009.09.030.

Abudunia, A-M, I Marmouzi, MEA Faouzi, Y Ramli, J Taoufik, N El Madani, EM Essassi, A Salama, K Khedid, M Ansar and A Ibrahimi. 2017. Anticandidal, Antibacterial, Cytotoxic and Antioxidant Activities of Calendula Arvensis Flowers. *Journal de Mycologie Médicale* 27 (1): 90–97. doi:10.1016/j.mycmed.2016.11.002.

Abutaha, N, FA Nasr, A-Z Mohammed, A Semlali, FA Al-Mekhlafi and MA Wadaan. 2019. Calendula Arvensis L. as an Anti-Cancer Agent against Breast Cancer Cell Lines. *Molecular Biology Reports* 46 (2): 2187–2196. doi:10.1007/s11033-019-04672-3.

Agcayazi, T, K Chatterjee, A Bozkurt and TK Ghosh. 2018. Flexible Interconnects for Electronic Textiles. *Advanced Materials Technologies* 3 (10): 1700277. doi:10.1002/admt.201700277.

Ahmed, S, M Ahmad, BL Swami and S Ikram. 2016. A Review on Plants Extract Mediated Synthesis of Silver Nanoparticles for Antimicrobial Applications: A Green Expertise. *Journal of Advanced Research* 7 (1): 17–28. doi:10.1016/j.jare.2015.02.007.

Ahmed, T, and RT Ogulata. 2021. A Review on Silver Nanoparticles -Green Synthesis, Antimicrobial Action and Application in Textiles. *Journal of Natural Fibers* 0 (0). Taylor & Francis: 1–22. doi:10.1080/15440478.2021.1964135.

Andreescu, D, C Eastman, K Balantrapu and DV Goia. 2007. A Simple Route for Manufacturing Highly Dispersed Silver Nanoparticles. *Journal of Materials Research* 22 (9). Cambridge University Press: 2488–2496. doi:10.1557/jmr.2007.0308.

Anil Kumar, S, MK Abyaneh, SW Gosavi, SK Kulkarni, R Pasricha, A Ahmad and MI Khan. 2007. Nitrate Reductase-Mediated Synthesis of Silver Nanoparticles from AgNO3. *Biotechnology Letters* 29 (3): 439–445. doi:10.1007/s10529-006-9256-7.

Annadhasan, M, VR SankarBabu, R Naresh, K Umamaheswari and N Rajendiran. 2012. A Sunlight-Induced Rapid Synthesis of Silver Nanoparticles Using Sodium Salt of N-Cholyl Amino Acids and Its Antimicrobial Applications. *Colloids and Surfaces B: Biointerfaces* 96 (August): 14–21. doi:10.1016/j.colsurfb.2012.03.009.

Asanović, K, T Mihailović, P Škundrić and L Simović. 2010. Some Properties of Antimicrobial Coated Knitted Textile Material Evaluation. *Textile Research Journal* 80 (16): 1665–1674. doi:10.1177/0040517510361805.

Baszkin, A, and W Norde. 1999. *Physical Chemistry of Biological Interfaces*. CRC Press.

Behravan, M, A Hossein Panahi, A Naghizadeh, M Ziaee, R Mahdavi and A Mirzapour. 2019. Facile Green Synthesis of Silver Nanoparticles Using Berberis Vulgaris Leaf and Root Aqueous Extract and Its Antibacterial Activity. *International Journal of Biological Macromolecules* 124 (March): 148–154. doi:10.1016/j.ijbiomac.2018.11.101.

Behzad, F, SM Naghib, MAJ kouhbanani, SN Tabatabaei, Y Zare and KY Rhee. 2021. An Overview of the Plant-Mediated Green Synthesis of Noble Metal Nanoparticles for Antibacterial Applications. *Journal of Industrial and Engineering Chemistry* 94 (February): 92–104. doi:10.1016/j.jiec.2020.12.005.

Benesty, J, Jingdong Chen, and Yiteng Huang. 2008. On the Importance of the Pearson Correlation Coefficient in Noise Reduction. *IEEE Transactions on Audio, Speech, and Language Processing* 16 (4): 757–765. doi:10.1109/TASL.2008.919072.

Bianchini, A, KC Bowles, CJ Brauner, JW Gorsuch, JR Kramer and CM Wood. 2002. Evaluation of the Effect of Reactive Sulfide on the Acute Toxicity of Silver (I) to Daphnia Magna. Part 2: Toxicity Results. *Environmental Toxicology and Chemistry* 21 (6): 1294–1300.

Burda, C, X Chen, R Narayanan and MA El-Sayed. 2005. Chemistry and Properties of Nanocrystals of Different Shapes. *Chemical Reviews* 105 (4). American Chemical Society: 1025–1102. doi:10.1021/cr030063a.

Cappitelli, F, and C Sorlini. 2008. Microorganisms Attack Synthetic Polymers in Items Representing Our Cultural Heritage. *Applied and Environmental Microbiology* 74 (3): 564–569. doi:10.1128/AEM.01768-07.

Chauhan, P, A Kumar and B Bhushan. 2019. Self-Cleaning, Stain-Resistant and Anti-Bacterial Superhydrophobic Cotton Fabric Prepared by Simple Immersion

Technique. *Journal of Colloid and Interface Science* 535 (February): 66–74. doi:10.1016/j.jcis.2018.09.087.

Choi, O, and Z Hu. 2008. Size Dependent and Reactive Oxygen Species Related Nanosilver Toxicity to Nitrifying Bacteria. *Environmental Science & Technology* 42 (12): 4583–4588. doi:10.1021/es703238h.

Christensen, FM, HJ Johnston, V Stone, RJ Aitken, S Hankin, S Peters and K Aschberger. 2010. Nano-Silver – Feasibility and Challenges for Human Health Risk Assessment Based on Open Literature. *Nanotoxicology* 4 (3). Taylor & Francis: 284–295. doi:10.3109/17435391003690549.

Dai, LL, R Sharma and C Wu. 2005. Self-Assembled Structure of Nanoparticles at a Liquid−Liquid Interface. *Langmuir* 21 (7): 2641–2643. doi:10.1021/la047256t.

Darroudi, M, MB Ahmad, R Zamiri, A Zak, AH Abdullah and NA Ibrahim. 2011. Time-Dependent Effect in Green Synthesis of Silver Nanoparticles. *International Journal of Nanomedicine* 6: 677–681. doi:10.2147/IJN.S17669.

Dibrov, P, J Dzioba, KK Gosink and CC Häse. 2002. Chemiosmotic Mechanism of Antimicrobial Activity of Ag^{+} in *Vibrio Cholerae*. *Antimicrobial Agents and Chemotherapy* 46 (8): 2668–2670. doi:10.1128/AAC.46.8.2668-2670.2002.

Dillard, CJ, and AL Tappel. 1986. Mercury, Silver, and Gold Inhibition of Selenium-Accelerated Cysteine Oxidation. *Journal of Inorganic Biochemistry* 28 (1): 13–20. doi:10.1016/0162-0134(86)80019-8.

Dong, X, X Ji, J Jing, M Li, J Li and W Yang. 2010. Synthesis of Triangular Silver Nanoprisms by Stepwise Reduction of Sodium Borohydride and Trisodium Citrate. *The Journal of Physical Chemistry C* 114 (5). American Chemical Society: 2070–2074. doi:10.1021/jp909964k.

Dong, X, X Ji, H Wu, L Zhao, J Li and W Yang. 2009. Shape Control of Silver Nanoparticles by Stepwise Citrate Reduction. *The Journal of Physical*

Chemistry C 113 (16). American Chemical Society: 6573–6576. doi:10.1021/jp900775b.

Durán, N, PD Marcato, GIH De Souza, OL Alves and E Esposito. 2007. Antibacterial Effect of Silver Nanoparticles Produced by Fungal Process on Textile Fabrics and Their Effluent Treatment. *Journal of Biomedical Nanotechnology* 3 (2): 203–208. doi:10.1166/jbn.2007.022.

El-Bisi, MK, H.M. El-Rafie, M.H. El-Rafie, and A.Hebeish. 2013. Honey Bee for Eco-Friendly Green Synthesis of Silver Nanoparticles and Application to Cotton Textile. *Egyptian Journal of Chemistry* 56 (3): 187–198. doi:10.21608/ejchem.2013.1107.

Engelbrekt, C, KH Sørensen, J Zhang, AC Welinder, PS Jensen and J Ulstrup. 2009. Green Synthesis of Gold Nanoparticles with Starch–Glucose and Application in Bioelectrochemistry. *Journal of Materials Chemistry* 19 (42): 7839. doi:10.1039/b911111e.

Erickson, RJ, LT Brooke, MD Kahl, FV Venter, SL Harting, TP Markee and RL Spehar. 1998. Effects of Laboratory Test Conditions on the Toxicity of Silver to Aquatic Organisms. *Environmental Toxicology and Chemistry* 17 (4): 572–578. doi:10.1002/etc.5620170407.

Fabrega, J, SN Luoma, CR Tyler, TS Galloway and JR Lead. 2011. Silver Nanoparticles: Behaviour and Effects in the Aquatic Environment. *Environment International* 37 (2): 517–531. doi:10.1016/j.envint.2010.10.012.

Fafal, T, P Taştan, BS Tüzün, M Ozyazici and B Kivcak. 2017. Synthesis, Characterization and Studies on Antioxidant Activity of Silver Nanoparticles Using Asphodelus Aestivus Brot. Aerial Part Extract. *South African Journal of Botany* 112 (September): 346–353. doi:10.1016/j.sajb.2017.06.019.

Feng, QL, J Wu, GQ Chen, FZ Cui, TN Kim and JO Kim. 2000. A Mechanistic Study of the Antibacterial Effect of Silver Ions on Escherichia Coli and Staphylococcus Aureus. *Journal of Biomedical Materials Research* 52 (4): 662–668. doi:10.1002/1097-4636(20001215)52:4<662::AID-JBM10>3.0.CO;2-3.

Firdhouse, MJ, and P Lalitha. 2016. Biogenic Silver Nanoparticles – Synthesis, Characterization and Its Potential against Cancer Inducing Bacteria. *Journal of Molecular Liquids* 222 (October): 1041–1050. doi:10.1016/j.molliq.2016.07.141.

Froelicher, Y, D Dambier, JB Bassene, G Costantino, S Lotfy, C Didout, V Beaumont, P Brottier, AM Risterucci, F Luro and P Ollitrault. 2008. Characterization of Microsatellite Markers in Mandarin Orange (Citrus Reticulata Blanco). *Molecular Ecology Resources* 8 (1): 119–122. doi:10.1111/j.1471-8286.2007.01893.x.

Gardea-Torresdey, JL, E Gomez, JR Peralta-Videa, JG Parsons, H Troiani and M Jose-Yacaman. 2003. Alfalfa Sprouts: A Natural Source for the Synthesis of Silver Nanoparticles. *Langmuir* 19 (4). American Chemical Society: 1357–1361. doi:10.1021/la020835i.

Gomathi, M, PV Rajkumar, A Prakasam and K Ravichandran. 2017. Green Synthesis of Silver Nanoparticles Using Datura Stramonium Leaf Extract and Assessment of Their Antibacterial Activity. *Resource-Efficient Technologies* 3 (3): 280–284. doi:10.1016/j.reffit.2016.12.005.

González-Ballesteros, N, JB Rodríguez-González and MC Rodríguez-Argüelles. 2018. Harnessing the Wine Dregs: An Approach towards a More Sustainable Synthesis of Gold and Silver Nanoparticles. *Journal of Photochemistry and Photobiology B: Biology* 178 (January): 302–309. doi:10.1016/j.jphotobiol.2017.11.025.

Gorup, LF, E Longo, ER Leite and ER Camargo. 2011. Moderating Effect of Ammonia on Particle Growth and Stability of Quasi-Monodisperse Silver Nanoparticles Synthesized by the Turkevich Method. *Journal of Colloid and Interface Science* 360 (2): 355–358. doi:10.1016/j.jcis.2011.04.099.

Gudikandula, K, P Vadapally and MA Singara Charya. 2017. Biogenic Synthesis of Silver Nanoparticles from White Rot Fungi: Their Characterization and Antibacterial Studies. *OpenNano* 2 (January): 64–78. doi:10.1016/j.onano.2017.07.002.

Guilger-Casagrande, M, and R de Lima. 2019. Synthesis of Silver Nanoparticles Mediated by Fungi: A Review. *Frontiers in Bioengineering and Biotechnology* 7. Frontiers. doi:10.3389/fbioe.2019.00287.

Haruta, M. 2004. Nanoparticulate Gold Catalysts for Low-Temperature CO Oxidation. *ChemInform* 35 (48). doi:10.1002/chin.200448226.

Hashem, M, NA Ibrahim, WA El-Sayed, S El-Husseiny and E El-Enany. 2009. Enhancing Antimicrobial Properties of Dyed and Finished Cotton Fabrics. *Carbohydrate Polymers* 78 (3). Elsevier Ltd: 502–510. doi:10.1016/j.carbpol.2009.05.007.

Hebeish, A, FA Abdel-Mohdy, MMG Fouda, Z Elsaid, S Essam, GH Tammam and EA Drees. 2011. Green Synthesis of Easy Care and Antimicrobial Cotton Fabrics. *Carbohydrate Polymers* 86 (4). Elsevier Ltd.: 1684–1691. doi:10.1016/j.carbpol.2011.06.086.

Hernández-Barrios, CA, CA Cuao, MA Jaimes, AE Coy and F Viejo. 2017. Effect of the Catalyst Concentration, the Immersion Time and the Aging Time on the Morphology, Composition and Corrosion Performance of TEOS-GPTMS Sol-Gel Coatings Deposited on the AZ31 Magnesium Alloy. *Surface and Coatings Technology* 325 (September): 257–269. doi:10.1016/j.surfcoat.2017.06.047.

Heydari, R, and M Rashidipour. 2015. Green Synthesis of Silver Nanoparticles Using Extract of Oak Fruit Hull (Jaft): Synthesis and In Vitro Cytotoxic Effect on MCF-7 Cells. Research Article. *International Journal of Breast Cancer*. Hindawi. doi:https://doi.org/10.1155/2015/846743.

Hiremath, L, S Narendra Kumar and P Sukanya. 2018a. Development of Antimicrobial Smart Textiles Fabricated with Magnetite Nano Particles Obtained Through Green Synthesis. *Materials Today: Proceedings* 5 (10): 21030–21039. doi:10.1016/j.matpr.2018.06.496.

Hiremath, L, S Narendra Kumar and P Sukanya. 2018b. Development of Antimicrobial Smart Textiles Fabricated with Magnetite Nano Particles Obtained Through Green Synthesis. *Materials Today: Proceedings* 5 (10). Elsevier Ltd: 21030–21039. doi:10.1016/j.matpr.2018.06.496.

House, JE, and KA House. 2016. Chapter 14 - Phosphorus, Arsenic, Antimony, and Bismuth. In *Descriptive Inorganic Chemistry (Third Edition)*, edited by James E. House and Kathleen A. House, 215–234. Boston: Academic Press. doi:10.1016/B978-0-12-804697-5.00014-2.

Ider, M, K Abderrafi, A Eddahbi, S Ouaskit and A Kassiba. 2017. Silver Metallic Nanoparticles with Surface Plasmon Resonance: Synthesis and Characterizations. *Journal of Cluster Science* 28 (3): 1051–1069. doi:10.1007/s10876-016-1080-1.

Im, SH, YT Lee, B Wiley and Y Xia. 2005. Large-Scale Synthesis of Silver Nanocubes: The Role of HCl in Promoting Cube Perfection and Monodispersity. *Angewandte Chemie International Edition* 44 (14): 2154–2157. doi:10.1002/anie.200462208.

Introduction to Bacteria. 2022. *Let's Talk Science*. Accessed April 26. https://letstalkscience.ca/educational-resources/backgrounders/introduction-bacteria.

Ji, JH, JH Jung, SS Kim, J-U Yoon, JD Park, BS Choi, YH Chung, IH Kwon, J Jeong, BS Han, JH Shin, JH Sung, KS Song and IJ Yu. 2007. Twenty-Eight-Day Inhalation Toxicity Study of Silver Nanoparticles in Sprague-Dawley Rats. *Inhalation Toxicology* 19 (10). Taylor & Francis: 857–871. doi:10.1080/08958370701432108.

Ji, M, X Chen, CM Wai and JL Fulton. 1999. Synthesizing and Dispersing Silver Nanoparticles in a Water-in-Supercritical Carbon Dioxide Microemulsion. *Journal of the American Chemical Society* 121 (11): 2631–2632. doi:10.1021/ja9840403.

Jiménez-Jiménez, C, VM Moreno and M Vallet-Regí. 2022. Bacteria-Assisted Transport of Nanomaterials to Improve Drug Delivery in Cancer Therapy. *Nanomaterials* 12 (2). Multidisciplinary Digital Publishing Institute: 288. doi:10.3390/nano12020288.

Kalimuthu, K, R Suresh Babu, D Venkataraman, Mohd Bilal and S Gurunathan. 2008. Biosynthesis of Silver Nanocrystals by Bacillus Licheniformis. *Colloids and Surfaces B: Biointerfaces* 65 (1): 150–153. doi:10.1016/j.colsurfb.2008.02.018.

Kanchi, S, and S Ahmed, Eds. 2018. *Green Metal Nanoparticles: Synthesis, Characterization and Their Applications*. Hoboken, NJ: Wiley-Scrivener.

Kara, R, and K Robert J. 2022. Britannica. Accessed April 26. https://www.britannica.com/science/bacteria.

Kashiwagi, Y, M Yamamoto and M Nakamoto. 2006. Facile Size-Regulated Synthesis of Silver Nanoparticles by Controlled Thermolysis of Silver Alkylcarboxylates

in the Presence of Alkylamines with Different Chain Lengths. *Journal of Colloid and Interface Science* 300 (1): 169–175. doi:10.1016/j.jcis.2006.03.041.

Khalil, MMH, EH Ismail, KZ El-Baghdady and D Mohamed. 2014. Green Synthesis of Silver Nanoparticles Using Olive Leaf Extract and Its Antibacterial Activity. *Arabian Journal of Chemistry* 7 (6): 1131–1139. doi:10.1016/j.arabjc.2013.04.007.

Kim, JS, E Kuk, KN Yu, J-H Kim, SJ Park, HJ Lee, SH Kim, YK Park, YH Park, C-Y Hwang, Y-K Kim, Y-S Lee, DH Jeong and M-H Cho. 2007. Antimicrobial Effects of Silver Nanoparticles. *Nanomedicine: Nanotechnology, Biology and Medicine* 3 (1): 95–101. doi:10.1016/j.nano.2006.12.001.

Kim, S-H, H-S Lee, D-S Ryu, S-J Choi and D-S Lee. 2011. Antibacterial Activity of Silver-Nanoparticles Against Staphylococcus Aureus and Escherichia Coli. *Microbiology and Biotechnology Letters* 39 (1). The Korean Society for Microbiology and Biotechnology: 77–85. https://www.koreascience.or.kr/article/JAKO201106737198819.page.

Kiran Pulidindi, HP. 2020. Antimicrobial Market. *Global Market Insights, Inc*. https://www.gminsights.com/industry-analysis/antimicrobial-textiles-market.

Kırmızıbekmez, H, C Bassarello, S Piacente, C Pizza and İ Çalış. 2006. Triterpene Saponins from Calendula Arvensis. *Zeitschrift Für Naturforschung B* 61 (9): 1170–1173. doi:10.1515/znb-2006-0920.

Km, F, H M and N S. 1996. Content of Carbon, Nitrogen, Oxygen, Sulfur and Phosphorus in Native Aquatic and Cultured Bacteria. *Aquatic Microbial Ecology* 10 (1): 15–27. doi:10.3354/ame010015.

Lansdown, ABG. 2010. A Pharmacological and Toxicological Profile of Silver as an Antimicrobial Agent in Medical Devices. *Advances in Pharmacological Sciences* 2010 (August). Hindawi: e910686. doi:10.1155/2010/910686.

Lee, PC, and D Meisel. 1982. Adsorption and Surface-Enhanced Raman of Dyes on Silver and Gold Sols. *The Journal of Physical Chemistry* 86 (17). American Chemical Society: 3391–3395. doi:10.1021/j100214a025.

Leung, TC-Y, CK Wong and Y Xie. 2010. Green Synthesis of Silver Nanoparticles Using Biopolymers, Carboxymethylated-Curdlan and Fucoidan. *Materials Chemistry and Physics* 121 (3): 402–405. doi:10.1016/j.matchemphys.2010.02.026.

Li, L, L Song, T Hua, WM au and KS Wong. 2013. Characteristics of Weaving Parameters in Microcapsule Fabrics and Their Influence on Loading Capability. *Textile Research Journal* 83 (2): 113–121. doi:10.1177/0040517512454184.

Li, S, Y Shen, A Xie, X Yu, L Qiu, L Zhang and Q Zhang. 2007. Green Synthesis of Silver Nanoparticles Using Capsicum Annuum L. Extract. *Green Chemistry* 9 (8): 852. doi:10.1039/b615357g.

Liao, C, Y Li and SC Tjong. 2019. Bactericidal and Cytotoxic Properties of Silver Nanoparticles. *International Journal of Molecular Sciences* 20 (2). Multidisciplinary Digital Publishing Institute: 449. doi:10.3390/ijms20020449.

Lim, DC, I Lopez-Salido and YD Kim. 2006. Characterization of Ag Nanoparticles on Si Wafer Prepared Using Tollen's Reagent and Acid-Etching. *Applied Surface Science* 253 (2): 959–965. doi:10.1016/j.apsusc.2006.01.040.

Lim, S-H, and SM Hudson. 2004. Application of a Fiber-Reactive Chitosan Derivative to Cotton Fabric as an Antimicrobial Textile Finish. *Carbohydrate Polymers* 56 (2): 227–234. doi:10.1016/j.carbpol.2004.02.005.

Lin, D, X Zeng, H Li, X Lai and T Wu. 2019. One-Pot Fabrication of Superhydrophobic and Flame-Retardant Coatings on Cotton Fabrics via Sol-Gel Reaction. *Journal of Colloid and Interface Science* 533 (January): 198–206. doi:10.1016/j.jcis.2018.08.060.

Lok, C-N, C-M Ho, R Chen, Q-Y He, W-Y Yu, H Sun, PK-H Tam, J-F Chiu and C-M Che. 2007. Silver Nanoparticles: Partial Oxidation and Antibacterial Activities. *JBIC Journal of Biological Inorganic Chemistry* 12 (4): 527–534. doi:10.1007/s00775-007-0208-z.

López-Téllez, G, P Balderas-Hernández, CE Barrera-Díaz, AR Vilchis-Nestor, G Roa-Morales and B Bilyeu. 2013. Green Method to Form Iron Oxide Nanorods in Orange Peels for Chromium(VI) Reduction. *Journal of Nanoscience and Nanotechnology* 13 (3): 2354–2361. doi:10.1166/jnn.2013.7093.

Luo, W, W Hu and S Xiao. 2008. Size Effect on the Thermodynamic Properties of Silver Nanoparticles. *The Journal of Physical Chemistry C* 112 (7). American Chemical Society: 2359–2369. doi:10.1021/jp0770155.

Magudapathy, P, P Gangopadhyay, BK Panigrahi, KGM Nair and S Dhara. 2001. Electrical Transport Studies of Ag Nanoclusters Embedded in Glass Matrix. *Physica B: Condensed Matter* 299 (1): 142–146. doi:10.1016/S0921-4526(00)00580-9.

Mahltig, B., and H Böttcher. 2003. Modified Silica Sol Coatings for Water-Repellent Textiles. *Journal of Sol-Gel Science and Technology* 27 (1): 43–52. doi:10.1023/A:1022627926243.

Mahltig, B., D Fiedler and H Böttcher. 2004. Antimicrobial Sol–Gel Coatings. *Journal of Sol-Gel Science and Technology* 32 (1): 219–222. doi:10.1007/s10971-004-5791-7.

Mahltig, Boris, H Haufe and H Böttcher. 2005. Functionalisation of Textiles by Inorganic Sol–Gel Coatings. *Journal of Materials Chemistry* 15 (41): 4385. doi:10.1039/b505177k.

Makarov, VV, AJ Love, OV Sinitsyna, SS Makarova, IV Yaminsky, ME Taliansky and NO Kalinina. 2014. “Green” Nanotechnologies: Synthesis of Metal

Nanoparticles Using Plants. *Acta Naturae* 6 (1): 35–44. https://www.ncbi.nlm.nih.gov/pmc/articles/PMC3999464/.

Mandal, D, ME Bolander, D Mukhopadhyay, G Sarkar and P Mukherjee. 2006. The Use of Microorganisms for the Formation of Metal Nanoparticles and Their Application. *Applied Microbiology and Biotechnology* 69 (5): 485–492. doi:10.1007/s00253-005-0179-3.

Maneewattanapinyo, P, W Banlunara, C Thammacharoen, S Ekgasit and T Kaewamatawong. 2011. An Evaluation of Acute Toxicity of Colloidal Silver Nanoparticles. *Journal of Veterinary Medical Science* advpub: 1106220557–1106220557. doi:10.1292/jvms.11-0038.

Mei, L, Z Teng, G Zhu, Y Liu, F Zhang, J Zhang, Y Li, Y Guan, Y Luo, X Chen and Q Wang. 2017. Silver Nanocluster-Embedded Zein Films as Antimicrobial Coating Materials for Food Packaging. *ACS Applied Materials & Interfaces* 9 (40): 35297–35304. doi:10.1021/acsami.7b08152.

Mendis, E, N Rajapakse, H-G Byun and S-K Kim. 2005. Investigation of Jumbo Squid (Dosidicus Gigas) Skin Gelatin Peptides for Their in Vitro Antioxidant Effects. *Life Sciences* 77 (17): 2166–2178. doi:10.1016/j.lfs.2005.03.016.

Meng, XK, SC Tang and S Vongehr. 2010. A Review on Diverse Silver Nanostructures. *Journal of Materials Science & Technology* 26 (6): 487–522. doi:10.1016/S1005-0302(10)60078-3.

Miller, SI, and NR Salama. 2018. The Gram-Negative Bacterial Periplasm: Size Matters. *PLoS Biology* 16 (1): e2004935. doi:10.1371/journal.pbio.2004935.

Mittal, AK, A Kaler and UC Banerjee. 2012. Free Radical Scavenging and Antioxidant Activity of Silver Nanoparticles Synthesized from Flower Extract of Rhododendron Dauricum. *Nano Biomedicine and Engineering* 4 (3): 118–124. doi:10.5101/nbe.v4i3.p118-124.

Molnár, Z, V Bódai, G Szakacs, B Erdélyi, Z Fogarassy, G Sáfrán, T Varga, Z Kónya, E Tóth-Szeles, R Szűcs and I Lagzi. 2018. Green Synthesis of Gold Nanoparticles by Thermophilic Filamentous Fungi. *Scientific Reports* 8 (1). Nature Publishing Group: 3943. doi:10.1038/s41598-018-22112-3.

Monica Periolatto, FFV. 2017. Novel Antimicrobial Agents and Processes for Textile Applications | IntechOpen. https://www.intechopen.com/books/antibacterial-agents/novel-antimicrobial-agents-and-processes-for-textile-applications.

Möritz, M, H Peters, B Nipko and H Rüden. 2001. Capability of Air Filters to Retain Airborne Bacteria and Molds in Heating, Ventilating and Air-Conditioning (HVAC) Systems. *International Journal of Hygiene and Environmental Health* 203 (5): 401–409. doi:10.1078/1438-4639-00054.

Morones, JR, JL Elechiguerra, A Camacho, K Holt, JB Kouri, JT Ramírez and MJ Yacaman. 2005. The Bactericidal Effect of Silver Nanoparticles. *Nanotechnology* 16 (10). IOP Publishing: 2346–2353. doi:10.1088/0957-4484/16/10/059.

Moses, J, and Venkataraman. 2016. Study of the Chemical Treatment on Cotton Fabrics to Increase the UV Protection and Anti-Odour Retention Properties. *Tekstil ve Konfeksiyon* 26 (4): 400–406.

Mowafi, S, M Rehan, HM Mashaly, AA El-Kheir and HE Emam. 2017. Influence of Silver Nanoparticles on the Fabrics Functions Prepared by In-Situ Technique. *The Journal of The Textile Institute* 108 (10). Taylor & Francis: 1828–1839. doi:10.1080/00405000.2017.1292649.

Nadiger, VG, and SR Shukla. 2016. Antibacterial Properties of Silk Fabric Treated with Silver Nanoparticles. *The Journal of The Textile Institute* 107 (12). Taylor & Francis: 1543–1553. doi:10.1080/00405000.2015.1129756.

Naika, HR, K Lingaraju, K Manjunath, D Kumar, G Nagaraju, D Suresh and H Nagabhushana. 2015a. Green Synthesis of CuO Nanoparticles Using Gloriosa Superba L. Extract and Their Antibacterial Activity . *Journal of Taibah University for Science* 9 (1). Taibah University: 7–12. doi:10.1016/j.jtusci.2014.04.006.

Naika, HR, K Lingaraju, K Manjunath, D Kumar, G Nagaraju, D Suresh and H Nagabhushana. 2015b. Green Synthesis of CuO Nanoparticles Using *Gloriosa Superba* L. Extract and Their Antibacterial Activity. *Journal of Taibah University for Science* 9 (1): 7–12. doi:10.1016/j.jtusci.2014.04.006.

Neal, AL. 2008. What Can Be Inferred from Bacterium–Nanoparticle Interactions about the Potential Consequences of Environmental Exposure to Nanoparticles? *Ecotoxicology* 17 (5): 362–371. doi:10.1007/s10646-008-0217-x.

Noël, J-M, MM Vieira, V Brasiliense, J-F Lemineur, C Combellas and F Kanoufi. 2020. Effect of the Driving Force on Nanoparticles Growth and Shape: An Opto-Electrochemical Study. *Nanoscale* 12 (5). The Royal Society of Chemistry: 3227–3235. doi:10.1039/C9NR09419A.

Orhan, M, D Kut and C Gunesoglu. 2007. Use of Triclosan as Antibacterial Agent in Textiles. *IJFTR Vol.32(1) [March 2007]*, March. CSIR. http://nopr.niscair.res.in/handle/123456789/302.

Paolini, J, T Barboni, J-M Desjobert, N Djabou, A Muselli and J Costa. 2010. Chemical Composition, Intraspecies Variation and Seasonal Variation in Essential Oils of Calendula Arvensis L. *Biochemical Systematics and Ecology* 38 (5): 865–874. doi:10.1016/j.bse.2010.07.009.

Parthiban, E, N Manivannan, R Ramanibai and N Mathivanan. 2019. Green Synthesis of Silver-Nanoparticles from Annona Reticulata Leaves Aqueous Extract and

Its Mosquito Larvicidal and Anti-Microbial Activity on Human Pathogens. *Biotechnology Reports* 21 (March): e00297. doi:10.1016/j.btre.2018.e00297.

Pastoriza-Santos, I, and LM Liz-Marzán. 2000. Binary Cooperative Complementary Nanoscale Interfacial Materials. Reduction of Silver Nanoparticles in DMF. Formation of Monolayers and Stable Colloids. *Pure and Applied Chemistry* 72 (1–2): 83–90. doi:10.1351/pac200072010083.

Pellieux, C, A Dewilde, C Pierlot and J-M Aubry. 2000. [18] Bactericidal and Virucidal Activities of Singlet Oxygen Generated by Thermolysis of Naphthalene Endoperoxides. In *Methods in Enzymology*, 319:197–207. Singlet Oxygen, UV-A, and Ozone. Academic Press. doi:10.1016/S0076-6879(00)19020-2.

Peng, X, J Wickham and AP Alivisatos. 1998. Kinetics of II-VI and III-V Colloidal Semiconductor Nanocrystal Growth: "Focusing" of Size Distributions. *Journal of the American Chemical Society* 120 (21): 5343–5344. doi:10.1021/ja9805425.

Perelshtein, I, G Applerot, N Perkas, G Guibert, S Mikhailov and A Gedanken. 2008. Sonochemical Coating of Silver Nanoparticles on Textile Fabrics (Nylon, Polyester and Cotton) and Their Antibacterial Activity. *Nanotechnology* 19 (24). IOP Publishing: 245705. doi:10.1088/0957-4484/19/24/245705.

Plotnikov, E, V Silnikov, A Gapeyev and V Plotnikov. 2016. Investigation of DNA-Damage and Chromosomal Aberrations in Blood Cells under the Influence of New Silver-Based Antiviral Complex. *Advanced Pharmaceutical Bulletin* 6 (1): 71–74. doi:10.15171/apb.2016.011.

Qin, Y, X Ji, J Jing, H Liu, H Wu and W Yang. 2010. Size Control over Spherical Silver Nanoparticles by Ascorbic Acid Reduction. *Colloids and Surfaces A: Physicochemical and Engineering Aspects* 372 (1–3): 172–176. doi:10.1016/j.colsurfa.2010.10.013.

Quadros, ME, and LC Marr. 2010. Environmental and Human Health Risks of Aerosolized Silver Nanoparticles. *Journal of the Air & Waste Management Association* 60 (7). Taylor & Francis: 770–781. doi:10.3155/1047-3289.60.7.770.

Quinteros, MA, V Cano Aristizábal, PR Dalmasso, MG Paraje and PL Páez. 2016. Oxidative Stress Generation of Silver Nanoparticles in Three Bacterial Genera and Its Relationship with the Antimicrobial Activity. *Toxicology in Vitro* 36 (October): 216–223. doi:10.1016/j.tiv.2016.08.007.

Ramakrishna, M, D Rajesh Babu, RM Gengan, S Chandra and G Nageswara Rao. 2016. Green Synthesis of Gold Nanoparticles Using Marine Algae and Evaluation of Their Catalytic Activity. *Journal of Nanostructure in Chemistry* 6 (1): 1–13. doi:10.1007/s40097-015-0173-y.

Ramamurthy, CH, M Padma, ID mariya samadanam, R Mareeswaran, A Suyavaran, MS Kumar, K Premkumar and C Thirunavukkarasu. 2013. The Extra Cellular Synthesis of Gold and Silver Nanoparticles and Their Free Radical Scavenging and Antibacterial Properties. *Colloids and Surfaces B: Biointerfaces* 102 (February): 808–815. doi:10.1016/j.colsurfb.2012.09.025.

Rana, M, B Hao, L Mu, L Chen and P-C Ma. 2016. Development of Multi-Functional Cotton Fabrics with Ag/AgBr–TiO2 Nanocomposite Coating. *Composites Science and Technology* 122 (January): 104–112. doi:10.1016/j.compscitech.2015.11.016.

Raveendran, P, J Fu and SL Wallen. 2003. Completely “Green” Synthesis and Stabilization of Metal Nanoparticles. *Journal of the American Chemical Society* 125 (46). American Chemical Society: 13940–13941. doi:10.1021/ja029267j.

Reidy, B, A Haase, A Luch, K Dawson and I Lynch. 2013. Mechanisms of Silver Nanoparticle Release, Transformation and Toxicity: A Critical Review of

Current Knowledge and Recommendations for Future Studies and Applications. *Materials* 6 (6): 2295–2350. doi:10.3390/ma6062295.

Rohani Shirvan, A, S Kordjazi and A Bashari. 2019a. Environmentally Friendly Finishing of Cotton Fabric via Star-like Silver Micro/Nano Particles Synthesized with Neem/Salep. *Journal of Natural Fibers* 00 (00). Taylor & Francis: 1–9. doi:10.1080/15440478.2019.1691122.

Rohani Shirvan, A, S Kordjazi and A Bashari. 2019b. Environmentally Friendly Finishing of Cotton Fabric via Star-like Silver Micro/Nano Particles Synthesized with Neem/Salep. *Journal of Natural Fibers*, November, 1–9. doi:10.1080/15440478.2019.1691122.

Roy, K, CK Sarkar and CK Ghosh. 2015. Photocatalytic Activity of Biogenic Silver Nanoparticles Synthesized Using Yeast (Saccharomyces Cerevisiae) Extract. *Applied Nanoscience* 5 (8): 953–959. doi:10.1007/s13204-014-0392-4.

Ruiz De Clavijo, E. 2005. The Reproductive Strategies of the Heterocarpic Annual Calendula Arvensis (Asteraceae). *Acta Oecologica* 28 (2): 119–126. doi:10.1016/j.actao.2005.03.004.

Sabri, MA, A Umer, GH Awan, MF Hassan and A Hasnain. 2016. Selection of Suitable Biological Method for the Synthesis of Silver Nanoparticles. *Nanomaterials and Nanotechnology* 6 (1): 1–20. doi:10.5772/62644.

Sadowski, Z, IH Maliszewska, B Grochowalska, I Polowczyk and T Ko. Synthesis of Silver Nanoparticles Using Microorganisms, 6.

Sahu, SC, and DA Casciano. 2009. *Nanotoxicity: From In Vivo and In Vitro Models to Health Risks*. John Wiley & Sons.

Sangeetha, G, S Rajeshwari and R Venckatesh. 2011. Green Synthesis of Zinc Oxide Nanoparticles by Aloe Barbadensis Miller Leaf Extract: Structure and Optical

Properties. *Materials Research Bulletin* 46 (12): 2560–2566. doi:10.1016/j.materresbull.2011.07.046.

Sasaki, K, M Tenjimbayashi, K Manabe and S Shiratori. 2016. Asymmetric Superhydrophobic/Superhydrophilic Cotton Fabrics Designed by Spraying Polymer and Nanoparticles. *ACS Applied Materials & Interfaces* 8 (1). American Chemical Society: 651–659. doi:10.1021/acsami.5b09782.

Sastry, PU, PSR Krishna, L Panicker and AB Shinde. 2008. Structural Behaviour of AgNO3 at Low Temperatures by Neutron Diffraction. *Pramana* 71 (5): 929–933. doi:10.1007/s12043-008-0202-1.

Sathishkumar, M, K Sneha and Y-S Yun. 2010. Immobilization of Silver Nanoparticles Synthesized Using Curcuma Longa Tuber Powder and Extract on Cotton Cloth for Bactericidal Activity. *Bioresource Technology* 101 (20): 7958–7965. doi:10.1016/j.biortech.2010.05.051.

Servi, H, C Vatansever, A Doğan and V Majeed. 2020. Antibacterial Activity and Essential Oil Composition of Calendula Arvensis L. *International Journal of Secondary Metabolite*, November, 229–236. doi:10.21448/ijsm.676985.

Shah, PS, JD Holmes, RC Doty, KP Johnston and BA Korgel. 2000. Steric Stabilization of Nanocrystals in Supercritical CO2 Using Fluorinated Ligands. *Journal of the American Chemical Society* 122 (17). American Chemical Society: 4245–4246. doi:10.1021/ja9943748.

Shahidi, S, M Rashidian and D Dorranian. 2018. Preparation of Antibacterial Textile Using Laser Ablation Method. *Optics & Laser Technology* 99 (February): 145–153. doi:10.1016/j.optlastec.2017.08.025.

Shankar, SS, A Rai, A Ahmad and M Sastry. 2004. Rapid Synthesis of Au, Ag, and Bimetallic Au Core–Ag Shell Nanoparticles Using Neem (Azadirachta Indica)

Leaf Broth. *Journal of Colloid and Interface Science* 275 (2): 496–502. doi:10.1016/j.jcis.2004.03.003.

Shengtai He, †, ‡ Jiannian Yao, † Peng Jiang, † Dongxia Shi, † Haoxu Zhang, † Sishen Xie, † and Shijin Pang and † Hongjun Gao*. 2001. Formation of Silver Nanoparticles and Self-Assembled Two-Dimensional Ordered Superlattice. Research-article. *ACS Publications*. American Chemical Society. World. doi:10.1021/la001239w.

Soenen, SJ, P Rivera-Gil, J-M Montenegro, WJ Parak, SC De Smedt and K Braeckmans. 2011. Cellular Toxicity of Inorganic Nanoparticles: Common Aspects and Guidelines for Improved Nanotoxicity Evaluation. *Nano Today* 6 (5): 446–465. doi:10.1016/j.nantod.2011.08.001.

Sondi, I, and B Salopek-Sondi. 2004. Silver Nanoparticles as Antimicrobial Agent: A Case Study on E. Coli as a Model for Gram-Negative Bacteria. *Journal of Colloid and Interface Science* 275 (1): 177–182. doi:10.1016/j.jcis.2004.02.012.

Sun, G. 2016. *Antimicrobial Textiles*. Woodhead Publishing.

Sun, Y, and Y Xia. 2002. Shape-Controlled Synthesis of Gold and Silver Nanoparticles. *Science* 298 (5601): 2176–2179. doi:10.1126/science.1077229.

Tang, S, X Meng, H Lu and S Zhu. 2009. PVP-Assisted Sonoelectrochemical Growth of Silver Nanostructures with Various Shapes. *Materials Chemistry and Physics* 116 (2–3): 464–468. doi:10.1016/j.matchemphys.2009.04.004.

Tao, A, P Sinsermsuksakul and P Yang. 2006. Polyhedral Silver Nanocrystals with Distinct Scattering Signatures. *Angewandte Chemie International Edition* 45 (28): 4597–4601. doi:10.1002/anie.200601277.

Tarimala, S, N Kothari, N Abidi, E Hequet, J Fralick and LL Dai. 2006. New Approach to Antibacterial Treatment of Cotton Fabric with Silver Nanoparticle–Doped

Silica Using Sol–Gel Process. *Journal of Applied Polymer Science* 101 (5): 2938–2943. doi:10.1002/app.23443.

Thakkar, KN, SS Mhatre and RY Parikh. 2010. Biological Synthesis of Metallic Nanoparticles. *Nanomedicine: Nanotechnology, Biology and Medicine* 6 (2): 257–262. doi:10.1016/j.nano.2009.07.002.

Trefry, JC, JL Monahan, KM Weaver, AJ Meyerhoefer, MM Markopolous, ZS Arnold, DP Wooley and IE Pavel. 2010. Size Selection and Concentration of Silver Nanoparticles by Tangential Flow Ultrafiltration for SERS-Based Biosensors. *Journal of the American Chemical Society* 132 (32). American Chemical Society: 10970–10972. doi:10.1021/ja103809c.

Tripathy, A, AM Raichur, N Chandrasekaran, TC Prathna and A Mukherjee. 2010. Process Variables in Biomimetic Synthesis of Silver Nanoparticles by Aqueous Extract of Azadirachta Indica (Neem) Leaves. *Journal of Nanoparticle Research* 12 (1): 237–246. doi:10.1007/s11051-009-9602-5.

TSE, L, and TL HO. 1975. The Hard Soft Acids Bases (Hsab) Principle and Organic Chemistry.

TÜBİVES Calendula Arvensis. 2021. Accessed September 1. http://194.27.225.161/yasin/tubives/index.php?sayfa=1&tax_id=4884.

Turkevich, J, PC Stevenson and J Hillier. 1951. A Study of the Nucleation and Growth Processes in the Synthesis of Colloidal Gold. *Discussions of the Faraday Society* 11 (0). The Royal Society of Chemistry: 55–75. doi:10.1039/DF9511100055.

Uğur, ŞS, M Sarıışık, AH Aktaş, MÇ Uçar and E Erden. 2010. Modifying of Cotton Fabric Surface with Nano-ZnO Multilayer Films by Layer-by-Layer Deposition Method. *Nanoscale Research Letters* 5 (7). SpringerOpen: 1204–1210. doi:10.1007/s11671-010-9627-9.

Vasireddy, R, R Paul and AK Mitra. 2012. Green Synthesis of Silver Nanoparticles and the Study of Optical Properties. *Nanomaterials and Nanotechnology* 2 (December). SAGE Publications Ltd STM: 8. doi:10.5772/52329.

Venkateswara Rao, A, and SD Bhagat. 2004. Synthesis and Physical Properties of TEOS-Based Silica Aerogels Prepared by Two Step (Acid–Base) Sol–Gel Process. *Solid State Sciences* 6 (9): 945–952. doi:10.1016/j.solidstatesciences.2004.04.010.

Vergara, JR, and PA Estévez. 2014. A Review of Feature Selection Methods Based on Mutual Information. *Neural Computing and Applications* 24 (1): 175–186. doi:10.1007/s00521-013-1368-0.

Veyrat-Charvillon, N, and F-X Standaert. 2009. Mutual Information Analysis: How, When and Why? In *Cryptographic Hardware and Embedded Systems - CHES 2009*, edited by Christophe Clavier and Kris Gaj, 429–443. Lecture Notes in Computer Science. Berlin, Heidelberg: Springer. doi:10.1007/978-3-642-04138-9_30.

Vijayaraghavan, K, SPK Nalini, NU Prakash and D Madhankumar. 2012. Biomimetic Synthesis of Silver Nanoparticles by Aqueous Extract of Syzygium Aromaticum. *Materials Letters* 75 (May): 33–35. doi:10.1016/j.matlet.2012.01.083.

Wan, Y, Z Guo, X Jiang, K Fang, X Lu, Y Zhang and N Gu. 2013. Quasi-Spherical Silver Nanoparticles: Aqueous Synthesis and Size Control by the Seed-Mediated Lee–Meisel Method. *Journal of Colloid and Interface Science* 394 (March): 263–268. doi:10.1016/j.jcis.2012.12.037.

Wang, J, J Shen, D Ye, X Yan, Y Zhang, W Yang, X Li, J Wang, L Zhang and L Pan. 2020. Disinfection Technology of Hospital Wastes and Wastewater: Suggestions for Disinfection Strategy during Coronavirus Disease 2019

(COVID-19) Pandemic in China. *Environmental Pollution* 262 (July): 114665. doi:10.1016/j.envpol.2020.114665.

Wiley, BJ, SH Im, Z-Y Li, J McLellan, A Siekkinen and Y Xia. 2006. Maneuvering the Surface Plasmon Resonance of Silver Nanostructures through Shape-Controlled Synthesis. *The Journal of Physical Chemistry B* 110 (32): 15666–15675. doi:10.1021/jp0608628.

Windler, L, M Height and B Nowack. 2013. Comparative Evaluation of Antimicrobials for Textile Applications. *Environment International* 53 (March): 62–73. doi:10.1016/j.envint.2012.12.010.

Xing, H, J Cheng, X Tan, C Zhou, L Fang and J Lin. 2020. Ag Nanoparticles-Coated Cotton Fabric for Durable Antibacterial Activity: Derived from Phytic Acid–Ag Complex. *The Journal of The Textile Institute* 111 (6): 855–861. doi:10.1080/00405000.2019.1668137.

Xu, Q, X Ke, L Shen, N Ge, Y Zhang, F Fu and X Liu. 2018. Surface Modification by Carboxymethy Chitosan via Pad-Dry-Cure Method for Binding Ag NPs onto Cotton Fabric. *International Journal of Biological Macromolecules* 111 (May): 796–803. doi:10.1016/j.ijbiomac.2018.01.091.

Xue, C, and CA Mirkin. 2007. pH-Switchable Silver Nanoprism Growth Pathways. *Angewandte Chemie* 119 (12): 2082–2084. doi:10.1002/ange.200604637.

Yamamoto, M, and M Nakamoto. 2003. New Type of Monodispersed Gold Nanoparticles Capped by Myristate and PPh3 Ligands Prepared by Controlled Thermolysis of [Au(C13H27COO)(PPh3)]. *Chemistry Letters* 32 (5). The Chemical Society of Japan: 452–453. doi:10.1246/cl.2003.452.

Yang, N, and W-H Li. 2013. Mango Peel Extract Mediated Novel Route for Synthesis of Silver Nanoparticles and Antibacterial Application of Silver Nanoparticles

Loaded onto Non-Woven Fabrics. *Industrial Crops and Products* 48 (July): 81–88. doi:10.1016/j.indcrop.2013.04.001.

Yazdankhah, DSP, AA Scheie, EA Høiby, B-T Lunestad, E Heir, TØ Fotland, K Naterstad and H Kruse. 2006. Triclosan and Antimicrobial Resistance in Bacteria: An Overview. Research-article. h*ttps://home.liebertpub.com/mdr*. Mary Ann Liebert, Inc. 2 Madison Avenue Larchmont, NY 10538 USA. 2 Madison Avenue Larchmont, NY 10538 USA. doi:10.1089/mdr.2006.12.83.

Yin, Y, Z-Y Li, Z Zhong, B Gates, Y Xia and S Venkateswaran. 2002. Synthesis and Characterization of Stable Aqueous Dispersions of Silver Nanoparticles through the Tollens ProcessElectronic Supplementary Information (ESI) Available: Photographs of Silver Mirror, and of Stable Dispersions of Silver Nanoparticles from Mixing Diluted Silvering Solutions under Sonication at Various Times. See Http://Www.Rsc.Org/Suppdata/Jm/B1/B107469e/. *Journal of Materials Chemistry* 12 (3): 522–527. doi:10.1039/b107469e.

You, C, C Han, X Wang, Y Zheng, Q Li, X Hu and H Sun. 2012. The Progress of Silver Nanoparticles in the Antibacterial Mechanism, Clinical Application and Cytotoxicity. *Molecular Biology Reports* 39 (9): 9193–9201. doi:10.1007/s11033-012-1792-8.

Zain, NM, AGF Stapley and G Shama. 2014. Green Synthesis of Silver and Copper Nanoparticles Using Ascorbic Acid and Chitosan for Antimicrobial Applications. *Carbohydrate Polymers* 112 (November): 195–202. doi:10.1016/j.carbpol.2014.05.081.

Zhang, C, F Cui, G Zeng, M Jiang, Z Yang, Z Yu, M Zhu and L Shen. 2015. Quaternary Ammonium Compounds (QACs): A Review on Occurrence, Fate and Toxicity in the Environment. *Science of The Total Environment* 518–519 (June): 352–362. doi:10.1016/j.scitotenv.2015.03.007.

Zhang, D, L Chen, C Zang, Y Chen and H Lin. 2013. Antibacterial Cotton Fabric Grafted with Silver Nanoparticles and Its Excellent Laundering Durability. *Carbohydrate Polymers* 92 (2): 2088–2094. doi:10.1016/j.carbpol.2012.11.100.

Zhang, F, X Wu, Y Chen and H Lin. 2009. Application of Silver Nanoparticles to Cotton Fabric as an Antibacterial Textile Finish. *Fibers and Polymers* 10 (4): 496–501. doi:10.1007/s12221-009-0496-8.

Zhao, G, and SE Stevens. 1998. Multiple Parameters for the Comprehensive Evaluation of the Susceptibility of Escherichia Coli to the Silver Ion. *Biometals* 11 (1): 27–32. doi:10.1023/A:1009253223055.

Zhou, Q, J Lv, Y Ren, J Chen, D Gao, Z Lu and C Wang. 2017a. A Green in Situ Synthesis of Silver Nanoparticles on Cotton Fabrics Using Aloe Vera Leaf Extraction for Durable Ultraviolet Protection and Antibacterial Activity. *Textile Research Journal* 87 (19): 2407–2419. doi:10.1177/0040517516671124.

Zhou, Q, J Lv, Y Ren, J Chen, D Gao, Z Lu and C Wang. 2017b. A Green in Situ Synthesis of Silver Nanoparticles on Cotton Fabrics Using *Aloe Vera* Leaf Extraction for Durable Ultraviolet Protection and Antibacterial Activity. *Textile Research Journal* 87 (19): 2407–2419. doi:10.1177/0040517516671124.

Zhou, Q, J Lv, Y Ren, J Chen, D Gao, Z Lu and C Wang. 2017c. A Green in Situ Synthesis of Silver Nanoparticles on Cotton Fabrics Using Aloe Vera Leaf Extraction for Durable Ultraviolet Protection and Antibacterial Activity. *Textile Research Journal* 87 (19). SAGE Publications Ltd STM: 2407–2419. doi:10.1177/0040517516671124.

Zhuang, X, B Cheng, W Kang and X Xu. 2010. Electrospun Chitosan/Gelatin Nanofibers Containing Silver Nanoparticles. *Carbohydrate Polymers* 82 (2): 524–527. doi:10.1016/j.carbpol.2010.04.085.

CURRICULUM VITAE

Toufique Ahmed completed his B.sc in Textile Engineering from the Bangladesh University of Textiles in 2012. In the same year started his career as a 'Production Engineer" in a weaving factory in Bangladesh. Next year, he enrolled in the same university's M.sc in Textile Engineering program. He joined in National Institute of Textile Engineering and Research (NITER) as a Lecturer in 2014. In 2016 he completed the M.sc in Textile Engineering degree. In the following year, he was upgraded to an Assistant Professor at that institute. He was admitted to Cukurova University for a Ph.D. in 2017 under the Turkish Government Scholarship program. He was awarded Ph.D. in Textile Engineering in 2022.